NOTE TO USERS

STRATEGIES FOR PREPARING SEGMENTALLY ISOTOPICALLY LABELED PROTEINS FOR PROBING DOMAIN-DOMAIN INTERACTIONS BY FTIR SPECTROSCOPY

By

Sarah Jane Martinez

Department of Food Science and Agricultural Chemistry

Macdonald Campus, McGill University

Montreal, Quebec

A thesis submitted to McGill University in partial fulfillment

of the requirements of the degree of Master of Science

December, 2004

Your file Votre référence
ISBN: 0-494-12501-2
Our file Notre référence
ISBN: 0-494-12501-2

Suggested short title:

Strategies for Probing Domain-Domain Interactions by FTIR Spectroscopy

ABSTRACT

Fourier transform infrared (FTIR) spectroscopy is a powerful tool for probing protein structure-function relationships. With the use of isotope editing, it can also be employed to elucidate protein-nucleic acid interactions. This technique was used to study the sequence of heat-induced unfolding of the uniformly labeled ^{13}C regulatory subunit (RSU) of *E. coli* aspartate transcarbamylase (ATCase) with its inhibitor CTP. The absorption of CTP in the amide I' region limits our ability to detect protein conformational changes upon binding of CTP. Therefore, by labeling the protein with ^{13}C shifts the amide I' band ~ 40 cm^{-1} and clearly separates the protein bands from those of CTP. Variable-temperature (VT) FTIR spectroscopy was then employed to monitor the thermal unfolding of the labeled RSU in the presence and absence of CTP.

In addition, isotope editing was further explored to probe domain-domain interactions of the two domains of RSU using intein technology. Intein technology provides a novel means by which isotope editing can be performed to extract information on protein inter-domain and inter-subunit interactions by spectroscopic analysis but has not yet been exploited in Fourier transform infrared (FTIR) spectroscopy. The objective of this project is to present for the first time the feasibility of segmental labeling through intein-mediated protein ligation (IPL) for the purpose of studying conformational changes by FTIR spectroscopy, using ATCase as a model enzyme. In the first phase of this project, the RSU of ATCase, which houses a Zn-binding domain and a nucleotide binding domain, was reconstructed from its isolated domains using commercially available intein-base expression vectors. As steps towards obtaining an isotope labeled RSU, we have fused each domain to separate inteins. Following affinity purification, the intein tags were chemically cleaved and the reactive ends of the two RSU domains were ligated together to form a peptide. Although ligation was successful, improved yields are required for the FTIR spectroscopic studies.

RÉSUMÉ

La spectroscopie infrarouge à transformée de Fourier (FTIR) est un outil puissant dans l'évaluation des rapports de structuro-fonctionels des protéines. Grâce à l'utilisation d'intégrations isotopiques elle peut également être utilisée pour élucider des interactions entre les protéines et les acides nucléiques. Cette technique a été employée pour étudier la séquence du déploiement provoqué par le chauffage de la sous-unité de normalisation (RSU) de la transcarbamylase d'aspartate de *E. coli* (ATCase), uniformément marquée de ^{13}C, avec son inhibiteur CTP. L'absorption du CTP dans la région amide I', limite notre capacité à détecter des changements conformationels de la protéine lors de son attachement avec le CTP. Le marquage de la protéine avec l'isotope 13C décale la région amide I' de 40 cm^{-1} permettant ainsi une séparation claire de l'absorption de la protéine de celle du CTP. La spectroscopie à température variable (VT) FTIR est alors utilisée pour surveiller le déploiement thermique du RSU marqué isotopiquement en présence et absence de CTP.

L'édition isotopique a été explorée plus loin afin de sonder les interactions inter-domaines entres les deux domaines du RSU en utilisant la technologie intein. La technologie intein fournit de nouveaux moyens par lesquels l'édition isotopique peut être effectuée pour extraire l'information sur des interactions entre les domaines et entre les sous-unités protéiques via analyse spectroscopique. Ce type de technologie n'a, à ce jour, pas été exploitée en spectroscopie FTIR. L'objectif de ce projet est de présenter pour la première fois la praticabilité du marquage des segments protéiques grâce à la fusion contrôlée par intein (IPL) de la protéine, afin d'étudier les changements conformationels par spectroscopie FTIR, en utilisant l'ATCase comme modèle enzymatique. Dans la première phase de ce projet, le RSU d'ATCase, qui abrite un domaine liant un Zn et un domaine d'attachement de nucléotide, a été reconstruit à partir de ses domaines respectifs en utilisant des vecteurs d'expression disponibles commercialement. Chaque domaine a été fusionné avec une intein, étape primordiale vers l'obtention du RSU marqué isotopiquement. Après la purification par affinité, les étiquettes d'intein ont été chimiquement scindées et les extrémités réactives des deux domaines de RSU fusionnées ensemble pour former un peptide. Bien que la ligature ait été réussie, de meilleurs rendements seraient nécessaires pour permettre des études spectroscopiques par FTIR.

ACKNOWLEDGMENTS

I wish to express my sincere gratitude to my supervisor, Dr. Ashraf A. Ismail, whose enthusiasm and brilliant vision has driven me to greater heights of clarity and cohesiveness. I would also like to thank Dr. Joanne Turnbull for her tremendous efforts in supervising my research work which I carried out in her laboratory at the Department of Chemistry and Biochemistry of Concordia University.

I would like to thank Dr. Ming-Ni Hung for her help in the molecular biology aspect of this work; Takrima Haque, for guiding me in the preparation of ^{13}C-labeled proteins; and Ziad Khoury, who has helped me set my thoughts down in an understandable way. I greatly appreciate the support and assistance from my colleagues at Concordia University; Julie Bonvin, John Manioudakis, Raphael Aponte and Kevork Mekhssian. I am sincerely grateful to the graduates from the McGill IRGroup, Nasser Aljundi and Pedro Alvarez for their friendships and generosity.

I am deeply indebted to my parents, who have never ceased their generous support of my endeavour. Their enthusiasm and positive outlook provided inspiration and energized my efforts. Lastly, I am grateful to my brother and sister, for all their support, encouragements and constant aid of all kinds.

TABLE OF CONTENTS

LIST OF FIGURES

CHAPTER 2:

CHAPTER 3:

CHAPTER 4:

CHAPTER 5:

LIST OF TABLES

CHAPTER 2:

CHAPTER 3:

CHAPTER 4:

CHAPTER 5:

LIST OF ABBREVIATIONS

1D	one-dimensional
2D	two-dimensional
°C	degrees Celsius
Abs	absorbance
Al domain	allosteric domain
Arg (R)	arginine
Asn (N)	asparagine
ATCase	aspartate transcarbamylase
ATP	adenosine triphosphate
bp	base pairs
C-	carboxy
Ca_2Fl	calcium fluoride
CBD	chitin binding domain
CD	circular dichroism
cm	centimeter
CSU	catalytic subunit
CTP	cytidine triphosphate
Cys (C)	cysteine
DNA	deoxyribonucleic acid
DTT	dithiothreitol
EDTA	ethylenediamine tetra-acetic acid
EPL	expressed protein ligation
FSD	Fourier self-deconvolution
FT	Fourier transform
g	grams
gly (G)	glycine
hr	hour
H-D	hydrogen-deuterium
IMPACT	intein-mediated purification with an affinity chitin-binding tag
IPL	intein-mediated protein ligation
IPTG	isopropyl-β-D-thiogalactopyranoside
IR	infrared
kbp	kilo base pairs

kDa	kilo Daltons
L	liter
LB	Luria broth
Lys (K)	lysine
M	Molar
μ	micro
MESNA	2-mercaptoethanesulfonic acid
Met (M)	methionine
min	minute
ml	milliliter
MS	mass spectroscopy
MW	molecular weight
N-	amino
N	nitrogen
NEB	New England Biolabs
NMR	nuclear magnetic resonance
O	oxygen
PAGE	polyacrylamide gel electrophoresis
PALA	N-phosphonoacetyl-L-asparate
PCR	polymerase chain reaction
PMSF	phenylmethylsulfonyl fluoride
r.p.m.	rotations per minute
RSU	regulatory subunit
s	second
S	sulfur
SDS	sodium dodecylsulfate
Ser (S)	serine
S/N	signal to noise
TCEP	tri(2-carboxyethyl)phosphine hydrochloride
Tris	tris(hydroxymethyl)aminomethan
U	units
UV	ultra violet
Val (V)	valine
VT	variable temperature
Zn	Zinc

CHAPTER 1
General Introduction

Fourier transform infrared (FTIR) spectroscopy is a common technique used for studying protein structure and unfolding. Isotope editing techniques can be employed to enhance FTIR spectroscopy by uniformly labeling the protein with heavy isotopes, such as ^{13}C and ^{15}N. This allows the displacement of the amide I bands by ~45 cm^{-1} to lower wavenumbers, and enables one to obtain structural information on an individual protein in the presence of an unlabeled protein, for studying protein-protein complexes (Harris et al. 1992). In addition, ^{13}C-labeling has been very useful in the study of enzyme-substrate, and protein-nucleic acid interactions where the ligand has an absorbance band that is close to, or overlaps the amide I band absorption. Uniform labeling of proteins can be achieved by directly supplying bacteria with labeled amino (Kainosho 1997; Gardner and Kay 1998), or by cell-free synthesis (Kigawa et al. 1995). Also, total chemical synthesis of producing isotopically labeled proteins is feasible; however, it is not economically practical and limited to peptides with less than 100 amino acids. This is an attractive approach because of the ability to label specific segments of a peptide or protein.

The latest method in producing segmentally labeled proteins employs the recently discovered intein (Otomo et al. 1999b; Xu et al. 1999). Inteins are inframe-intervening sequences that disrupt the coding region of a host protein. After translation, the protein undergoes a process called protein splicing, which results in the excision of the intervening sequences (inteins) and joining of the lateral sequences (exteins). This process has been shown to involve the formation of a thioester group, which is essential for protein ligation. Since the discovery of protein splicing, commercially available intein-base expression vectors have been developed to purify proteins of any size. The advantage of this system is the ability to generate an N-terminal Cys and C-terminal thioesters on separate proteins, which can then ligate together chemically to form a peptide bond. Hence, this method is called intein-mediated protein ligation (IPL). Intein technology can also be used to selectively label a peptide segment, containing an active site, to study its structure and function upon ligand binding. Isotope editing using intein technology is less than 6 years old

and there are only a few proteins that have been labeled using this technique (Otomo et al. 1999b; Xu et al. 1999; Perler and Adam 2000). The objective of this thesis is to outline the overall strategy that will be employed to investigate for the first time the feasibility of segmental labeling through IPL of the regulatory subunit (RSU) of aspartate transcarbamylase (ATCase), for the purpose of studying conformational changes that occur in selected segments/domains of RSU by isotope edited FTIR spectroscopy.

The first part of this thesis will deal with a general overview of inteins and their use in peptide ligation. The chapter will also cover the structure and enzymatic properties of ATCase and its subunits. The second part will cover the synthesis of uniformly ^{13}C-labeled RSU and the use of 2D variable-temperature FTIR spectroscopy to elucidate its thermally induced unfolding pathway in the presence and absence of its allosteric effector, cytidine triphosphate (CTP). The third part will cover the assignment of the Raman bands of ATCase and its subunits, as well as the application of Raman spectroscopy to elucidate their secondary and tertiary structure. The forth part will cover the detailed protocols and their implementation in the production of two independently expressed domains of the regulatory subunit and their ligation to form an intact RSU.

CHAPTER 2
Literature Review

2.1 Introduction

Native chemical ligation involves a fusion of two synthetic peptides under relatively mild conditions. This technique requires one peptide with a C-terminal thioester and another peptide with an N-terminal cysteine. The N-terminal sulfhydryl moiety on the cysteine acts as a nucleophile and attacks the carbonyl of the thioester on the former peptide. This reaction is called *trans*-thioesterification and is followed by a covalent attachment of the two peptides through a thioester bond with a native peptide bond between the reacting species (Dawson et al. 1994; Tam et al. 1995). This chemistry of native chemical ligation reaction along with the mechanism of protein splicing is the theory behind producing semisynthetic peptides through intein technology.

Small proteins or peptides (~50 amino acids) can be easily produced by total synthesis, however it becomes challenging to produce peptides with > 100 amino acid residues. A solution to this problem is to link together two synthetic peptide segments. This approach is technically demanding to perform. Therefore, a semi-synthetic approach was developed to combine synthetic peptides and recombinantly derived polypeptides for ligation building blocks. This method alters the covalent structure of proteins, which is not possible by standard site-directed mutagenesis techniques. Through peptide ligation, fully unprotected polypeptide building blocks can be region-selectively joined together in aqueous solution to produce a target protein molecule (Cotton and Muir 1999). This process can be achieved chemically through chemical ligation or enzymatically by reverse proteolytic technique (Wallace 1995; Braisted et al. 1997). This paper will focus on the recent technologies in the field of peptide ligation, particularly using protein splicing elements (inteins) in the preparation of target protein molecules.

Inteins are inframe-intervening sequences that disrupt the coding region of a host protein. After translation, the protein undergoes a process called protein splicing, which results in the excision of the intervening sequences (inteins) and the joining of the lateral

sequences (exteins). The mechanism of protein splicing was first discovered in the 69 kDa subunit of the vascular ATPase from *Saccharomyces cerevisiae* (Gimble and Thorner 1992). Since that initial discovery, over 100 inteins were reported in an intein database called InBase (www.neb.com/neb/inteins.html). A large number of inteins are found in host proteins involved in nucleic acid metabolism (Perler and Adam 2000), particularly in DNA replication and DNA repair. Inteins have a broad phylogenetic distribution and they are found in eubacterias, archaeas, and eukaryotes (Perler and Adam 2000). Inteins are bifunctional enzymes comprised of an endonuclease and a splicing domain (Figure 2.1). The endonuclease domain is encoded by in the central region of the gene and is essential for intein mobility. The protein splicing activity is located in the two terminal regions and is directly involved in peptide bond cleavage and formation. The protein splicing mechanism is well defined, but the evolution and biological function of inteins are still unknown.

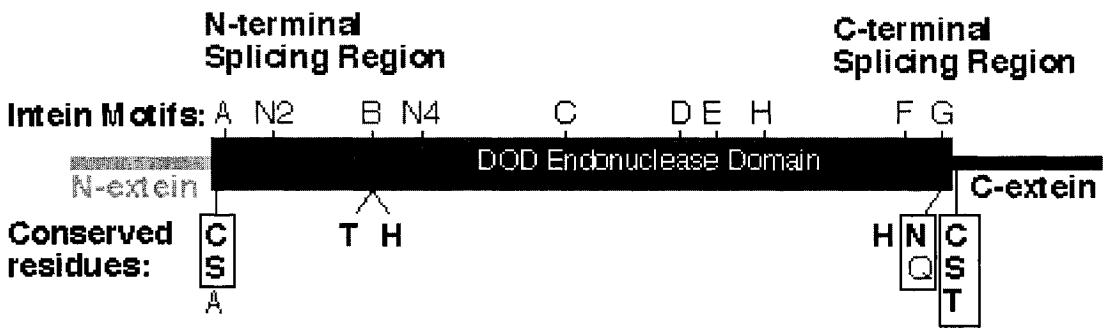

Figure 2.1: Structure of inteins. Inteins consists of two domains, the endonuclease domain and the splicing domains. The endonuclease domain is essential for the mobility of the gene, and the N- and C- terminal regions are involved in protein splicing activity (www.neb.com/neb/inteins.html).

2.2 Protein Splicing

The mechanism of protein splicing (Perler et al. 1997; Shao and Kent 1997) is summarized in Figure 2.2. The first step involves the N→S or N→O acyl shift in which the N-terminal extein (N-extein) is transferred to the side chain sulfhydryl/hydroxyl group of the first residue in the intein. This first residue is usually a cysteine, serine or threonine. It is speculated that intein structure is the driving force of this N-O or (N-S) acyl shift. After the initial N→(S/O) rearrangement, a slow *trans* esterification step occurs, in which the N-extein unit is transferred to the first conserved residue (cysteine, serine or threonine) of the C-extein. The next step involves the cyclization of the intein C-terminal Asn resulting in cleavage at the downstream splice junction and release of the excised intein. In the final step of the process, a peptide bond is formed between the N-extein and C-extein following an (S/O) →N acyl shift.

2.3 Application of Inteins

The knowledge of protein splicing has enabled researchers to exploit recombinant protein thioesters for use in native chemical ligation. Perler's groups in New England Biolabs (NEB) have created commercially available intein-base expression vectors. The controlled cleavage at a single intein splice junction, led to the design of a single-step protein purification system for purifying proteins of any size. The advantage of this system is the ability to generate N-terminal Cys and C-terminal thioesters on separate proteins, which can then ligate together chemically to form a peptide bond. Hence, this method is called intein-mediated protein ligation (IPL) (Evans et al. 1998; 1999) or also called expressed protein ligation (EPL)(Muir et al. 1998; Severinov and Muir 1998). This topic will be discussed in greater detail. The chemistry behind this reaction is very similar to the chemistry described for native chemical ligation (Chong et al. 1997; Klabunde et al. 1998).

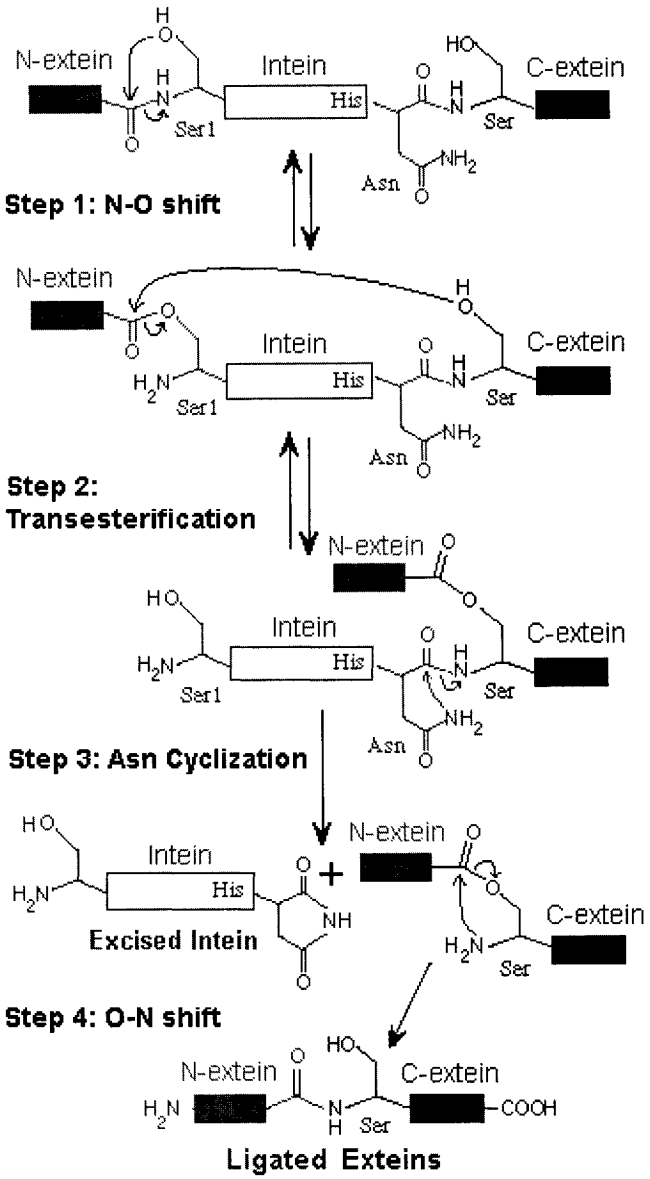

Figure 2.2: The chemical mechanism of protein splicing. The first step involves the N→S or N→O acyl shift in which the N-terminal extein (N-extein) is transferred to the side chain sulfhydryl/hydroxyl group of the first residue at the intein N-terminus. The second step involves a slow *trans*-esterification step where the N-extein unit is transferred to the first conserved residue of the C-extein. Then the intein is excised after asparagine cyclization, followed by an O-N or (S-N) acyl shift to form an amide bond (www.neb.com/neb/inteins.html).

2.4 Generation of Thioester-Tagged Proteins

The method of creating a specific C-terminal alpha-carbon was based on the studies of peptide bond cleavage at the N-terminal splice junction of an intein. Chong and coworkers showed that incubating the Sce VMA intein (N454A) mutant with hydroxylamine or with thiol reagent dithiothreitol (DTT), would lead to the cleavage of the thioester bond and result in the formation of a hydroxamate or thioester, respectively, on the C-terminus of the released N-extein (Chong et al. 1996; Chong et al. 1997). The activity of the intein enabled thiol-inducible cleavages which lead to the development of the system Intein Mediated Purification with an Affinity Chitin-binding Tag (IMPACT). This purification system is designed to isolate proteins containing a C-terminal thioester by fusing the protein of interest in-frame to the N-terminus of a modified intein. Furthermore, a chitin-binding domain (CBD) derived from *Bacillus circullans* (Watanabe et al. 1994) is used to separate the fusion protein from other cellular proteins based on its high affinity for chitin resin. Once the fusion protein (target protein-intein-CDB) is bound to the chitin resin, an inducible cleavage reaction occurs by incubating the mixture overnight with thiol reagents such as DTT, 2-mercaptoethanesulfonic acid (MESNA), or thiolphenol.

The IMPACT kit uses inteins called self-splicing mini-inteins (modified inteins). An example of a mini-intein that is commercially available through the kit is the *Mxe* GyrA intein (Telenti et al. 1997). This intein has a known crystal structure and is used because it possesses the ability to cleave the target protein from the intein tag in bacterial expressed proteins. The IMPACT system can be used to express intein fusion proteins in *E.coli*, an example of this is in the production of the Human Thionein/Metallothionein (Hong et al. 2001). The system produced high-yields of Human Thionein/Metallothionein proteins that are otherwise difficult to produce by conventional methods. Other researchers have used this method to obtain a C-terminal thioester- containing protein for chemical ligation with a reactive N-terminal cysteine-containing protein. (Chong et al. 1997; Evans et al. 1998; Severinov and Muir 1998; Evans et al. 1999; Hoang et al. 1999; Mathys et al. 1999; Blaschke et al. 2000; Cowburn and Muir 2001; Takeda et al. 2004)

2.5 Creation of an N-terminal Cysteine

In order for a native chemical ligation reaction to occur, proteins or peptides require an N-terminal cysteine as a complementary reactive group to the C-terminal thioester of another protein or peptide. Proteins or peptides containing an N-terminal cysteine can be obtained through proteolytic cleavage of an expressed protein at a site adjacent to a cysteine (Mathys et al. 1999; Xu et al. 1999). The use of proteases in cleavage reactions can result in non-specific proteolysis, and can be difficult to separate the protease from the products of interest.

An alternative method to produce a protein with an N-terminal cysteine (without the use of proteases) can be obtained by using intein expression vectors. New England Biolabs have created the intein vector for expression of a target protein fused to the C-terminal of a CBD-intein tag. Following expression of the fusion protein (CBD-intein-target protein), the precursor protein can be bound to the chitin resin. Incubating the system at room temperature and with specific cleavage buffer (usually below neutral pH), the target protein will be released from the intein-tag that contains an N-terminal cysteine. Note that since the first naturally occurring residue of a C-extein is a cysteine, serine or threonine , the cleavage at the C-terminus of an intein should result in the release of a protein with an N-terminal cysteine, serine or threonine. The advantage of this technique lies in the generation of a purified protein without extra residues at the cleavage site. In addition, the one-step purification system makes this process fairly simple. Several investigators have used this method to obtain an N-terminal cysteine-containing protein for chemical ligation with a C-terminal thioester-containing protein, and they are: (Chong et al. 1998; Evans et al. 1999; Mathys et al. 1999; Southworth et al. 1999; Wood et al. 1999; Wood et al. 2004)

2.6 Intein-Mediated Protein Ligation

IPL is a condensation reaction mediated by inteins and involves the fusion of a protein containing a C-terminal thioester, with an N-terminal cysteine (Figure 2.3). Only a few applications have been exploited using this technique, Some include: expressing cytotoxic proteins and kinase substrates (Evans et al. 1998), inserting nonnatural amino acid into proteins (Muir et al. 1998) and generating circular proteins for increased structure stability and enhance activity (Camarero and Muir 1997; Evans et al. 1999; Iwai and Pluckthun 1999; Scott et al. 1999).

IPL technology has been used in the production of cytotoxic proteins such as bovine pancreatic ribonuclease A (RNase A) and a restriction enzyme *Haemophilus parainfluenzae* (*Hpa*I) (Evans et al. 1998). They have used a truncated form of the cytotoxic protein and fused it with the modified *Mxe* GryA intein using the IMPACT kit. Following its purification via thiol-induced cleavage, the truncated RNase A is eluted from the chitin column, and then ligated with synthetic peptides (*Hpa*I) to complete the amino acid sequence of the enzyme. Regrettably, both proteins were misfolded; only RNase A regained activity but only after it was refolded. Several researchers have been successful in using IPL, and they are listed in Table 2.1.

Another example of the use of IPL is in the creation of segmentally labeled proteins for nuclear magnetic resonance (NMR) structural analysis. NMR spectroscopy has been instrumental in determining protein structures in solution. Uniformly labeling a protein with ^{13}C and ^{15}N enables the assignment of the resonances of the protein's atoms. This is beneficial for proteins up to ~ 25 K Da (Clore and Gronenborn 1994). However, for analyzing proteins of high molecular masses, NMR signal overlapping makes it difficult to assign resonances unequivocally. In the past, amino acid-specific labeling has been employed to decrease the number of NMR signals (Muchmore et al. 1989). Now with intein technology, the use of IPL is gaining popularity in the creation of segmentally labeling proteins for NMR spectroscopy.

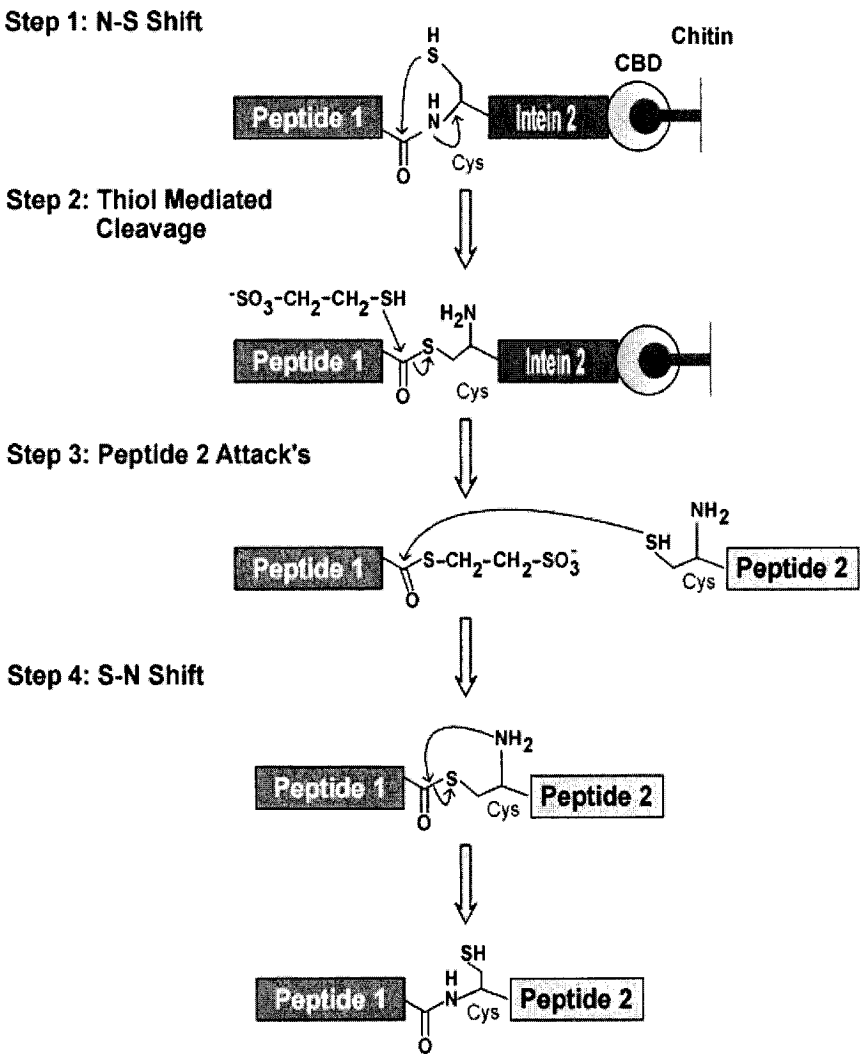

Figure 2.3: Strategy of intein-mediated protein ligation. Once the fusion protein is loaded on the column, cleavage of the target protein can be induced by thiol-reagents such as MESNA, DTT or β-mercaptoethanol. The release of the target protein from the intein tag creates a C-terminal thioester which can then undergo chemical protein ligation with a peptide (or protein) containing an N-terminal Cys. Chemical protein ligation will occur by just mixing the peptides to form a peptide bond (www.neb.com/neb/inteins.html).

Table 2.1: Application of inteins for IPL/EPL and segmental isotope labeling of proteins

IPL /EPL	
Semisynthesis of Ribonuclease A using Intein-Mediated Protein Ligation	(Arnold et al. 2002)
Intein-mediated protein ligation: harnessing nature's escape artists	(Evans et al. 1999)
Synthesis of adenoviral targeting molecules by intein-mediated protein ligation.	(Nyanguile et al. 2003)
Generation of an affinity column for antibody purification by intein-mediated protein ligation	(Sun et al. 2003)
Establishment of Intein-Mediated Protein Ligation under Denaturing Conditions: C-Terminal Labeling of a Single-Chain Antibody for Biochip Screening	(Sydor et al. 2002)
Phosphorylation of eIF4E attenuates its interaction with mRNA 5' cap analogs by electrostatic repulsion: Intein-mediated protein ligation strategy to obtain phosphorylated protein	(Zuberek et al. 2003)
Introduction of unnatural amino acids into proteins using expressed protein ligation	(Ayers et al. 1999)
Protein engineering by expressed protein ligation	(Blaschke et al. 2000)
Synthesis of Multi-domain Proteins using Expressed Protein Ligation: Strategies for Segmental labeling of Internal Regions	(Blaschke et al. 2000)
Expressed protein ligation: Method and applications	(David et al. 2004)
Recent advances in the application of expressed protein ligation to protein engineering	(Hofmann and Muir 2002)
Selenocysteine in native chemical ligation and expressed protein ligation	(Hondal et al. 2001)
Synthesis of protein-nucleic acid conjugates by expressed protein ligation	(Lovrinovic et al. 2003)
Expressed protein ligation: A general method for protein engineering	(Muir et al. 1998)
Development and Application of Expressed Protein Ligation	(Muir 2001)
Semisynthesis of Proteins by Expressed Protein Ligation	(Muir 2003)
Expressed protein ligation to probe regiospecificity of heterocyclization in the peptide antibiotic microcin B17	(Roy et al. 1999)
Merging fluorescence resonance energy transfer and expressed protein ligation to analyze protein-protein interactions	(Scheibner et al. 2003)
Expressed Protein Ligation, a Novel Method for Studying Protein-Protein Interactions in Transcription	(Severinov and Muir 1998)
Site-specific conjugation of oligonucleotides to the C-terminus of recombinant protein by expressed protein ligation	(Takeda et al. 2004)
The role of C-terminal tyrosine phosphorylation in the regulation of SHP-1 explored via expressed protein ligation	(Zuberek et al. 2003)

Segmental Isotope Labeling of Proteins	
New developments in isotope labeling strategies for protein solution NMR spectroscopy	(Goto and Kay 2000)
Improved seqmental isotope labeling of proteins and application to a larger protein	(Otomo et al. 1999b)
NMR observation of selected segments in a larger protein: central-segment isotope labeling through intein-mediated ligation	(Otomo et al. 1999a)
Segmental isotope labeling for protein NMR using peptide splicing	(Yamazaki et al. 1998)
Segmental isotopic labeling using expressed protein ligation	(Cowburn and Muir 2001)

Stable isotope labeling of peptide segments in protein samples has recently been achieved through the use of intein-mediated protein splicing. Xu and coworkers expressed src homology type 3 and 2 independently (SH3 and SH2, respectively) which are domains of the Abelson protein tyrosine kinase. Under normal physiological conditions, they were able to ligate the domains using expressed protein ligation (Xu et al. 1999). The samples were prepared in quantities suitable for NMR analysis. One domain was homogenously labeled by biosynthetic incorporation of ^{15}N, and the other domain was unlabeled or remained spectroscopically silent for NMR. The NMR results showed well-resolved peaks for the labeled portion of the protein. Hence, selective labeling of the protein was used to overcome the problem of spectral crowding, as observed when the whole protein is a homogenous biosynthetic ^{15}N labeled complex of multidomain proteins. The main idea to this approach is to study the protein domains in the context of larger multidomain complexes by NMR.

2.7 Protein Splicing in *Trans*

Semi-synthetic *trans*-splicing is an alternative method to expressed protein ligation. *Trans*-splicing is a strategy that can be used to chemically ligate (splice) two recombinant polypeptide chains which have been expressed and purified separately. It involves using a split intein and expressing each intein fragment with a portion of the protein target. The chemical ligation is facilitated by reconstituting the intein-fusion proteins *in vitro,* and the two intein segments will noncovalently associate to give a folded intein capable of supporting protein splicing (see Figure 2.4) (Noren et al. 2000). An example of this application is shown in Figure 2.5, which enabled the isotopic labeling of a central segment of the maltose binding protein. Otomo and coworkers created three plasmids, each containing portions of two different inteins fused to three segments of a target protein (Maltose Binding Protein); the protein expressed on plasmid #2 were isotopically labeled (Otomo et al. 1999a) (Otomo et al. 1999a). In this example, once the three intein fusion proteins were expressed and purified, gene products were mixed to perform the splicing reaction. This results in the production of a central-segment isotopic labeled protein (Maltose Binding Protein).

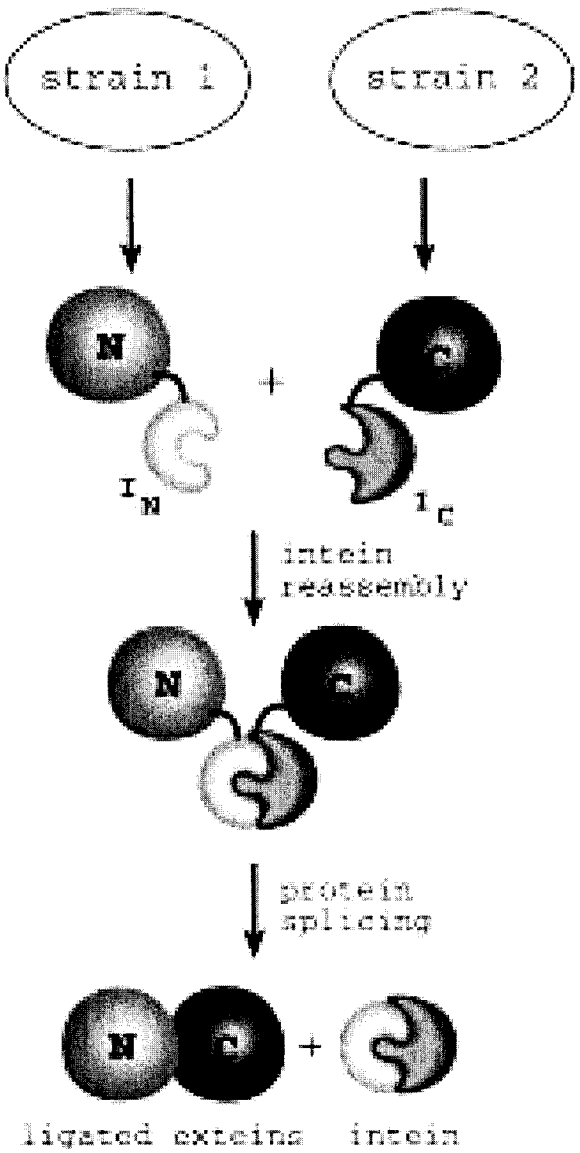

Figure 2.4: Schematic representation of protein splicing in *trans*. *Trans*-splicing involves expressing and purifying the intein-fusion proteins separately. By reconstituting the purified intein-fusion proteins *in vitro*, the intein reassembles and protein splicing occurs to ligate the exteins (Noren et al. 2000).

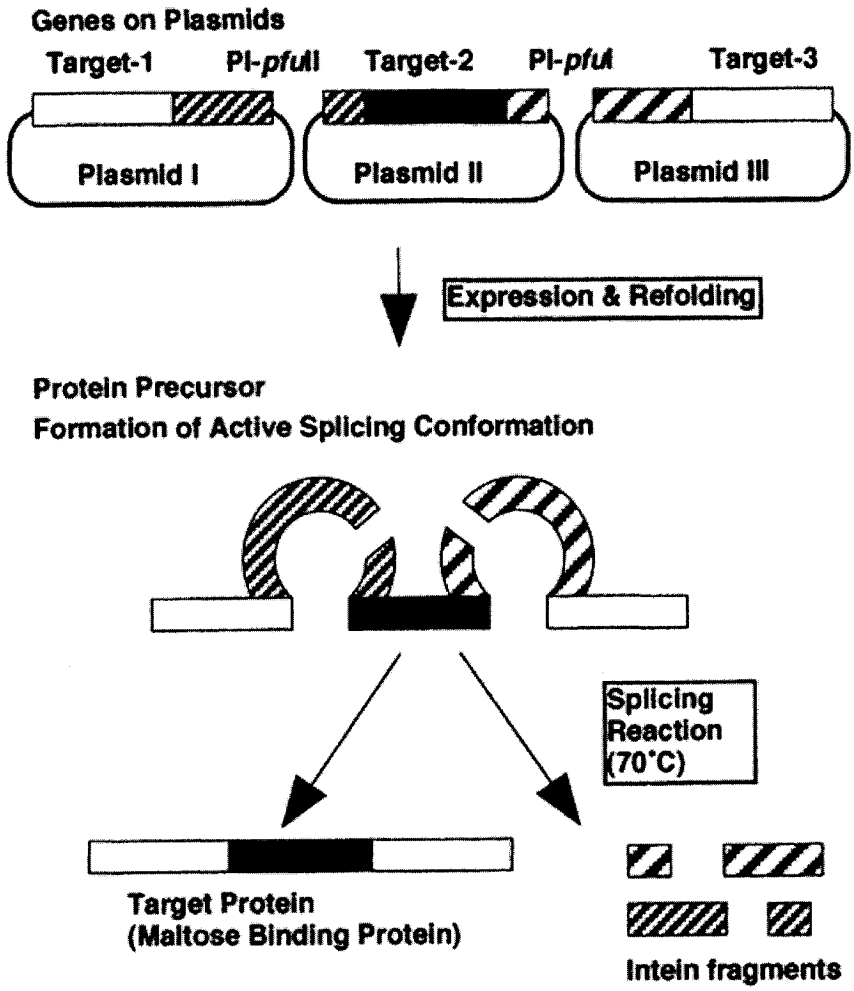

Figure 2.5: Strategy for segmental isotope labeling using split inteins. Otomo and coworkers have designed three plasmids encoding each containing portions of two different inteins fused to three segments of a target protein (Maltose Binding Protein); the protein expressed on plasmid #2 were isotopically labeled. In this example, once the three intein fusion proteins were expressed and purified, gene products were mixed to perform the splicing reaction. This results in the production of a central-segment isotopic labeled protein (Otomo et al. 1999a).

This powerful technique is ideally suited for large proteins for NMR spectroscopy and for the investigation of ligand protein interactions and drug design using SARS (structure-activity relationships). In addition, other researchers have also isotopically labeled their proteins of interest using protein splicing in *trans* (Table 2.1) (Goto and Kay 2000) (Otomo et al. 1999b) (Yamazaki et al. 1998) (Otomo et al. 1999a).

2.8 IPL/EPL versus Splicing of Split Inteins

The application of IPL/EPL versus split inteins to facilitate protein ligaiton depends on the product desired. IPL/EPL is the only method that incorporates moieties for peptide ligation, which can not be introduced during ribosomal synthesis. In terms of producing segmentally isotopic labeled protein, IPL/EPL is used for the terminal-segment isotope labeling by ligating two independently folded domains (one domain is isotopically labeled). The *trans*-splicing technique is optimized for central-segment labeling with the advantage of labeling any segment between structural flexibility residues in a single domain.

There are disadvantages of both techniques. For example, it may be difficult to choose a portion to separate the target protein, especially if it does not possess independently folded domains. Furthermore, expressed protein fragments may aggregate due to exposure of normally buried hydrophobic regions (Perler and Adam 2000). To overcome this problem, denaturants have been used to assist in the reassembly of the two proteins or peptide products (Perler and Adam 2000). Ligated proteins may require refolding for its activity. Most inteins require specific residues for optimized cleavage and splicing reactions, since different inteins may have different requirements (see Table 2.2). Also, crystallography data of the target protein can be instrumental in identifying a surface exposed loop for positioning the intein, which may in turn, result in an increase in cleavage efficiency and reduced perturbation of the target protein structure.

Table 2.2: Intein-based protein purification vectors (Perler and Adam 2000)

Intein	Vector	Mutation	Incompatible proximal aa[1]	Cleavage method[2]	IPL[3]	Reference
Vectors with the carboxy-terminus of the target protein fused to the intein amino-terminus						
Sce VMA	pTYB	N454A	P,C,N,D,R	Thiol	Yes	(Chong et al. 1997)
Sce VMA	pNam[4]	N454A	P,C,N,D,R	Thiol	Yes	(Hoang et al. 1999)
Mxe GyrA	pTXB	N198A	S,P,E,D	Thiol	Yes	(Evans et al. 1998) (Southworth et al. 1999)
Mth RIR1	pTRB	P(1)G/N134A	n.d.	Thiol	Yes	(Evans et al. 1999)
Ssp DnaB	pTSB	N154A	n.d.	Thiol, pH, T	Yes	(Mathys et al. 1999)
Vectors with the amino-terminus of the target protein fused to the intein carboxy-terminus						
Sce VMA	pTYB	H509Q	P,S,C	Thiol	Yes	(Chong et al. 1998)
Mxe GyrA	pMBX	Y(-1)S	n.d.	T	Yes	(Southworth et al. 1999)
Mth RIR1	pBRC	P(-1)G/C1A	n.d.	pH, T	Yes	(Evans et al. 1999)
Ssp DnaB	pBSC	C1A	Q,N,L,I,R,K,P	pH, T	Yes	(Mathys et al. 1999)
Mtu RecA	pDI-CM	4 mutations[5]	n.d.	pH, T	Yes	(Wood et al. 1999)

[1] In model fusions, theses amino acids immediately adjacent to the active junction result in cleavage in vivo or failure to cleave in vitro. [2] Another nucleophile may be substituted for the thiol reagent. pH and T indicate that the cleavage reaction can be activated by a change in pH or temperature, respectively. [3] An IPL-compatible amino-terminal splice junction vector yields a target protein with a carboxy-terminal α-thioester and a carboxy-terminal splice junction vector yields a target protein with an amino-terminal cysteine. [4] pNam is a derivative of TYB1 on a low copy number plasmid.
[5] C1→A, D24→ G, V67→L and D422→G.

2.9 *E.coli* ATCase as a Model for Studying Conformational Changes within Proteins

2.9.1 Structural Organization and Mode of Regulation

Aspartate transcarbamoylase (ATCase) is an enzyme that catalyzes the first committed step in pyrimidine biosynthesis, mainly the condensation of carbamyl phosphate with L-aspartate to produce N-carbamyl-L-aspartate and inorganic phosphate (Figure 2.6). Pyrimidines are building blocks of nucleic acids (DNA and RNA). Consequently, this enzyme is an important target in the design of inhibitory compounds that can act as antineoplastic (Johnson et al. 1978), antiparasitic and antimicrobial agents (Dutta and Foye 1990).

ATCase from *E. coli* is a regulatory enzyme and therefore can control the levels of pyrimidines in the cell. The end product of the pyrimidine biosynthetic pathway, cytidine triphosphate (CTP), can bind to the enzyme and reduce enzyme activity. In contrast, the end product of purine synthesis, adenine triphosphate (ATP), can activate the enzyme (Figure 2.6). ATCase is also regulated at the level of transcription by attenuation (Hervé 1989). In this manner, levels of pyrimidines and purines remain balanced in the cell for nucleic acid synthesis.

ATCase from *E. coli* is a multi-subunit enzyme of 310 kDa. It is composed of six catalytic chains organized as two catalytic trimers (100 kDa each); each trimer is known as a catalytic subunit (CSU). The enzyme also has six regulatory chains organized as three regulatory dimers (35 kDa each), with each dimer denoted as a regulatory subunit (RSU) (Figure 2.7) (Kantrowitz and Lipscomb 1990). The site where the carbamylation reaction is catalyzed is distinct from the site of regulation of activity. Substrates and the antineoplastic bisubstrate analogue, N-phosphonoacetyl-L-asparate (PALA) bind to each chain of the CSU portion of the enzyme, while nucleotides bind to the RSU.

In this project, the RSU is the main region of interest. It is composed of two domains, the allosteric (Al) domain and the zinc (Zn)-binding domain (Figure 2.8). The allosteric domain contains the binding site for the nucleotide triphosphate (NTP) effectors CTP and ATP, and the Zn-binding domain contains a structural Zn atom that is bound.

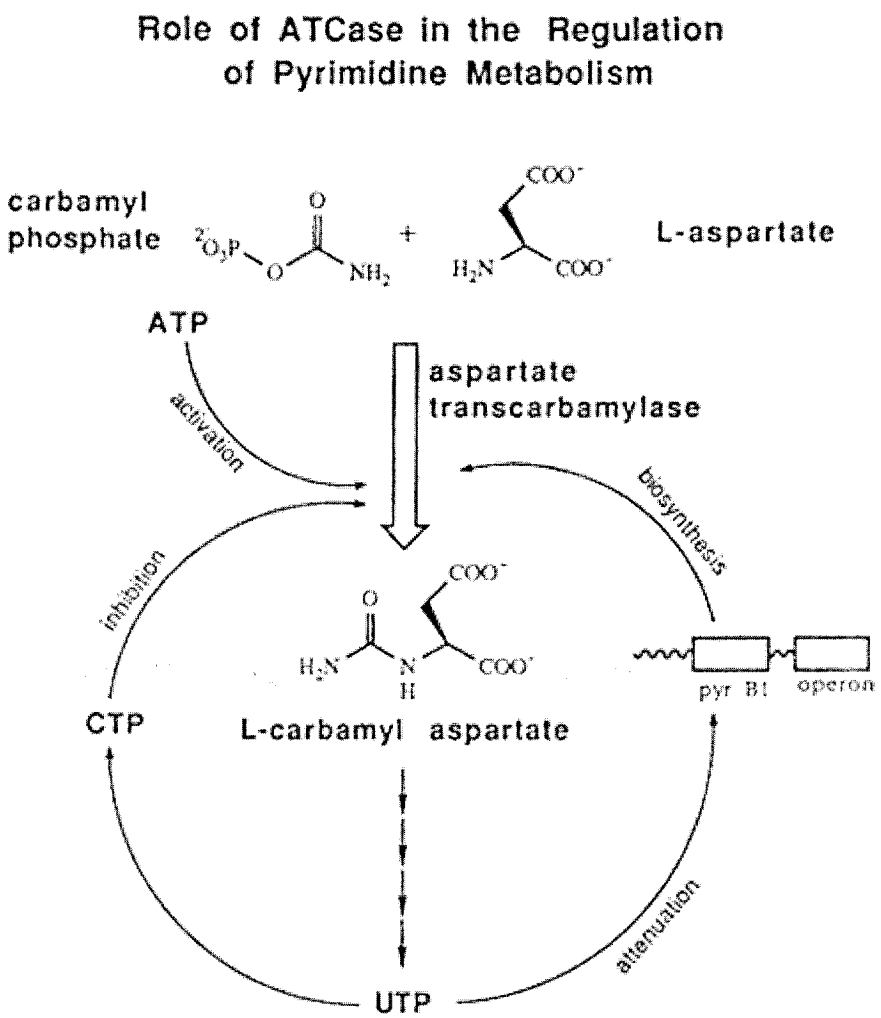

Figure 2.6: Regulation of ATCase in the pyrimidine pathway (Hervé 1989).

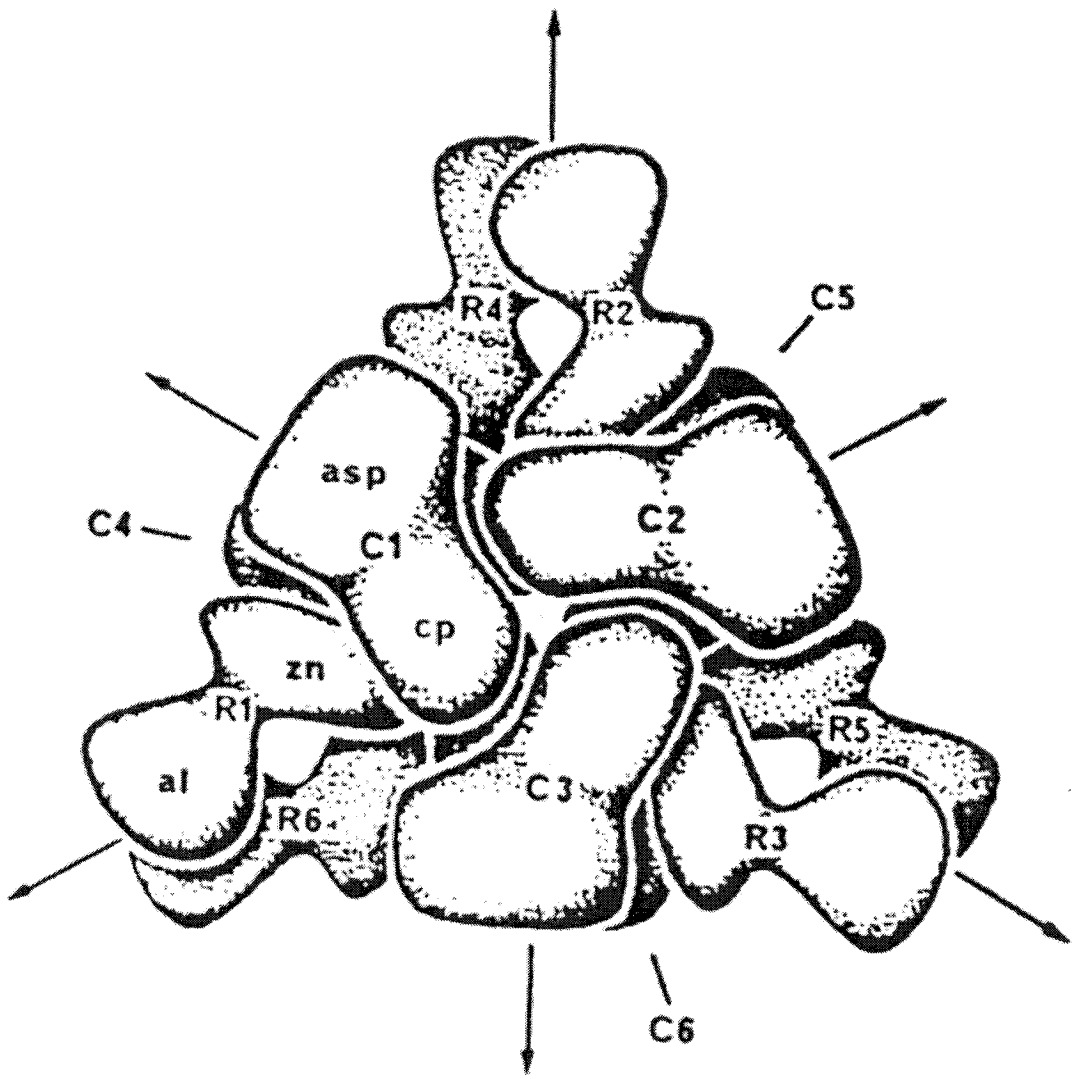

Figure 2.7 The quaternary structure of aspartate transcarbamylase (the view is down the threefold axis). It is composed of six catalytic chains organized as two catalytic trimers, (C1, C2, C3; C4, C5, C6), each trimer is known as a catalytic subunit (CSU). The enzyme also has six regulatory chains organized as three regulatory dimers (R1, R6; R2, R4; R3, R5), with each dimer denoted as a regulatory subunit (RSU). The catalytic chain is composed of the aspartate (Asp) and the carbamyl phosphate (Cp) domains. The regulatory chain is composed of the allosteric (Al) and zinc (Zn)-binding domains (Krause et al. 1985).

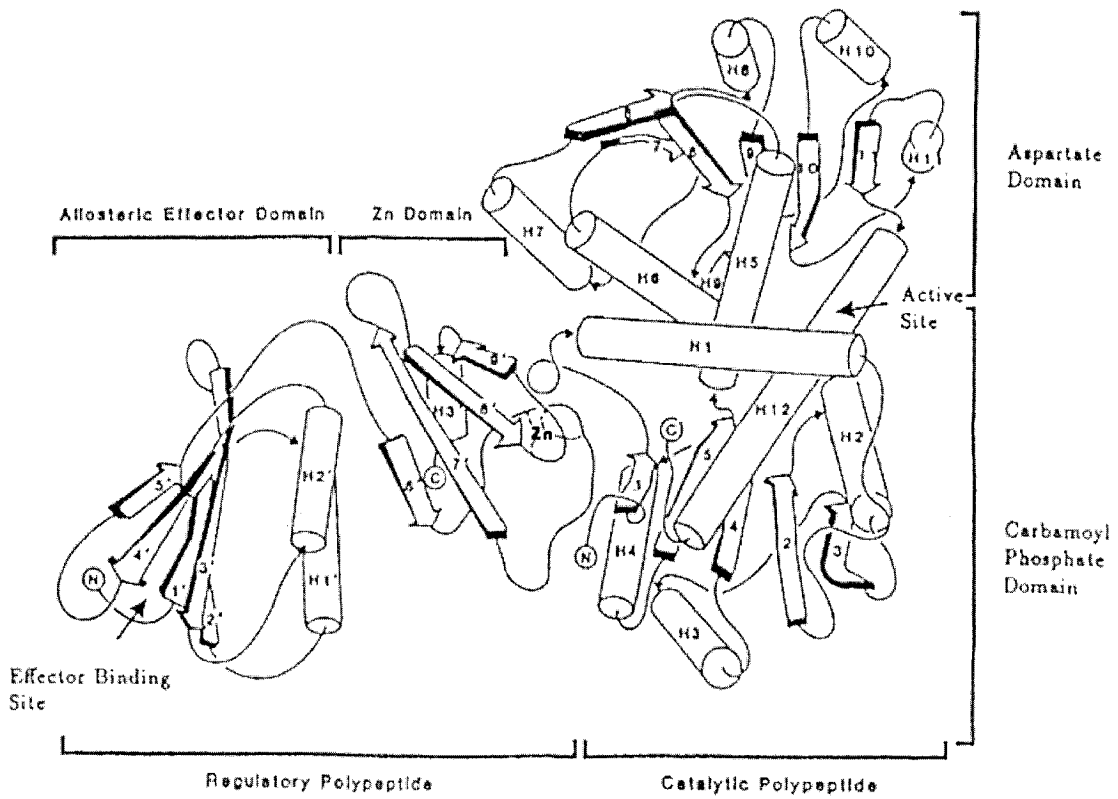

Figure 2.8: Schematic trace of one catalytic and regulatory pair of ATCase (the view is down the threefold axis). The regulatory chain is composed of two domains, the allosteric domain and the Zn-binding domain. The allosteric domain contains the binding site for the nucleotide triphosphate effectors CTP and ATP, and the Zn-binding domain contains a structural Zn atom that is bound tetrahedrally to four cysteine residues. The carbamylation reaction occurs in the catalytic chain which is composed of the aspartate domain and the carbamoyl phosphate domain (Krause et al. 1985).

The two-state model proposed by Monod and coworkers hypothesized that there is a dynamic equilibrium between two (or more) conformational states called T for taut, constrained, or low affinity (activity state) and R for the relaxed, expanded, or high affinity (activity) state (Monod et al. 1965). The binding of ligands to the molecules, at either of the two states would perturb the equilibrium population of the unliganded molecules. CTP shifts the equilibrium in favor of the T state and ATP shifts it in favor of the R state conformation. The conversion of the molecule from T → R state occurs upon the cooperative binding of two substrates, aspartate and carbamoyl phosphate to the catalytic subunit. Structural studies reveal that in the transition between T → R states, the enzyme's catalytic trimers separate along the molecule's 3-fold state by 11^{o} and reorient around the axis, relative to each other by 12^{o}, and the regulatory dimers rotate clockwise by 15^{o} around their two-fold axes and separate by 4^{o} along the 3-fold axis (LiCata and Allewell 1997; Sakash et al. 2000).

The binding of N-phosphonacetyl-L-aspartate (PALA), a bisubstrate analogue, to the catalytic trimers mimics the binding of aspartate and carbamoyl phosphate and induces conformational changes to occur. This binding brings the two domains of the CSU closer together so that the two substrates bond and undergo a condensation reaction to form N-carbamyl-L-aspartate and inorganic phosphate.

The allosteric behavior is not observed when the CSU is dissociated from the RSU; hence, the interaction of CSU and RSU are essential for the binding of a substrate to one catalytic subunit triggering ATCase to go from T → R quaternary shift. Moreover, the binding of the substrates to one of the CSU causes substrate-binding affinity to increase, leading to the increase in catalytic activity of the other 5 CSU, hence explaining the enzyme's cooperative substrate binding occur (Stevens and Lipscomb 1990; Stevens et al. 1991; Lipscomb 1994).

There are several crystal structures available for the holoenzyme (Honzatko et al. 1982), also, bound with substrate analogue PALA (Lipscomb 1994; Hoang et al. 1999; Jin et al. 1999) and nucleotides (Stevens et al. 1990; Kosman et al. 1993). Crystal structures are also available for the CSU, unliganded and liganded form (Williams et al. 1998; Beernink et al. 1999; Stieglitz et al. 2004). However, there is no structure for the isolated RSU. It would be important to have structural information for both the isolated

CSU and RSU components in order to further dissect the role of the conformational changes that occur within the protein upon binding ligands. These studies would ultimately help us understand how the enzyme regulates nucleotide metabolism.

CHAPTER 3

VT-FTIR and 2D Correlation Analysis of ^{13}C-Labeled Regulatory Subunit of Aspartate Transcarbamylase

3.1 Introduction

FTIR spectroscopy in conjunction with 2D correlation analysis is employed to monitor changes in the sequence of heat-induced unfolding that occurs upon interaction of RSU of ATCase with its allosteric effector CTP. The holoenzyme ATCase was expressed and purified from *E.coli* strain HS1061. The RSU was then isolated from the CSU by treating the holoenzyme with the mercury containing reagent neohydrin, followed by separation of the two subunit types by anion exchange chromatography (Yang et al. 1978). Since some of the IR absorption bands of CTP occur near the absorption of the amide I' bands of RSU, it was necessary to displace the amide I' absorption bands by isotope-edited techniques. Thus by uniformly labeling all the ^{12}C with ^{13}C in RSU, the amide I' absorption is shifted by ~ 45 cm^{-1}. This allows a clear differentiation between the IR bands of CTP and the amide I' band of the protein. It is important to note that the amide band (1600-1700 cm^{-1}), is referred to amide I' when the spectra of the proteins are recorded in D_2O. This band is frequently employed to elucidate secondary structure of proteins. In this chapter, the protocol to uniformly label holoenzyme is described, as well as the isolation of the ^{13}C-labeled RSU. 2D-FTIR spectroscopy is employed to ascertain if the unfolding pathway is altered upon isotope-editing of RSU. The unfolding pathway of ^{13}C-labeled RSU in the presence of CTP is subsequently elucidated.

3.2 Materials and Methods

3.2.1 Materials

ATCase was prepared from *E. coli* HS1061, a generous gift from H.K. Schachman, University of California, Berkeley. The HS1061 strain contains the multicopy plasmid pPYRB3 (Navre and Schachman 1983) and carries the intact pyrB-pyrI operon encoding the catalytic and regulatory subunit of ATCase (Pauza et al. 1982).

D-Glucose (U-$^{13}C_6$, 99%) was obtained from Cambridge Isotope Laboratories. Neohydrin ([1-(chloromercuri)-2-methloxypropyl] urea) was synthesized by D. Christendat according to the method of (Rowland et al. 1950). Q-Sepharose (Fast Flow) anion exchange resin was purchased from Pharmacia Biotech. NAP^{TM} buffer exchange columns were purchased from Amersham Pharmacia. D_2O was obtained from Aldrich. All other chemicals were of the highest grade available and were purchased from Bio-Rad or Amersham.

3.2.2 Purification of ^{13}C-Labeled Aspartate Transcarbamylase Holoenzyme

An overnight culture was made by inoculating a single colony of *E.coli* HS1061 in 2.5 ml of Luria broth (LB), supplemented with ampicillin (100 μg /ml final concentration) at 37°C with agitation at 225 rpm. The 2.5 ml culture was then transferred into minimal media containing salts with a total volume of 250 ml. The salt solution consists of 2.1g Na_2HPO_4, 1.3 g KH_2PO_4, 0.5 g NH_4Cl, and 0.001 g Ca $(NO_3)_2$ dissolved in 243 ml distilled water and sterilized by autoclaving. The minimal media was prepared by mixing the following filter sterilized solutions: 0.10 ml 1M $MgSO_4.7H_2O$, 0.04 ml 10mM $ZnSO_4$. $7H_2O$, 0.15 ml 20 mM $Fe(NH_4)_2(SO_4)$. $7H_2O$, 4.0 ml ^{13}C-labeled glucose (25%), 0.50 ml 0.2 % uracil, 0.25 ml 0.2% histidine (not- ^{13}C enriched), 0.25 ml 1.0% vitamin B1 and 0.250 ml of 100 mg/ml ampicillin. The percent concentrations are expressed as w/v.

The cell culture was incubated at 37 °C for 24 hrs with continuous shaking at 250 rpm. Subsequently, the cells were harvested by centrifugation at 9000 rpm for 20 min at 4 °C. The resulting pellet was then resuspended in 20 ml of ice cold lysis buffer consisting of 50 mM Tris-HCl (pH 8.7), 0.5 mM EDTA and 50 mM NaCl. The total cell extract was obtained by lysing the cells by a French Press (2 passages) and the cellular debris was removed by centrifugation at 38 000 x g for 45 min at 4 °C. The clarified cell extract (supernatant) containing the cellular proteins was dialyzed against 50 mM Tris-HCl (pH 8.7), 0.5 mM EDTA overnight at 4°C. The protein solution was loaded onto a Q-Sepharose anion exchange column (bed volume of 18 ml) that was previously equilibrated against the same buffer used for dialyzing the protein. The column was then washed with 200 ml of the equilibration buffer and the protein was eluted with an 80 ml

linear salt gradient of 0-0.8 M KCl in the same buffer. The fraction collector was set at collecting 60 drops per tube (~ 2 ml) at a flow rate of 3-4 ml/min. The fractions containing the holoenzyme were identified by running native polyacrylamide gel electrophoresis (PAGE) and the protein fractions were then pooled and precipitated overnight by dialyzing against a 1L solution of 3.6 M ammonium sulfate.

3.2.3 Isolation of CSU and RSU from ^{13}C-Labeled Holoenzyme

The ammonium sulfate precipitated fractions obtained above (~ 31.53 mg of protein) were spun down at 10,000 x g for 10 min at 4°C to obtain a pellet. The pellet was resuspended with 2 ml of 10 mM Tris HCl, 0.1 KCl (pH 8.7) and dialyzed overnight against 1L of the same buffer at 4°C. The concentration of the holoenzyme after dialysis was calculated by absorbance measurements at 280 nm in a 1 ml cuvette using the extinction coefficient of 0.59 cm^2/mg (Gerhart and Holoubek 1967). The mercurial reagent neohydrin (20 mg neohydrin per 100 mg holoenzyme) was prepared in 100 mM Tris-HCl (pH 8.7) at room temperature. The neohydrin solution was then added to the holoenzyme solution drop wise with continuous stirring. The reaction proceeded for 30 min at room temperature. The resulting solution was loaded onto the Q-Sepharose Fast Flow anion exchange column (bed volume of 18 mL) and the ^{13}C-RSU was eluted by applying 3 column volumes of 10 mM Tris-HCl, 0.1 KCl pH 8.7 in 4°C. Each fraction had 60 drops per tube (~2 ml each). The ^{13}C –labeled CSU was eluted by washing the column with 10 mM Tris-HCl, 0.5 M KCl (pH 8.7). Native PAGE was used to identify which protein fractions were enriched with ^{13}C-labeled RSU and CSU. The RSU fractions were pooled and were supplemented with 10 mM β-mercaptoethanol and 1 mM Zn acetate, and then concentrated with a Centriprep apparatus (Millipore Corporation, Bedford, MA), and stored at 4°C until further use. The CSU fractions were pooled and supplemented with 5 mM β-mαercaptoethanol and dialyzed against 1.5 L ammonium to precipitate overnight at 4 °C. The precipitate was also stored at 4 °C until further use.

3.2.4 Purification of ^{12}C Unlabeled ATCase

ATCase was purified by standard methods as described by (Turnbull et al. 1992).

3.2.5 Determination of Protein Concentration

Protein concentration was determined using the BioRad Protein Assay with bovine serum albumin as the calibration standard. The concentration of RSU, CSU and holoenzyme was also calculated by absorbance measurements at 280 nm in a 1 ml cuvette using the extinction coefficients 0.32 cm^2/mg, 0.72 cm^2/mg, and 0.59 cm^2/mg, respectively (Gerhart and Holoubek 1967).

3.2.6 Microwave Silver Staining Method for Protein Visualization

After PAGE, the gel was washed with 50 ml of 50% methanol and was heated in a microwave for one minute at maximum power. The gel was then shaken for 1 min at room temperature. The methanol solution was discarded. The procedure was repeated another time and the methanol solution was replaced with 50 ml of silver stain solution (2 ml of 20% silver nitrate solution added dropwise to 10.5 ml 0.36 % NaOH, 0.9 ml 30 % NH_4OH, diluted to 50 ml with dH_2O). The gel was shaken for 2-3 min at room temperature. Then the solution was discarded and the gel was washed with dH_2O four times. The development solution (1.25 ml of 1% citric acid, 0.125 ml 37.38 % formaldehyde, diluted to 250 ml in dH_2O) was then added, and heated for 15-20 sec in the microwave and shaken for ~ three min, or until the bands reached the desired staining intensity. The development reaction was stopped by discarding the solution and replacing it with dH_2O. Finally, the reaction was quenched with 10% methanol (personal communication by Dr. Judith Kornblatt, Concordia University).

3.2.7 VT-FTIR Analysis of ^{13}C-Labeled RSU with and without CTP

RSU samples at a concentration of 0.9 mg/ml were freeze-dried overnight using Labconco Freeze dry system Lyph-Lock4.5, in 1.0 ml aliquots. The samples were resuspended in 8 µl of D_2O for use in VT-FTIR analysis. The samples were used immediately after reconstituting in D_2O. For ligand binding studies, 8 µl of the CTP solution (68.2 µM in a 1M Tris buffer in D_2O (pH 8.7)) was added to 0.9 mg of freeze dried RSU and used for VT-FTIR studies.

The FTIR spectra were recorded using a Nicolet Magna-IR 550 spectrophotometer series II, supplied with a deuterated triglycine sulfate (DTGS)

detector. The sample compartment was continuously purged with dry air. Sample volumes of 8 µl were placed in a temperature-controlled IR cell between two CaF_2 windows separated by a 50 µM Teflon™ spacer. FTIR spectra were recorded at various temperatures between 25 and 80 °C in 2.5 °C increments, with a 10 min equilibration time. Data was collected by the co-addition of 512 scans from 4000 cm^{-1} to 1000 cm^{-1} at a resolution of 4 cm^{-1}. Resolution enhancement was performed using Fourier self-deconvolution (FSD) with a bandwidth of 18.7 cm^{-1} and a resolution enhancement factor (k) of 2.7.

3.2.8 VT-Far Ultraviolet-Circular Dichroism (UV-CD) of ^{12}C RSU

VT-CD spectra were recorded on a J710 spectropolarimeter (Jasco, Japan). A 200 µl protein solution (0.05 mg/ml) was placed in a 0.05 cm pathlength temperature-controlled water-jacketed quartz cell. The 5 scans were co-added and the data was acquired between 205 and 260 nm at a scan rate of 50 nm/min. A step resolution of 0.2 nm was acquired, with a response time of 0.5 sec. The bandwidth of 1.0 nm and a sensitivity of 50 mdeg were chosen. Variable temperature scans in the far UV-CD were recorded from 25 °C to 70 °C in 2.5 °C increments with a 10 min equilibration time. The data were collected using the Jasco software.

3.2.9 2D Correlation Analysis of ^{13}C-Labeled RSU with and without CTP

The amide I' absorption bands (in the region between 1700 and 1600 cm^{-1}) obtained after FSD of the VT-FTIR spectra acquired every 2.5 °C between 35 - 55 °C for ^{13}C-labeled RSU and 35-65 °C for ^{13}C -labeled RSU-CTP were employed to generate synchronous and asynchronous correlation maps using the KG2D software written by Y. Wang (Wang et al. 1998).

3.3 Results and Discussion

3.3.1 Purification of ^{13}C-Labeled and Unlabeled Aspartate Transcarbamylase

ATCase can be isolated in large amounts after expression in the E. *coli* strain HS1061, which houses a multi-copy plasmid encoding both the catalytic and regulatory

subunit of ATCase. ^{13}C-labeled ATCase is obtained by growing E. *coli* HS1061 in 250 ml of minimal media supplemented with ^{13}C-labeled glucose. The holoenzyme was recovered after purification by anion-exchange chromatography following a procedure developed by Turnbull and coworkers (Turnbull et al. 1992). The protein elution profile of the clarified cell extract from the anion-exchange column is shown in Figure 3.1. The absorbance reading at 280 nm for various fractions revealed one major broad peak which represents the holoenzyme. The proteins eluted from the linear salt gradient were analyzed by native PAGE (Figure 3.2). The bands from this gel correspond to the holoenzyme, which was eluted with a salt gradient between 0.4-0.7 M KCl (Figure 3.1, fractions 57-67). The integrity of ATCase in fractions 57-67 were confirmed by an activity assay (Turnbull et al. 1992). None of the holoenzyme remained bound to the column as judged by the native PAGE analysis (Figure 3.2, lanes 11-15) of the eluate from the 1.5M KCl wash (fractions 76-88). Fractions 57-67 containing the holoenzyme in solution (20 ml, ~ 32 mg) were pooled together and precipitated by dialyzing the protein against a saturated solution of ammonium sulfate. The protein in this salt form is stable indefinitely when stored at 4°C.

The RSU was isolated from CSU by treating the holoenzyme with mercurial reagent neohydrin. Figure 3.3 shows the elusion profile of neohydrin-treated ^{13}C-labeled holoenzyme (27 mg) from an anion exchange column. The absorbance readings at 280 nm were recorded for each fraction throughout the stepwise addition of a gradient of 0.1 KCl and 0.5 KCl in 10 mM Tris-HCl (pH 8.7). A native PAGE (Figures 3.4 and 3.5) were used to determine which fractions contained the RSU (Figure 3.4) and CSU (Figure 3.5).

The regulatory subunit was eluted from the anion exchange column at a salt concentration of 0.1 M, and is shown as the first small peak in the elution profile (Figure 3.3, fractions 6-15). Selected fractions between 7 and 19 were loaded on to an electrophoresis gel under native conditions in order to identify the presence of RSU (Figure 3.4). Fractions 6-15 (18 ml) were pooled and supplemented with β-mercaptoethanol to deactivate residual neohydrin, while zinc acetate was added to stabilize the RSU. The protein was then concentrated down to 2.6 ml and the RSU solution (~ 0.9 mg/ ml) was freeze dried over night in 1 ml aliquots and stored at 4°C.

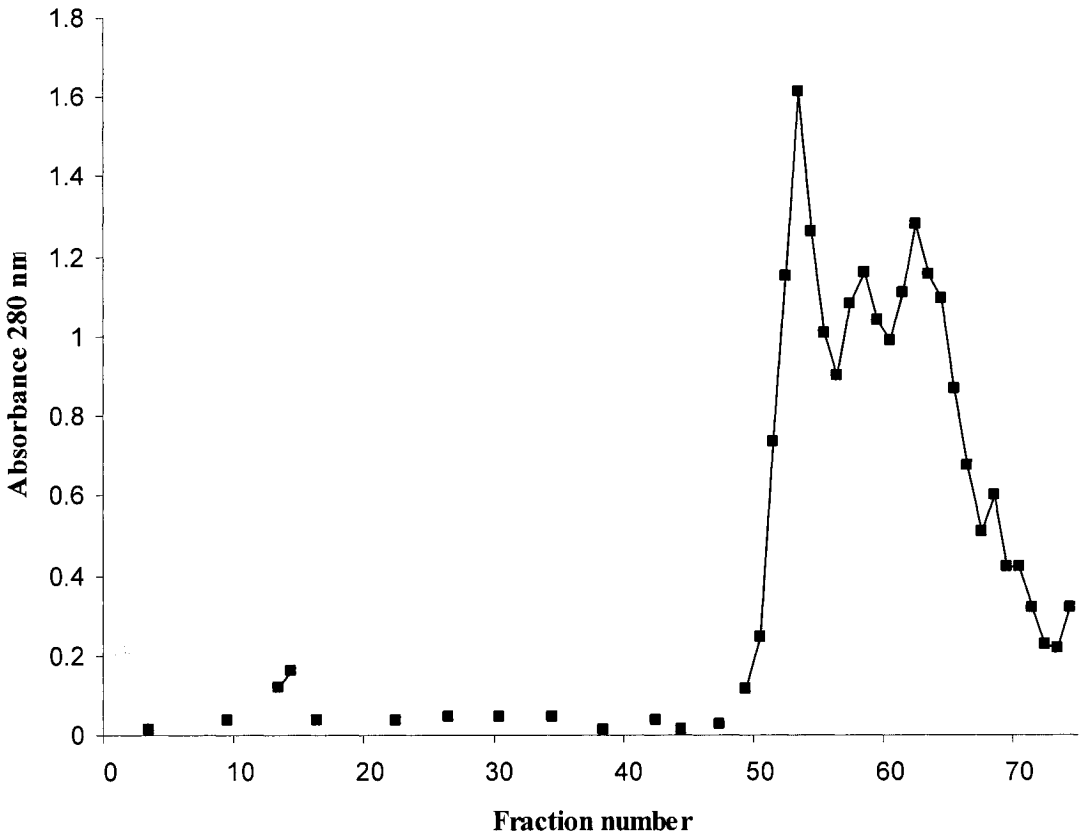

Figure 3.1: Protein elution profile from Q-Sepharose Fast Flow column. Clarified cell lysate containing ^{13}C labeled ATCase holoenzyme was loaded onto an anion exchange column (bed volume 18 ml). Fractions of 2 ml were collected at a flow rate of 3-4 ml/min and A_{280} readings were taken throughout the elution procedure. Fractions 1-10 represents the flow-through during sample application, while fractions 11-35 were collected as the column was washed with 50 ml of equilibration buffer (50 mM Tris HCl (pH 8.7), 0.5 mM EDTA). A linear salt gradient of 0-0.8 M KCl was applied between fractions 36-75 to elute the holoenzyme, followed by a high salt wash (1.5 M KCl) from fractions 76-88.

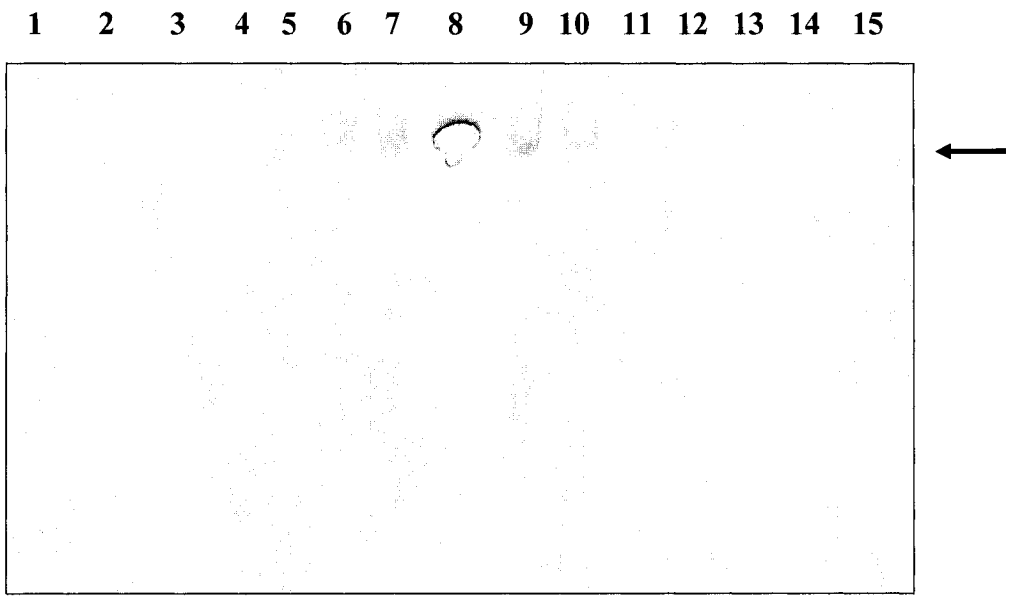

Figure 3.2: Native PAGE (7.5 % acrylamide) of selected fractions from Q-Sepharose Fast Flow chromatography shown in Figure 3.1. 10 µl of aliquots were loaded onto each well and proteins were visualized by Coomassie Blue staining. Lane 1, marker (not shown); lanes 2-4 represents the column wash (fractions 52, 54, 56); lanes 5-7,9-12 represents proteins eluted from the linear salt gradient (fractions 58, 60, 62, 64, 66, 69, 72); lanes 13-15 indicate protein eluted from the high salt wash (fractions 78, 81, 88).

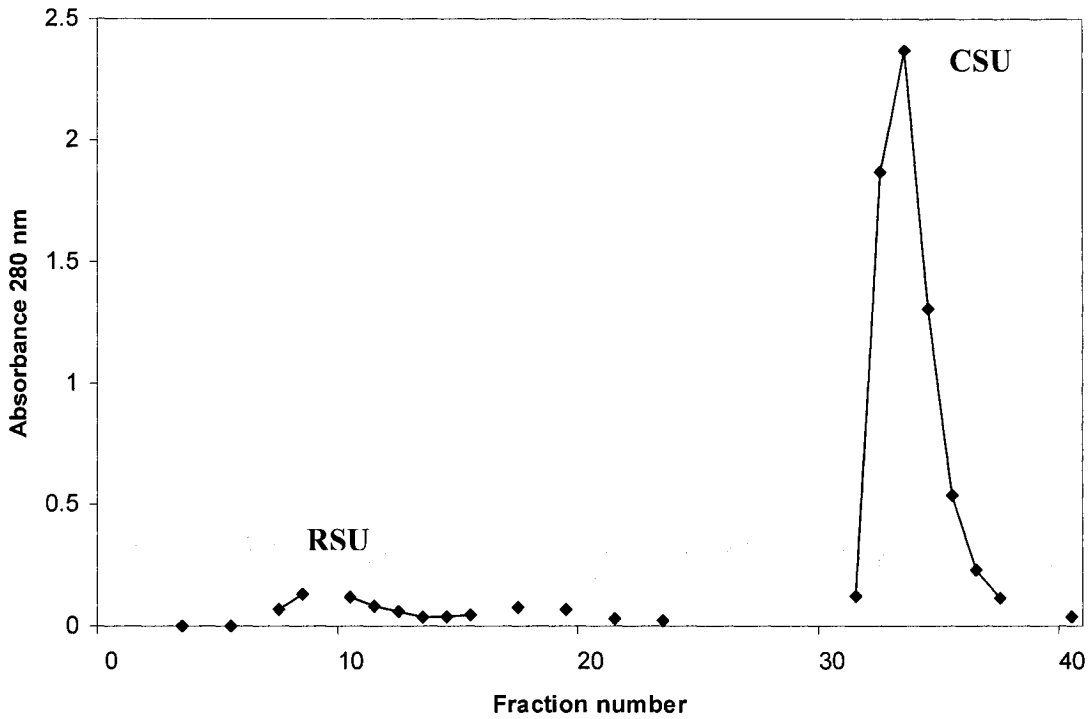

Figure 3.3: Protein elution profile of neohydrin-treated ^{13}C-labeled holoenzyme from Q-Sepharose Fast Flow column. ^{13}C-labeled holoenzyme solution (27 mg) was incubated with neohydrin then loaded onto an anion exchange column (bed volume 18 ml). The column was then washed with 60 ml each of a two-step salt gradient in 10 mM Tris-HCl (pH 8.7). Fractions of 2 ml were collected at a flow rate of 3-4 ml/min. Fractions 1-30 were collected during the low salt (0.1 M KCl) wash, while fractions 31-40 were collected during the high salt (0.5 M KCl) wash. A_{280} readings were taken throughout the elution process.

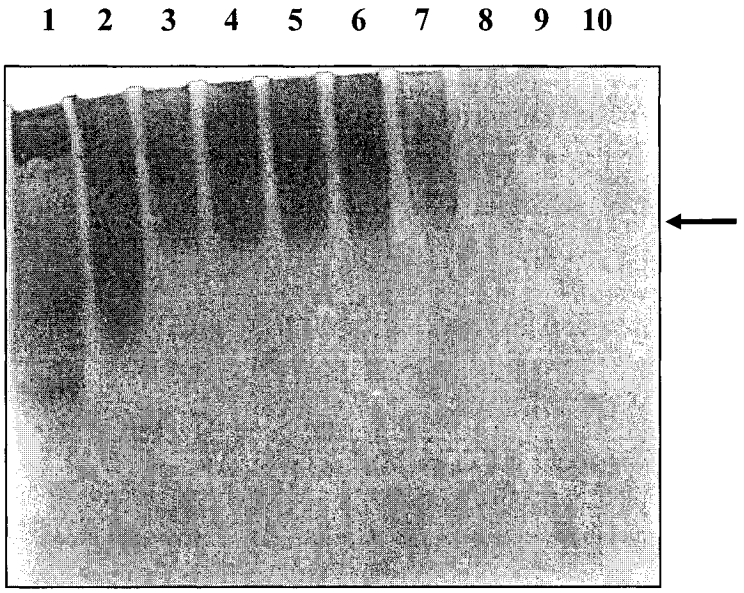

Figure 3.4: Native PAGE (7.5 % acrylamide) of selected fractions from Q-Sepharose Fast Flow chromatography (first peak region) shown in Figure 3.3. 18 µl aliquots were loaded into wells and proteins were visualized by silver staining. Lanes 1 and 2: ATCase holoenzyme and ^{12}C RSU standards, respectively; lanes 3-10: proteins eluted during the low salt wash (fractions 7, 8, 10, 11, 12, 15, 17, 19). The arrow indicates the isolated C^{13} RSU.

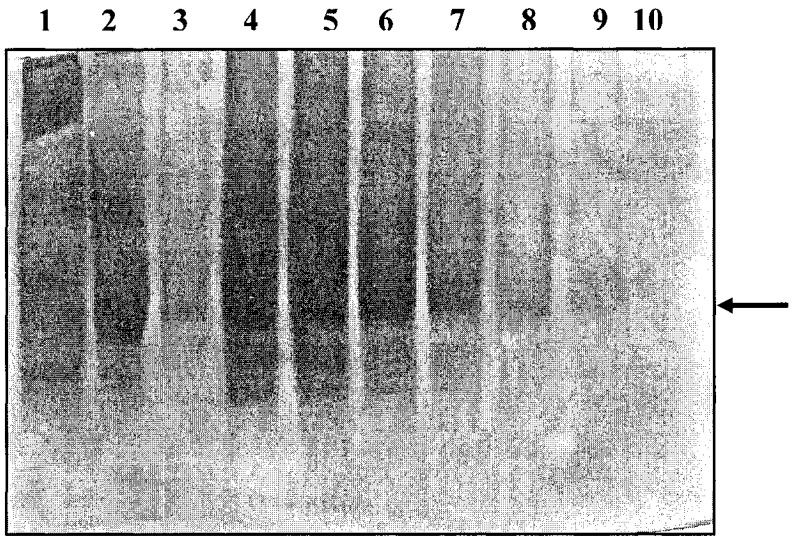

Figure 3.5: Native PAGE (7.5 % acrylamide) of selected fractions from Q-Sepharose Fast Flow chromatography (second peak region) shown in Figure 3.3. 18 µl aliquots were loaded into wells and proteins were visualized by silver staining. Lanes 1 and 2: ATCase holoenzyme and ^{12}C CSU standards, respectively; lanes 2-9: ^{13}C-labeled CSU eluted during the high salt wash (fractions 31, 32, 33, 34, 35, 35, 37, 40). The arrow indicates the isolated ^{13}C RSU.

The CSU was eluted from the anion exchange column at a salt concentration of 0.5 M, and is shown as the second peak in the elution profile (Figure 3.3). Selected fractions between 31 and 40 were analyzed by native PAGE to identify the presence of CSU (Figure 3.5). Fractions 31-38 (15 ml) were pooled and supplemented with β-mercaptoethanol, followed by an overnight dialysis of the protein in ammonium sulphate. The CSU sample (16.7 mg) was then stored at 4°C until further use. Table 3.1 summarizes the overall yield of protein after selected purification steps.

In addition, unlabeled ^{12}C RSU was also prepared using a similar procedure for the labeled protein (Turnbull *et al.*, 1992). Native PAGE of the pure protein is shown in Figure 3.6.

Table 3.1: Purification table of ^{13}C-labeled aspartate transcarbamylase.

Purification Step	**Total Protein (mg)**	**% Recovery**
Anion-Exchange Column	31.5	100
Ammonium Sulphate Precipitate	27	85.6
Anion-Exchange Column after Neohydrin Treatment:		
Regulatory Subunit	**2.4**	7.6
Catalytic Subunit	16.7	52.9

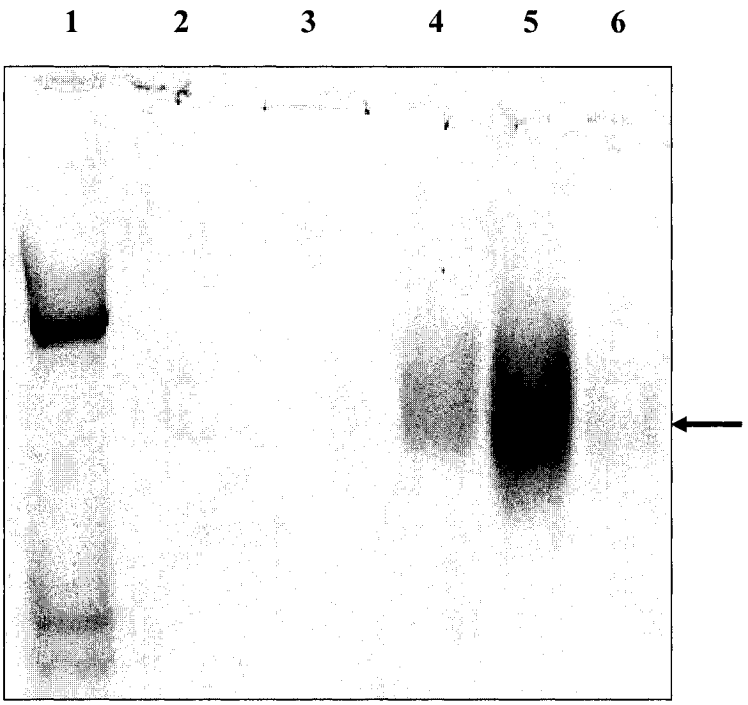

Figure 3.6: Native PAGE (7.5 % acrylamide) of selected fractions from Q-Sepharose Fast Flow chromatography of ^{12}C RSU (unlabeled protein). 18 µl aliquots were loaded into wells and proteins were visualized by Coomassie Blue staining. Lanes 1: pure unlabeled holoenzyme, lanes 4-6: ^{12}C RSU protein used for FTIR analysis. The arrow indicates the isolated ^{12}C RSU.

3.3.2 VT-FTIR Analysis of ^{12}C RSU

The changes in the secondary structure of unlabeled RSU were monitored by VT-FTIR spectroscopy. Figure 3.7 shows the overlaid deconvolved VT-FTIR spectra in the amide I' (1700-1600 cm^{-1}) region as a function of increasing temperature from 25 to 80°C. The bands in the amide I' region arise from the carbonyl stretching vibration of the peptide linkages. At room temperature, the strong band at 1627 cm^{-1} is assigned to the β-sheet structure (Ismoyo et al. 2000). The band at 1651 cm^{-1} is assigned to α-helix while the small band at 1677 cm^{-1} is assigned to β-turns and/or antiparallel β-sheet structure. Although there is no crystal structure of the isolated regulatory subunit available, the X-ray structure of the ATCase holoenzyme show that the RSU constitutes mainly antiparallel β-sheets (~33%), with 17% α-helix and 5.2% turns (Honzatko et al. 1982) Therefore, the FTIR data is consistent with the crystal structure of RSU in ATCase. Note that only three peaks are analyzed: β-sheets at 1627 cm^{-1}, α -helix at 1651 cm^{-1}, and the aggregation band at 1618 cm^{-1}, since these peaks are more observable (Ismoyo et al. 2000).

A 3 cm^{-1} shift to lower frequency is observed in the 1627 cm^{-1} band (to 1624 cm^{-1}) when RSU is heated from 25°C to 29°C. This shift is attributed to an increase in hydrogen-deuterium (H-D) exchange resulting from a partial unfolding of RSU, allowing the deuterium to exchange with protons located in the more shielded and less polar environment of the molecule. Above 29°C no additional peak shift is observed, however, the intensity of the RSU bands drop significantly with increasing temperature and new bands are attributed to aggregation of the protein (Tm ~ 47°C). Since the α-helices tends to be solvent exposed and undergo H-D exchange more rapidly, H-D exchange with β-sheets and high frequency β-sheets are observed and not α-helices.

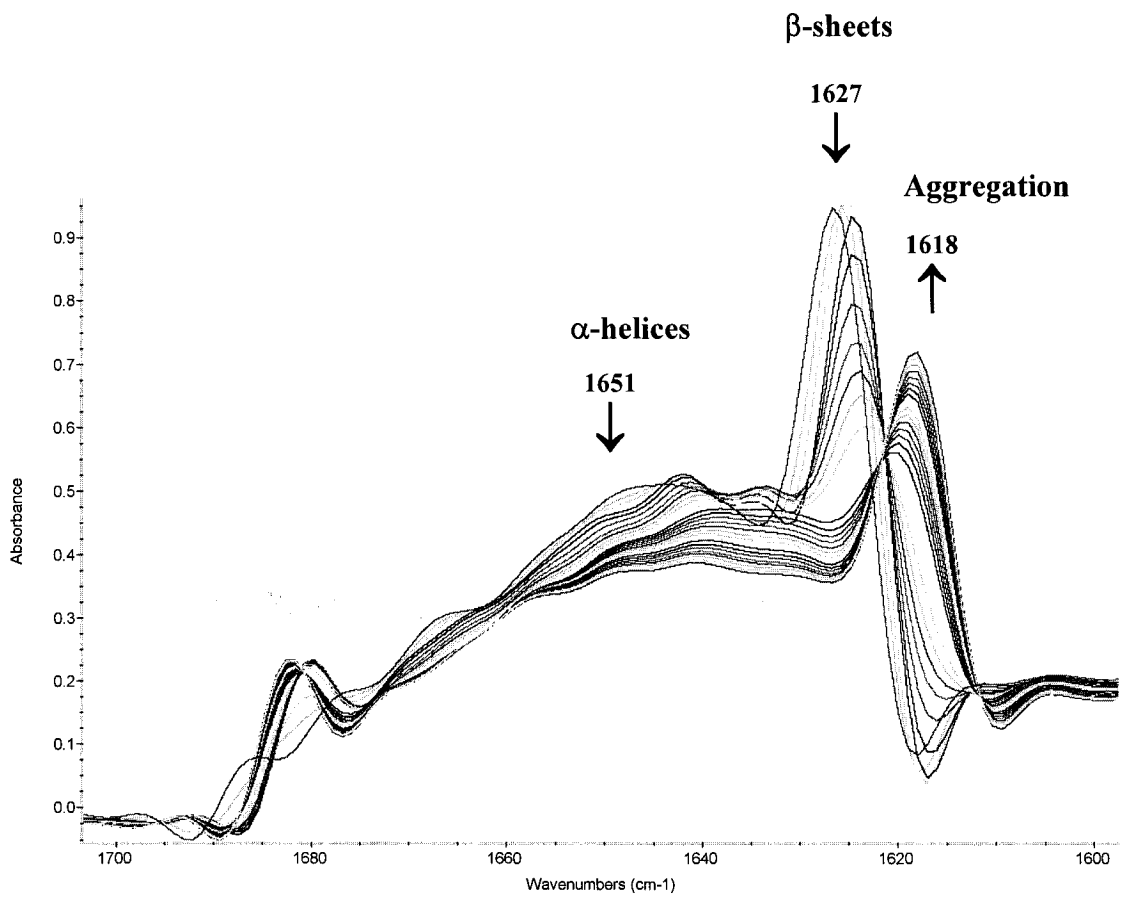

Figure 3.7: Overlaid deconvolved VT-FTIR spectra of ^{12}C RSU in the amide I' region as a function of increasing temperature from 25°C to 80°C. The arrows represent the direction of changes of intensity as a function of increasing temperature.

3.3.3 VT-Far UV-CD Analysis of ^{12}C RSU

VT-Far UV-CD was performed to corraborate the findings obtained from the VT-FTIR studies of RSU. One local minimum was observed at 217 nm, which is typical for proteins with a significant amount of β-sheet structures shown (data not shown). Figure 3.8 shows the disappearance of the secondary structure, mainly β-sheets, monitored at 217 nm as a function of increasing temperature. The CD bands remains relatively constant at temperatures between 25 and 47°C, and start to decrease at 47°C, which indicates a change in the secondary structure. It is interesting to note that the CD instrument cannot distinguish between intramolecular β-sheets and intermolecular β-sheets (aggregation). In the case of the RSU, where it contains primarily β-sheet structures, the increase in the negative ellipticity is most likely due to the two forms of β-sheet structures in the temperature range of 47-70°C. Comparing the results obtained from both the VT-FTIR and VT-far UV-CD reveals that the onset of extensive denaturation occurs above 47°C.

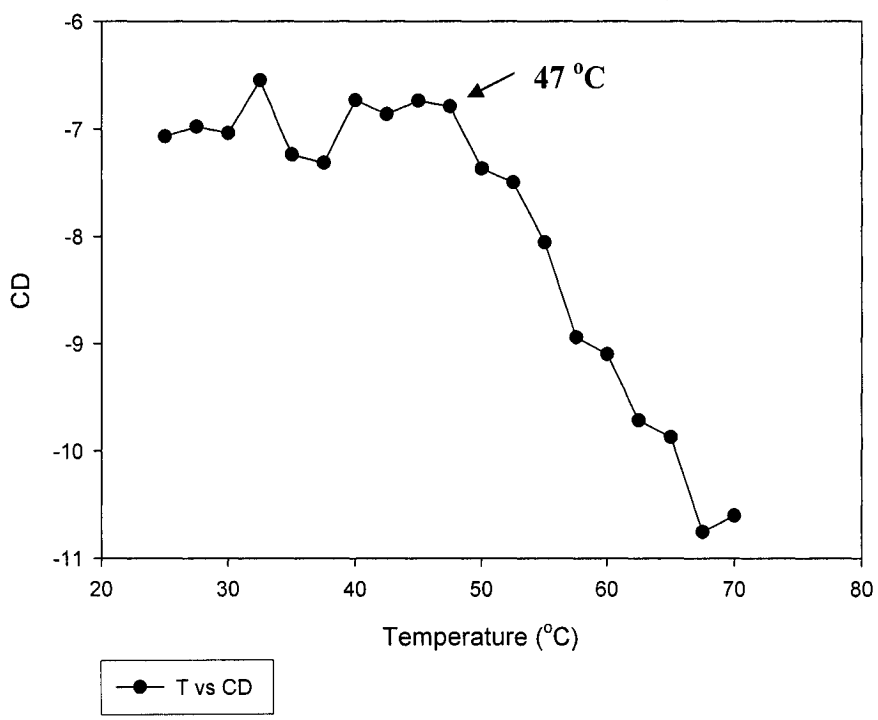

Figure 3.8: VT-far UV-CD of intact RSU monitored at 217 nm as a function of increasing temperature from 25°C to 70°C.

3.3.4 VT-FTIR Analysis of Ligand CTP

The VT-FTIR spectra of CTP in D_2O were recorded as a function of increasing temperatures between 25 and 80°C (Figure 3.9). The nucleotide CTP has a strong band (at 1656 cm^{-1}) in the amide region; attributed to the carbonyl stretching vibrations in the cytosine ring of CTP (Figure 3.9). A 2 cm^{-1} shift to lower frequency is observed in the 1656 cm^{-1} band (to 1654 cm^{-1}) when CTP is heated from 25°C to 29°C. Although this shift is attributed to an increase in hydrogen-deuterium (H-D) exchange, allowing the deuterium to exchange with protons located in the more shielded and less polar environment of the molecule, CTP does not unfold.

3.3.5 VT-FTIR Analysis of the RSU-CTP Complex

The effect of binding CTP to the regulatory subunit of ATCase was investigated by VT-FTIR spectroscopy. Previous studies using continuous flow-dialysis have shown that the binding of CTP to the holoenzyme results in a Scatchard plot, indicating three high-affinity and three low affinity binding sites available for the nucleotide (Gray et al. 1973). The dissociation constants for the interaction of RSU and CTP at the high and low affinity sites are 20 μM and 420 μM, respectively. In this study, it is assumed that the RSU dimer has one site that has a K_d value of 22 μM for CTP. Accordingly, a quadratic equation was used to obtain the percentage of CTP bound to the RSU dimer: K_d = ([RSU]*[CTP])/ [RSU-CTP], where K_d = 22 μM, [CTP] = 68.2 μM and [RSU] = 6.62 μM. This yields 99% of the RSU bound to CTP. CTP is not a tight binding ligand, therefore significant amounts (10 times excess) of ligand is needed to bind to the enzyme for conformational changes to occur. The objective of this study is to assess the effect of CTP binding on the structure and structural stability of RSU in the RSU-CTP complex.

Figure 3.10 shows the VT-FTIR difference spectra of RSU complexed with CTP in the amide I' region as a function of increasing temperature between 25°C and 80°C. These spectra were obtained by subtracting the spectrum CTP recorded as a function of increasing temperature from the spectrum of CTP-RSU recorded at the same temperature. At 25°C, RSU in the CTP-RSU complex exhibits a predominant β-sheet structure (1627 cm^{-1}), with α-helix (1651 cm^{-1}) and β-turns/β-sheet (1677 cm^{-1}).

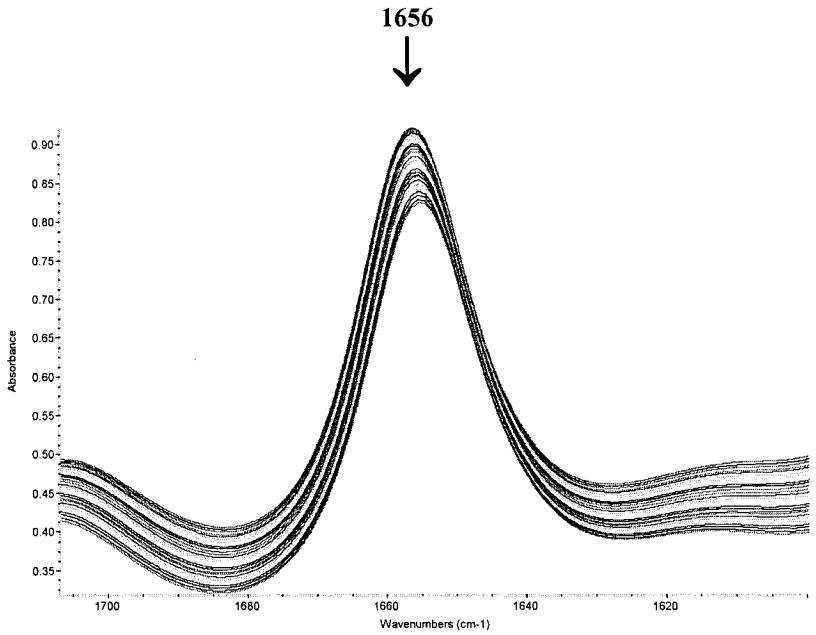

Figure 3.9: Overlaid non-deconvolved VT-FTIR spectra of CTP in D_2O in the amide I' region as a function of increasing temperature from 25°C to 80°C.

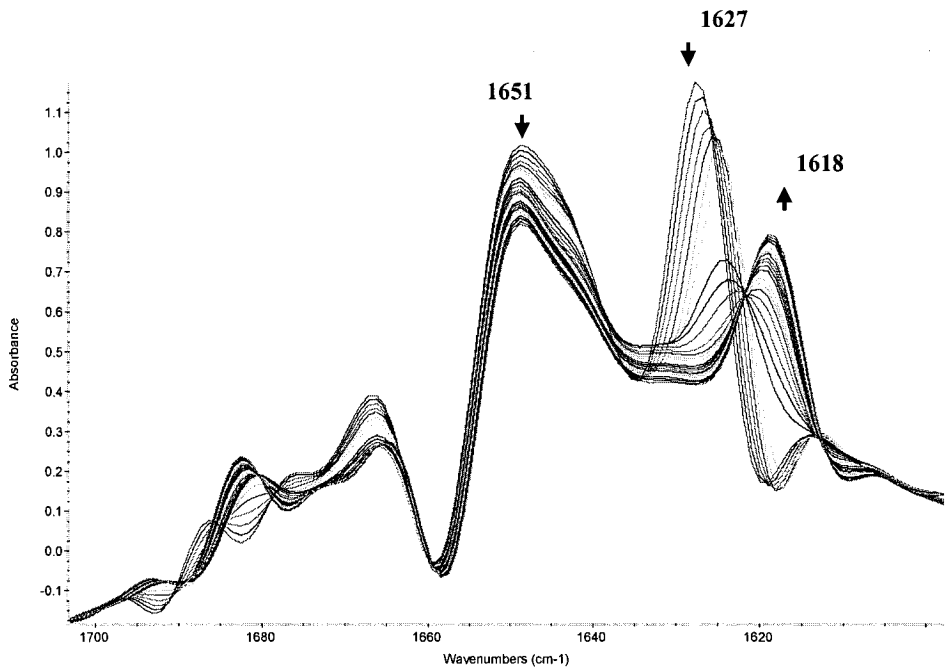

Figure 3.10: Overlaid deconvolved difference VT-FTIR spectra of RSU complexed with CTP in the amide I' region as a function of increasing temperature from 25°C to 80°C. The directions of the arrows indicate the change in intensity of the main secondary structures of the protein with increasing temperature.

This structure is similar to that of RSU in the absence of CTP (Figure 3.7) with the notable exception of the intensity of α -helix peak (1651 cm^{-1}) which is doubled upon binding of CTP to RSU. The increase in the intensity in the α-helix region may be attributed to the underlying residual absorption of CTP which is not completely subtracted. Thus, the absorption band of CTP (1656 cm^{-1}) which overlaps with the band assigned to α-helical structure of RSU (1650 cm^{-1}) limits our ability to detect protein conformational changes upon binding of CTP. A way to observe the amide I' vibrations of the protein is to isotopically label the RSU with ^{13}C which results in a significant shift of the amide I' band to lower wavenumber (~ 45 cm^{-1}) and in turn, away from the carbonyl absorption of CTP (Figure 3.11 A and B). The 1677, 1651 and 1627 cm^{-1} bands of RSU are shifted to 1634, 1610 and 1585 respectively in ^{13}C-labeled RSU.

3.3.6 VT-FTIR of ^{13}C-Labeled RSU and 2D Correlation Analysis

VT- FTIR spectroscopy was employed to monitor the thermal unfolding of the ^{13}C-labeled RSU in the presence and absence of CTP. First, the thermal unfolding of the ^{13}C-labeled RSU was monitored by increasing temperatures from 25-80°C. Below 35°C, there is a two wavenumber shift of the β-sheet band from 1585 to 1583 cm^{-1} (data not shown); this shift is most likely due to H-D exchange. To analyze changes in secondary structure of the ^{13}C-labeled RSU, only spectra from 35-79°C were examined (Figure 3.12A).

Figures 3.12 A and B show the 1D overlaid spectra and difference spectra, respectively, of the temperature-induced unfolding of the ^{13}C-labeled RSU. The plots show a decrease in the intensities of β-sheet and α-helix peaks that occurs with increasing temperature.

Between 35 and 43°C, the protein appears to resist temperature mediated changes. This is illustrated in Figure 3.12 A and B as well as by an absorbance versus temperature plot (Figure 3.13). Moreover, when the protein was heated to 80°C, two new bands emerged at 1574 cm^{-1} and 1637 cm^{-1} which correspond to intermolecular β-sheets, or aggregated protein (see Figure 3.12 A and B). Also, significant levels of aggregation appear at 55 °C as shown by Figure 3.13.

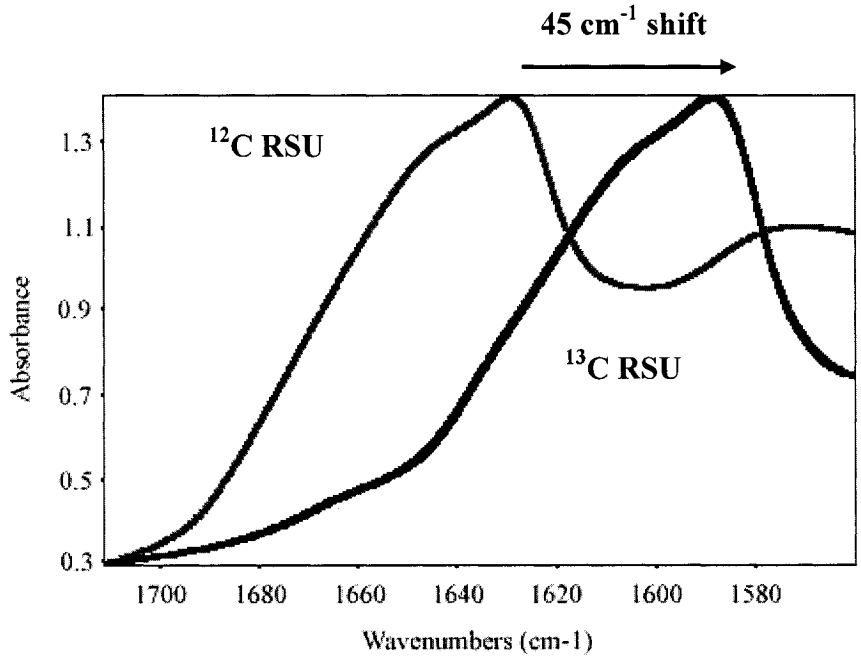

Figure 3.11 A: Amide I' band of ^{12}C RSU and ^{13}C RSU at room temperature (25 °C). Amide I' band of RSU has shifted 45 cm^{-1} lower as a result of ^{13}C labeling. No secondary structural changes have occurred in the labeled protein.

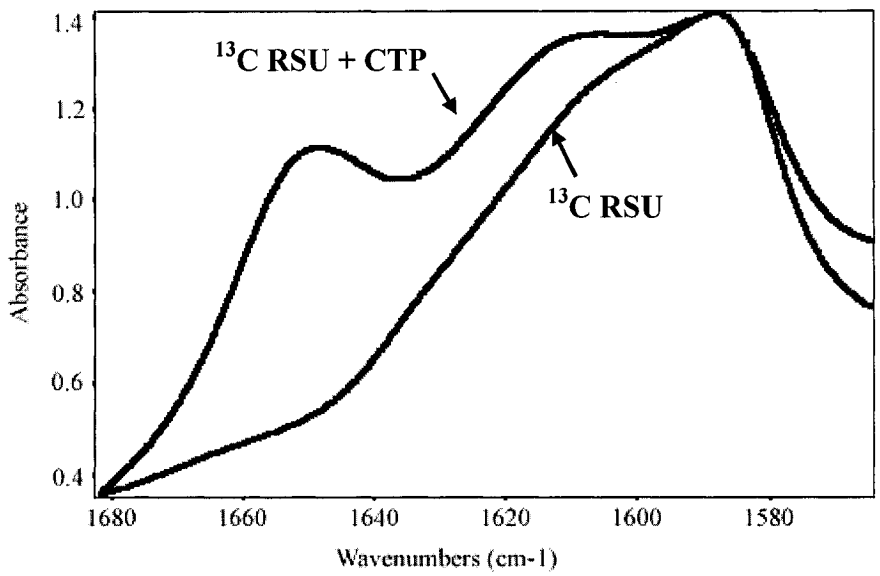

Figure 3.11 B: Uniform ^{13}C-labeling of RSU provides a spectral window allowing the thermal denaturation of RSU to be monitored in the presence of CTP.

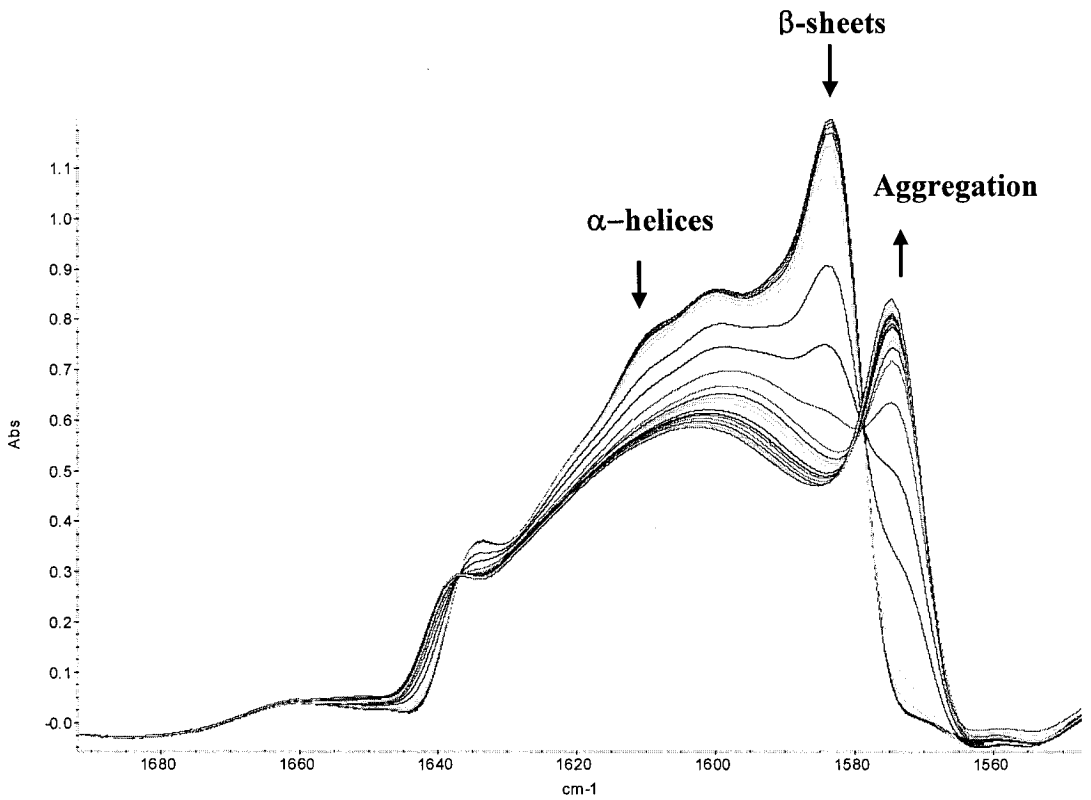

Figure 3.12 A: Overlaid deconvolved spectra of ^{13}C RSU VT-FTIR from 35-79°C. The directions of the arrows indicate the change in intensity of the main secondary structures of the protein with increasing temperature. The directions of the arrows indicate the change in intensity of the main secondary structures of the protein with increasing temperature.

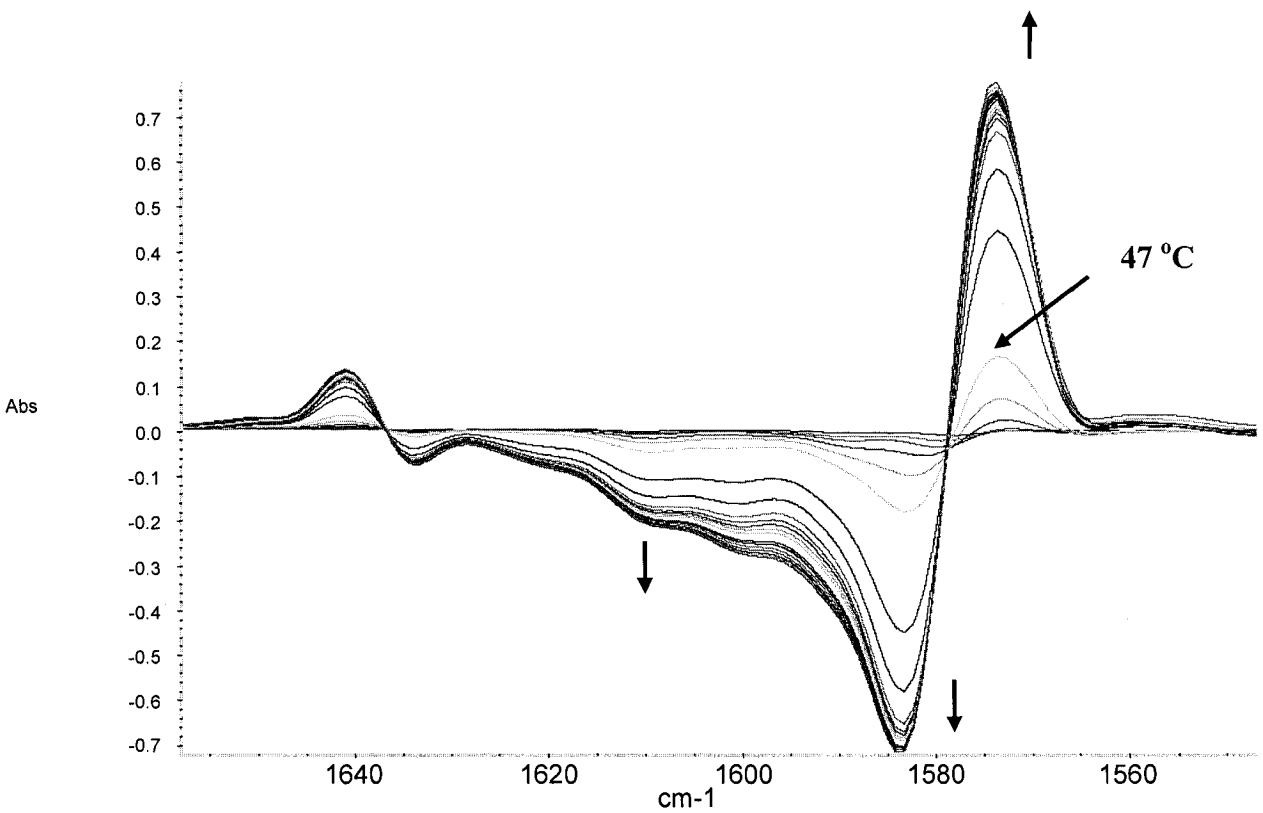

Figure 3.12 B: Overlaid deconvolved difference spectra of ^{13}C RSU, VT-FTIR from 35-79°C. The difference spectra were obtained by baseline correction with the spectrum at 35°C. The arrows indicate the direction of the change of intensity with increasing temperature.

The temperature at which the ^{13}C-labeled RSU starts to denature can be identified by a plot of the variation of intensity versus temperature (Figure 3.13), obtained from the deconvolved spectra in Figure 3.12B. The curves in Figure 3.13 highlight the changes in absorbance of the main secondary structures of RSU as a function of increasing temperature. Figure 3.13 shows three major bands that undergo changes as a function of increasing temperature between 35 and 55°C: 1610 cm^{-1} (α-helices), 1583 cm^{-1} (intramolecular β-sheets) and 1574 cm^{-1} (intermolecular β-sheets). The peak heights for the α-helices and intramolecular β-sheets structures decreases while the 1574 cm^{-1} band increases with increasing temperature. The figure shows the disappearance of the β-sheets and α -helices and the appearance of the aggregation band (or intermolecular β-sheets). This graph shows that the β-sheets and α-helices decrease with increasing temperature and the onset of aggregation occurs at 47°C.

The overall unfolding of the protein and its thermal stability can be deduced by the one-dimensional spectral analysis. However, in order to obtain or confirm the sequence of unfolding, 2D correlation analysis was used. The 2D correlation analysis uses data obtained from the deconvolved difference spectra (i.e. subtracting the initial deconvolved spectrum at 35°C from those recorded during the heat treatment). Spectral data reflecting changes in the amide I' absorption of RSU in the temperature range between 35 and 55°C (Figure 3.12 B) were used to generate 2D correlation maps (Ismoyo et al. 2000). At temperatures below 35°C, the minor changes in the amide I' band occurs due to H-D exchange, while above 55°C, the proteins had undergone extensive aggregation. Accordingly, the 2D- correlation analysis was carried out between 35 and 55°C.

Figure 3.14 shows the synchronous and asynchronous 2D maps generated from the deconvolved difference spectra in the amide I' region of ^{13}C RSU. It is interesting to note that only the top quadrants of the synchronous and asynchronous maps are analyzed (both maps are symmetrical across the diagonal). The synchronous map shows two strong autopeaks (on the diagonal) at 1583 cm^{-1} and 1574 cm^{-1}. These peaks represent the variation of intensity that occurred as a function of increasing temperature.

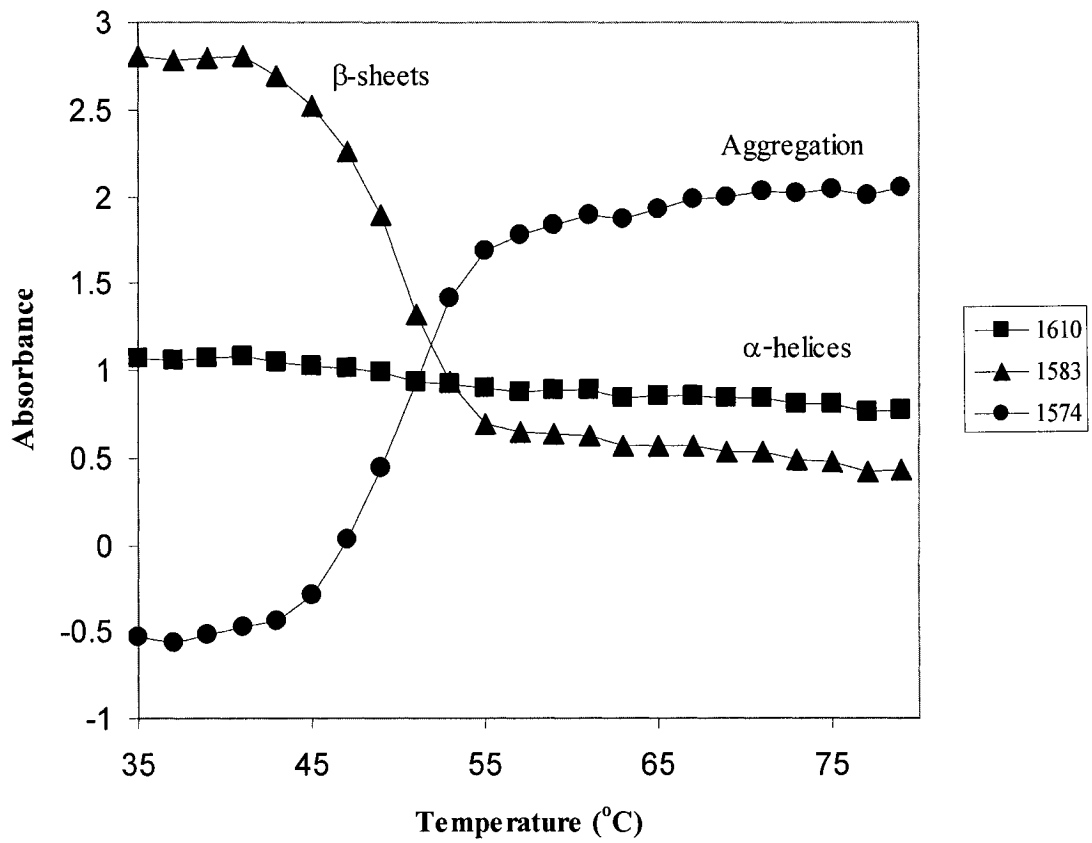

Figure 3.13: Peak heights of amide I' band components of ^{13}C RSU as a function of increasing temperature.

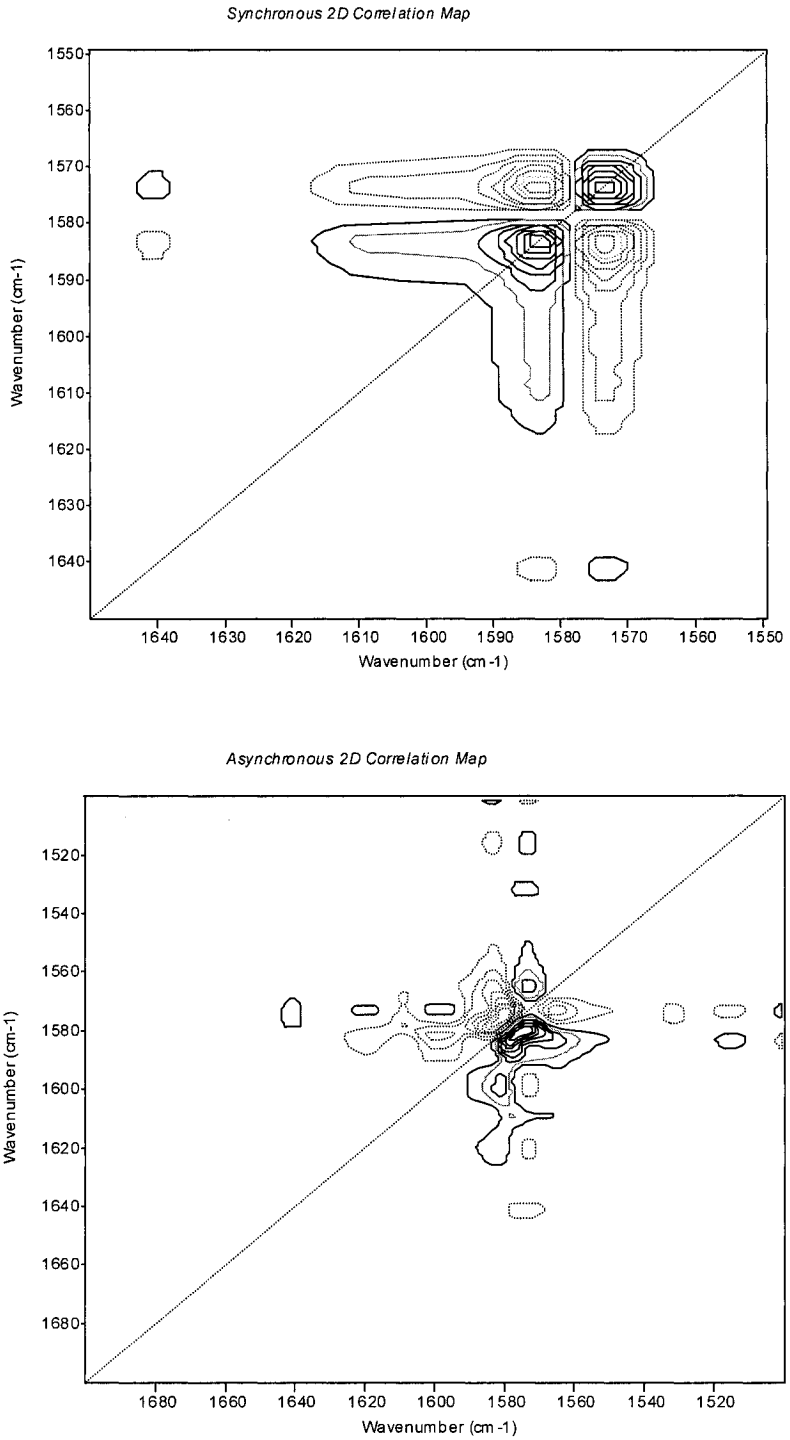

Figure 3.14: Synchronous and asynchronous 2D correlation map of ^{13}C-labeled RSU over a temperature range of 35-55°C.

The positive cross correlation peaks (solid lines) on the 2D maps, represent the intensity changes that occur in the same direction. The negative cross correlation peaks (dashed lines), represent the intensity changes that occur in the opposite direction. For example, the cross correlation peak of 1610 (x-axis) and 1583 (y-axis) cm^{-1} gives a positive sign, indicating that the intensities are changing in the same direction. In contrast, the cross correlation peak between 1610 and 1574 cm^{-1} and between 1583 and 1574 cm^{-1} give negative signs, meaning that the intensities of the 1610 and 1583 cm^{-1} bands are changing in opposite direction of the 1574 cm^{-1} band.

The sequence of events leading to the unfolding of the RSU domains can be deduced by examining the asynchronous 2D map (Figure 3.14) in conjunction with the signs of the cross correlation bands in the synchronous map. An asynchronous 2D map represents sequential changes of spectral intensities measured at two wavenumbers. A positive sign of a cross correlation peak indicates that the change in intensity at the wavenumber on the x-axis occurs first, followed by the change in intensity at the wavenumber on the y-axis. If the corresponding cross-peak in the synchronous map is also positive, then the same order applies. However, if the corresponding cross-peak in the synchronous map is of the opposite sign (i.e., negative in this case), then the rule is reversed.

The cross correlation peak between 1610 (x-axis) and 1583 (y-axis) cm^{-1} in the asynchronous map is negative. Since the corresponding peak in the synchronous map shows a positive sign, the change in intensity at 1583 cm^{-1} occurs before 1610 cm^{-1}. The cross correlation peak between 1610 and 1574 cm^{-1} is negative and since the corresponding peak in the synchronous map is also negative, then the intensity at 1610 cm^{-1} changes prior to 1574 cm^{-1}. And lastly, the cross correlation peak between 1583 and 1574 cm^{-1} gives a negative sign in the asynchronous map, and shows a negative sign in the synchronous map, therefore the intensity at 1583 cm^{-1} changes before that at 1574 cm^{-1}.

The sequence of events leading to the unfolding aggregation of RSU can be summarized in Table 3.2. The wavenumbers on the X- axis (row) and Y-axis (column) of the table represents the bands of interest; the up and down arrows (↑ or ↓) indicate the change in intensity for each peak with increasing temperature as deduced from the 1D spectra. Note that the column excludes the highest wavenumber while the row omits the lowest wavenumber. A positive sign means that the peak intensities are changing in the *same* direction (↑ and ↑) or (↓ and ↓), and a negative sign (–) means that the peak intensities are changing in the *opposite* direction (↑ and ↓). The first symbol (+ / -) for each peak correlation pertains to the peak intensities in the synchronous map and the second symbol (+/-) represents the analysis of the cross correlation peaks in the asynchronous 2D map. The directional arrows indicate the sequential changes of spectral intensities measured at two wavenumbers. By respecting the directions of all the arrows in each cell, the sequence of unfolding can be obtained. Lastly, the summary of the sequence of events are written in the bottom of the table. The sequence of intensity changes of the ^{13}C-labeled RSU obtained from the 2D maps up to the point of aggregation are as follows: first, loss of some of the β-sheet structures occurs followed by a loss of α-helices, and finally leading to aggregation.

Table 3.2: Sequence of unfolding of ^{13}C-labeled RSU from 35-55 °C

	1610 ↓	1583 ↓
1574 ↑	- - ⇐	- - ⇐
1583 ↓	+ - ⇒	
Sequence of events of individual components		
⇓	Intramolecular β-sheets (1583 cm^{-1}) α-Helices (1610 cm^{-1}) Intermolecular β-sheets (1574 cm^{-1})	

3.3.7 VT-FTIR of ^{13}C-Labeled RSU Complexed with CTP and 2D Correlation Analysis

Figure 3.15A shows the VT-FTIR spectra in the amide I' absorption region as a function of increasing temperature of the ^{13}C-labeled RSU-CTP complex. The band that represents the carbonyl absorption of CTP at 1656 cm^{-1} is now clearly separated from the amide I' band of the ^{13}C-labeled RSU. The thermal unfolding of the ^{13}C RSU-CTP was monitored by increasing the temperature from 25 to 80 °C. Below 41 °C, there is a two wavenumber shift from 1585 to 1583cm^{-1} assigned to the β-sheet structures in RSU and this shift is attributed to H-D exchange. For RSU alone, the increase in the temperature from 35°C to 41°C indicates that the tertiary structure of the protein may be stabilized by CTP or that CTP is blocking access of D_2O to the interior of the protein.

The changes in the secondary structures due to conformational changes are analyzed using spectral data acquired between temperatures 35 and 79°C (Figure 3.15 A). The absorption bands of CTP (Figure 3.9) were not subtracted from the spectra of RSU-CTP complex since the amide I' components are clearly separated from those of CTP, which enables analysis of the changes in the secondary structure. The intensity of the α-helix band increases and indicates that the RSU has a higher α-helical content when bound to CTP.

The overlaid deconvolved difference spectrum (Figure 3.15 B) illustrates the change in intensity more clearly. In addition, the changes in peak heights were plotted as a function of increasing temperature (Figure 3.16). This graph shows that the β-sheets and α-helices decrease with increasing temperature. The onset of aggregation occurs at 55°C (in comparison with 47°C in the absence of CTP).

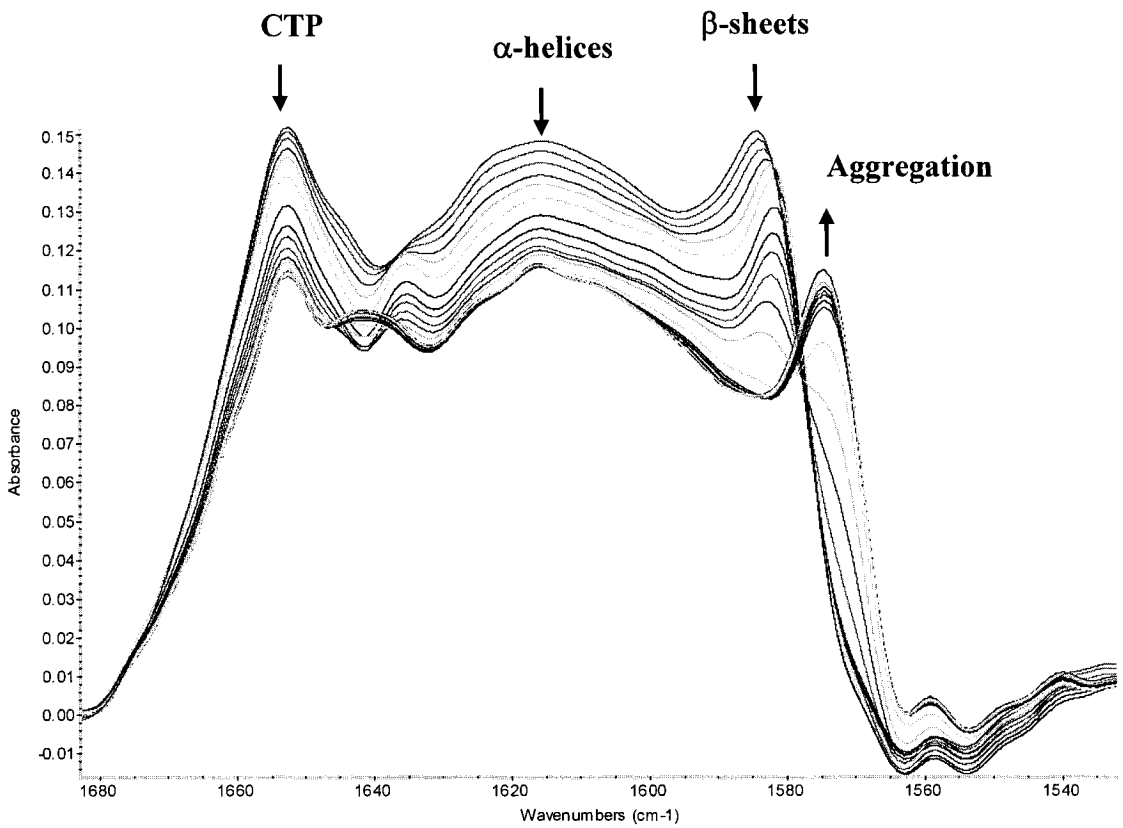

Figure 3.15 A: Overlaid deconvolved spectra of ^{13}C RSU complexed with CTP, VT-FTIR from 35-80°C.

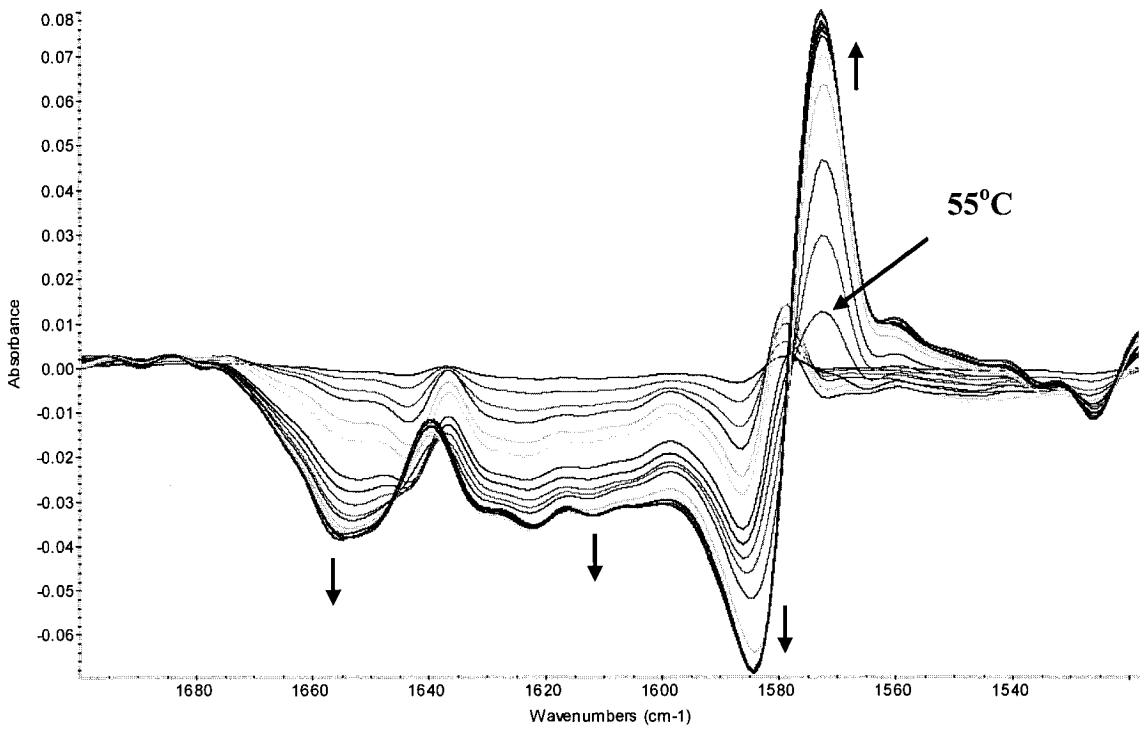

Figure 3.15 B: Overlaid deconvolved difference spectra of ^{13}C RSU complexed with CTP, VT-FTIR from 35-80°C.

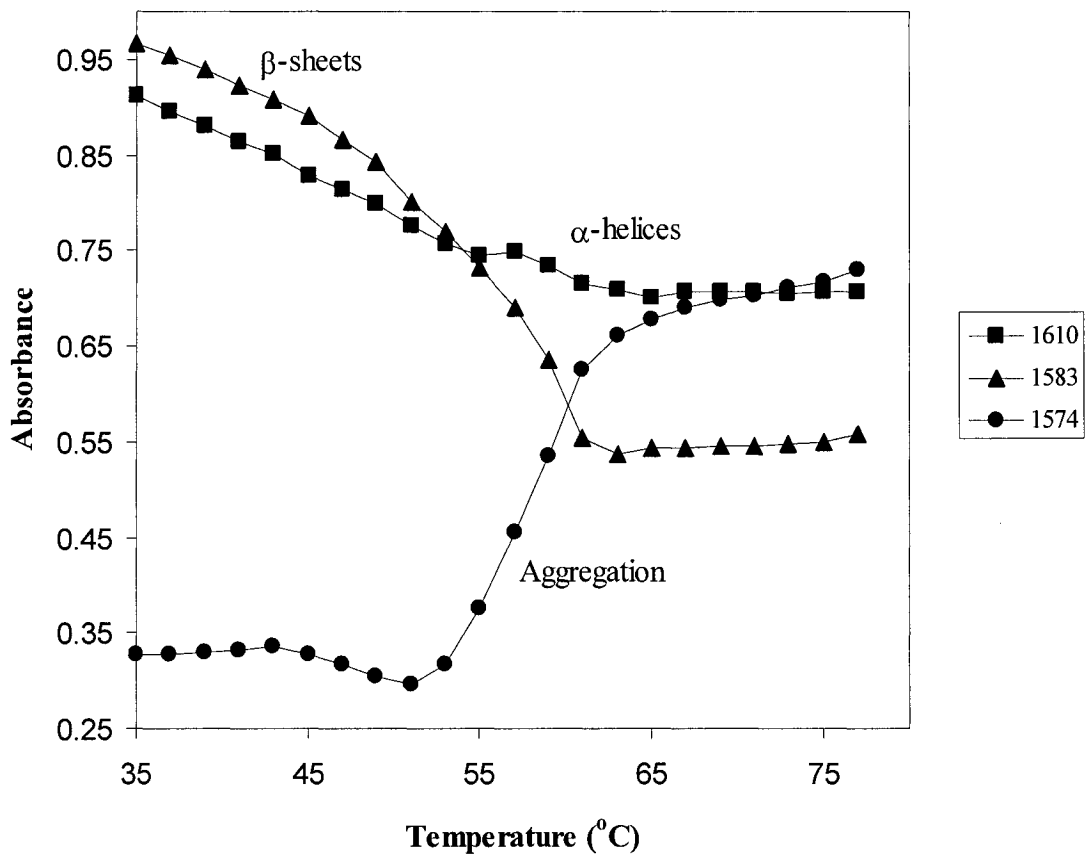

Figure 3.16: Peak heights of amide I' band components of ^{13}C-labeled RSU complexed with CTP as a function of increasing temperature.

To elucidate the changes that occur when CTP binds to RSU, the relative absorbance of the α-helix and β-sheet bands observed in the deconvolved spectra were plotted as a function of increasing temperature. The relative absorbance is computed as 100 × [Abs (T) – Abs (79°C)]/[Abs (35°C) – Abs (79 °C)] (Figure 3.17 A and B). The curves in Figure 3.17A show that the α-helical content of the isolated RSU, monitored by analyzing the 1610 cm^{-1} band remains stable until 39°C, and then progressively decreases with increasing temperature up to 55°C. Between 55-65°C, the signal remains constant and is gradually lost upon heating to 77°C. In contrast, the α-helical intensity of the RSU-CTP complex decreases immediately as temperature increases up to 65°C, then the signal remains constant from 65-77°C. This indicates that the α-helical structures are less stable when ligand is bound. Only 15% of the α -helical content in RSU remains at 55°C when CTP is bound to RSU in comparison with 35% α-helical content in RSU at the same temperature. Similarly, the β-sheet content was monitored by the changes in the intensity of the band at 1583 cm^{-1} (Figure 3.17 B). For the isolated RSU, the band intensity remains unchanged up to 39°C then rapidly decreases until 53°C, (~ 20% of β-structure remains), and finally the signal decreases slowly from 55-77°C. These findings are consistent with the results obtained from the VT-far UV-CD data of the unlabeled RSU (Figure 3.8).

Examination of the VT-FTIR spectra of CTP-RSU complex reveals that the 1583 cm^{-1} band intensity decreases progressively from 35-60°C, resulting in the elimination of all β-structure at 60°C. The β-sheet structures shows uncooperative unfolding in the RSU-CTP complex; between 49-59°C, the presence of CTP significantly destabilizes the β-sheets of the RSU against temperature-induced unfolding.

The onset of aggregation was monitored by the appearance and increase in the intensity of the band at 1574 cm^{-1} corresponding to the formation of intermolecular β-sheets. Figure 3.18 shows the plot of the increase in the band intensity as a function of increasing temperature. For both the isolated and ligand bound RSU, the amounts of intermolecular β-sheets increase as the temperature increases. However, the onset of aggregation occurs at a significantly higher temperature for the protein complexed with ligand. The RSU alone begins to aggregate at 47°C, compared to 55°C in the presence of CTP.

A

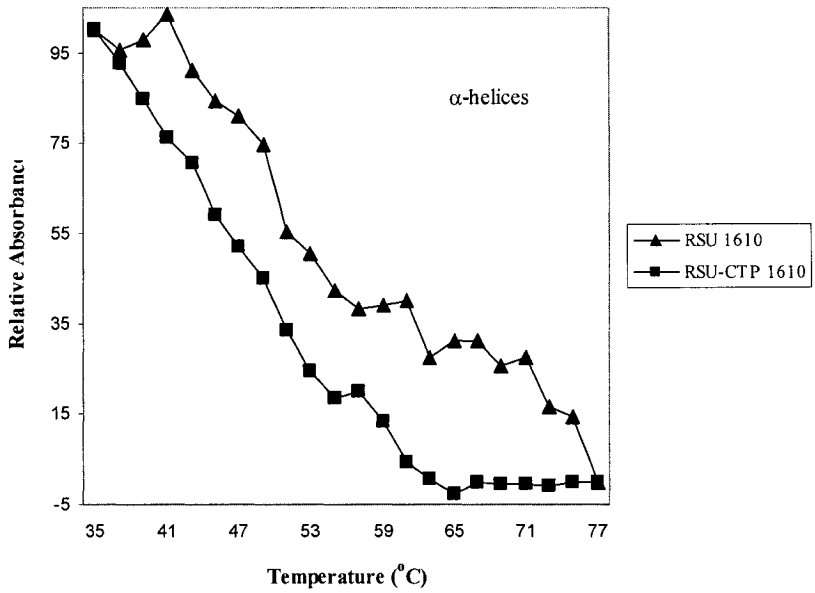

B

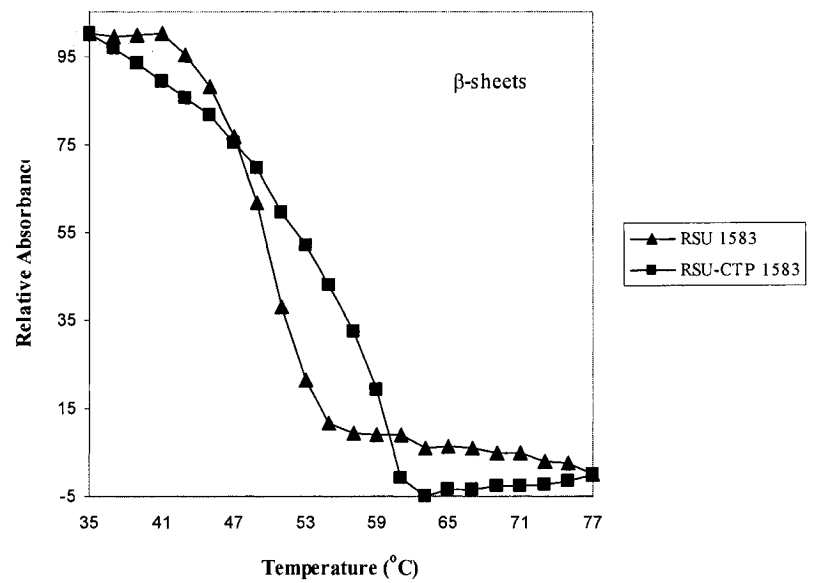

Figures 3.17 A, B: Plot of relative absorbance of the α-helix and β-sheet bands, respectively, in the deconvolved spectra as a function of increasing temperature (T), where relative absorbance is computed as 100 × [Abs(T) - Abs(79°C)]/[Abs(35°C) - Abs(79°C)].

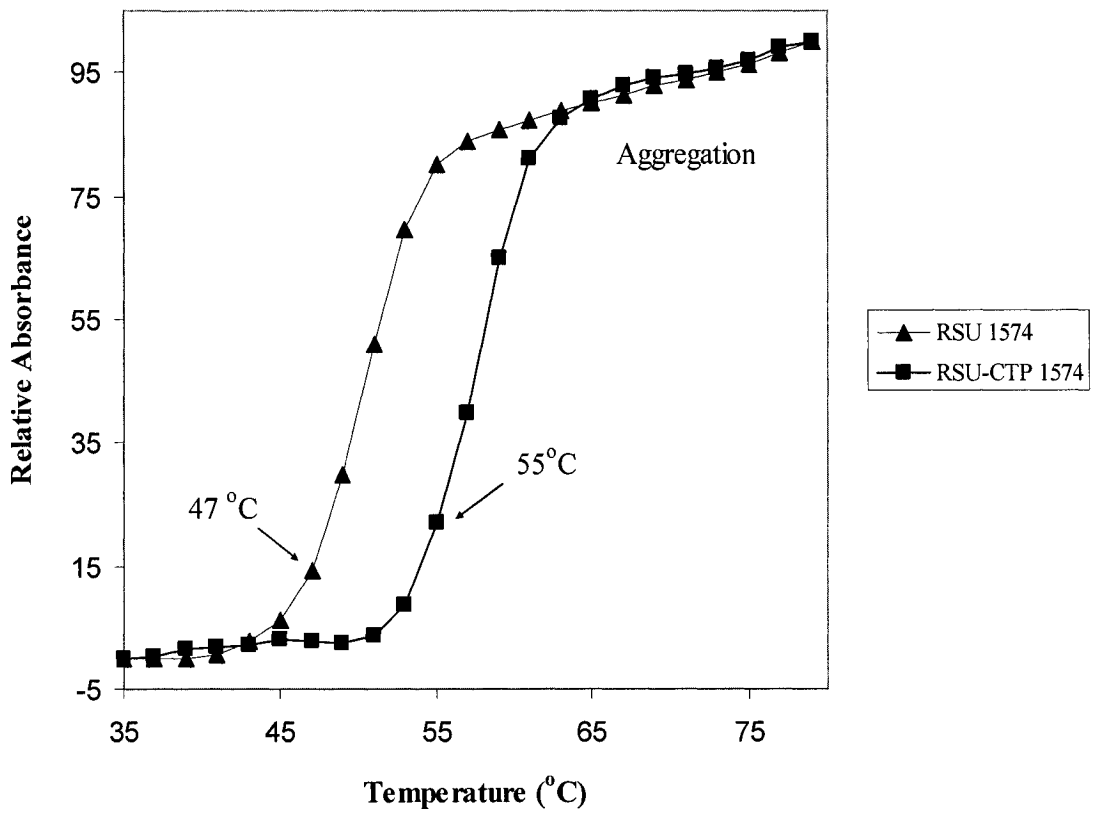

Figure 3.18: Plot of relative absorbance of the aggregation band in the deconvolved spectra as a function of increasing temperature (T), where relative absorbance is computed as 100 × [Abs(T) – Abs(79°C)]/[Abs(35°C) - Abs(79°C)]. The labeled temperatures indicate the onset of aggregation.

The sequence of unfolding of ^{13}C-labeled RSU complexed with CTP was obtained using the 2D correlation maps (Figure 3.19). The synchronous and asynchronous 2D correlation maps were constructed using the overlaid deconvolved spectra from Figure 2.15B. Table 3.3 summarizes the results obtained from the 2D maps. The sequence of event leading to the unfolding and aggregate formation of CTP- ^{13}C RSU complex commenced with the loss of α-helix structures followed by a loss of β-sheet, and finally leading to aggregation. Thus, the binding of CTP to RSU does not alter the sequence of unfolding of the protein but rather, delay the onset of unfolding and aggregate formation. The delay in the unfolding may be a result in the significant increase in the α-helical content in RSU upon binding to CTP. Furthermore, the decrease in H-D exchange upon CTP binding may suggest that the tertiary structure of the protein is also altered.

The allosteric domain holds the binding sites for the nucleotides effectors, and it is distinct from the catalytic active sites (Lipscomb 1994). From the crystal structure (Figure 3.20), it is known that the Zn-binding domain provides all the interactions between the catalytic subunit and in turn, the heterotrophic binding effects is mediated between the allosteric and Zn-binding domain interface (Rastogi et al. 1998). There are three allosteric models that are based on this interface. Tanner and coworkers postulated that a global conformational change occurs upon the interaction of nucleotides; this model is based on the 'hinge-bending' at the interface (Tanner et al. 1993). The second model involves the 'effector-modulated transition' model, and it directly involves the nature of hydrophobic core of the allosteric domain (Xi et al. 1991; Xi et al. 1994). The third model, termed 'nucleotide pertubation', suggests that a direct signal is transmitted from the hydrophobic core to the allosteric-Zn binding domain interface (Stevens and Lipscomb 1992).

This present work may support the first proposed model, in which the overall change in tertiary structure is minimal by the binding of the nucleotide. The presence of CTP has shown to increase the helical content, possibly due to 'hinge-bending' at the interface. This in turn, allows the buried helical structures in the allosteric domain to become more surface exposed.

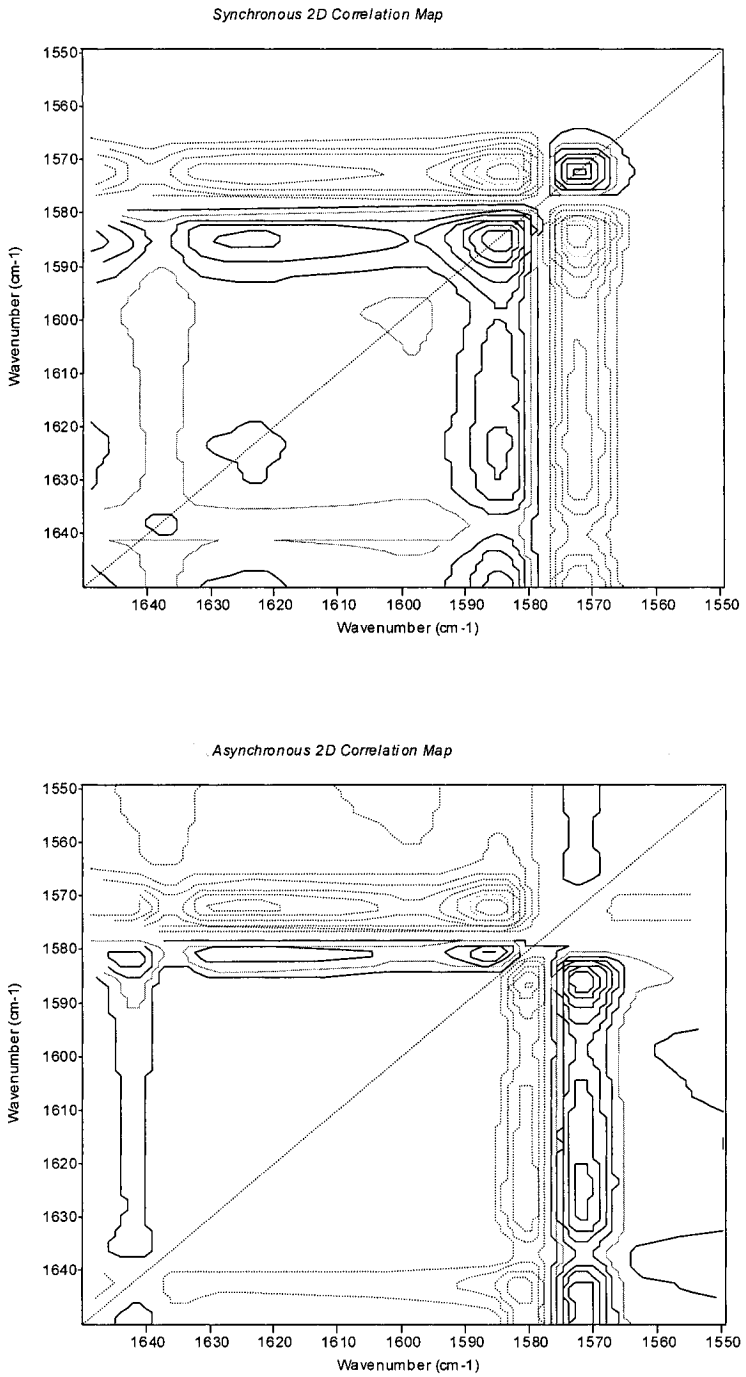

Figure 3.19: Synchronous and asynchronous 2D correlation map of ^{13}C-labeled RSU complexed with CTP over a temperature range of 37-65°C.

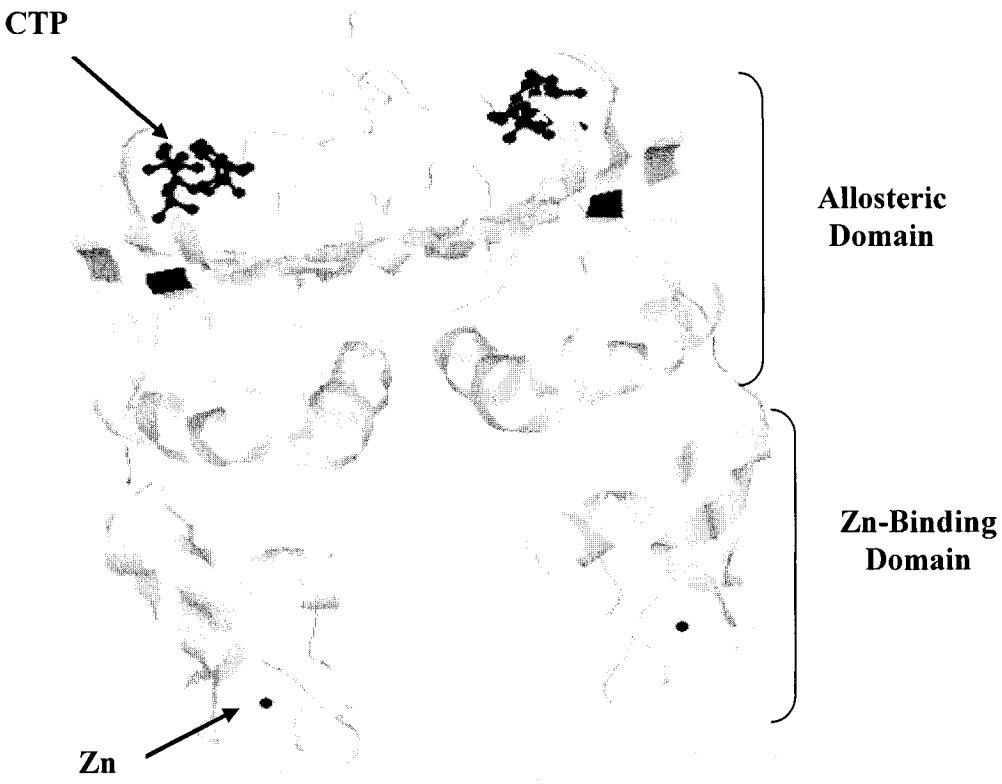

Figure 3.20: Crystal structure of the RSU dimer (Kosman et al. 1993).The allosteric and Zn-binding domains were uniformly labeled with ^{13}C glucose.

Table 3.3: Sequence of unfolding of ^{13}C-labeled RSU-CTP from 35-65 °C

	1610 ↓	**1583 ↓**
1574 ↑	- - ⇐	- - ⇐
1583 ↓	+ + ⇐	
Sequence of events of individual components		
⇓	**α-Helices (1610 cm^{-1})** **Intramolecular β-sheets (1583 cm^{-1})** **Intermolecular β-sheets (1574 cm^{-1})**	

3.4 Summary

The thermal unfolding of uniformly ^{13}C-labeled RSU bound to CTP was investigated using FTIR spectroscopy. The ~ 45 cm^{-1} band shift of the amide I' band of RSU upon ^{13}C labeling provided a clear separation between the protein amide I' band and the absorption of the ligand. This significantly facilitated the study of the changes in the secondary structure of the protein upon ligand binding and thermal denaturation of the CTP-RSU complex. In the presence of CTP, RSU was observed to be more heat-stable as aggregate formation occurred at 53°C as opposed to 47°C for RSU alone. 1D and 2D correlation analysis confirmed that the CTP stabilizes the overall structure of the RSU, and revealed that the α-helical structures were more thermally labile compared to the β-sheet in the protein. Furthermore, the change in the α-helical content (which increased upon the binding of CTP to RSU) decreased more rapidly and more extensively in the CTP-RSU complex. Similar findings were observed for the β-sheet structures.

Isotopic labeling of each domain of the RSU will allow us to study the structural changes of each domain in the presence and absence of CTP by VT-FTIR spectroscopy in conjunction with 2D correlation analysis. Future studies will be used to determine the structural contribution of the allosteric portion of the protein and the Zn-binding ***independently*** upon interaction with catalytic subunit, CTP or Zn. These studies will ultimately help us understand how the enzyme structure helps to regulate nucleotide metabolism.

CHAPTER 4

FT-Raman Spectroscopy of *E. coli* Aspartate Transcarbamylase

4.1 Introduction

The Raman shifts are based on discrete vibrational transitions that occur in the ground electronic state of the molecule, which correspond to various stretching and bending deformation modes of the chemical bonds. Hence, a Raman spectrum (a plot of the intensity of scattered light as a function of the Raman shift) can give information about the molecule's structure. Molecules will undergo inelastic light scattering if irradiation causes a change in the polarizability of the functional groups, that is, in the shape of the electron density cloud around the molecule. Some important advantages of Raman spectroscopy include its ease of sample preparation and its ability to obtain structural information, particularly vibrational information that can't be obtained by infrared (IR) spectroscopy. IR spectroscopy results from absorption of energy by vibrating chemical bonds, whereas Raman scattering results from the same transition but records the emission of scattered laser light. The two techniques are complementary to each other because of the selection rule; generally vibration bands formed from strong dipole moment are strong in IR and weak in Raman, while non-polar functional group vibrations give a strong signal in Raman and a weak one in IR. In addition, since the water band in Raman spectrum is weak, it provides a means of obtaining vibrational data from aqueous systems. The latter enables Raman spectroscopy to be a useful tool in studying proteins in solution. Tables 4.1 and 4.2 outlines the main band frequencies that are particularly useful in studying protein structure.

The interpretation of Raman data of biological systems can be limited by a poor signal-to-noise (S/N) ratio because only a few molecules (~0.0001%) undergo Raman scattering. It is important to have high concentrations of protein samples (~2-20 mg/ml). Another very important consideration is the effect of fluorescence emission which may overpower the Raman signal. One way to overcome this effect is through proper selection of the laser frequency, particularly in the near-infrared (NIR) region.

Table 4.1: Summary of Raman modes used in the interpretation of protein structure (Li-Chan 1996; Li-Chan et al. 2002).

Origin	Wavenumber (cm^{-1})	Assignment	Structural Information Obtained
Cystine, cysteine, methionine	510	S-S stretch	Presence of *gauche-gauche* conformation; band broadening and/or shifts may indicate conformational heterogeneity of cystine residue
	525	S-S stretch	*Gauche-gauche-trans* conformation
	545	S-S stretch	*Trans-gauche-trans*-conformation
	630-670	C-S stretch	*Gauche*-conformation
	700-745	C-S stretch	*Trans*-conformation
	2550-2580	S-H stretch	Presence of thiol cysteine residues
Tyrosine	850/830	Fenni resonance between ring fundamental and overtone	State of phenolic OH group (exposed or buried, hydrogen-bond donor or acceptor)
Tryptophan	760, 880, 1360	Indole ring	Sharp intense band indicates buried residues; sensitive to environment polarity
Phenylalanine	1006	Ring breath	Conformation insensitive; useful as an internal intensity standard
Histidine	1409	*N*-deuteroimidazole	Probe of ionization state, metalloprotein structure, proton transfer in deuterated solution
Aspartic and glutamic acids	1400-1430	C=O stretch of COO^-	Ionized carboxyl groups
	1700-1750	C=O stretch of COOH or COOR	Undissociated carboxyl, ester or metal complexation
Aliphatic residues	1450, 1465	C-H bending	Microenvironment, polarity
	2800-3000	C-H stretching	Microenvironment, polarity
Amide I	1655 ± 5	Amide C=O stretch, N-H wag	α-helix
	1670 ± 3	Amide C=O stretch, N-H wag	Anti-parallel β-sheet
	1666 ± 3	Amide C=O stretch, N-H wag	Disordered structure (solvated)
	1685	Amide C=O stretch, N-H wag	Disordered structure (non-hydrogen bonded)
Amide III	>1275	N-H in-plane bend, C-N stretch	α-helix
	1235 ± 5 (sharp)	N-H in-plane bend, C-N stretch	Anti-parallel β-sheet
	1245 ± 5 (broad)	N-H in-plane bend, C-N stretch	Disordered structure
	1235	N-H in-plane bend, C-N stretch	Disordered structure (non-hydrogen bonded)

Table 4.2: Characteristic Raman bands of ATCase, CSU and RSU

Wavenumber (cm^{-1})	Assignment
	ATCase
1650	Amide I α-Helix
1670	Amide I β-sheets
1660 (faint shoulder)	Amide I Unordered
1284	Amide III α-Helix
1235 (sharp)	Amide III β-sheets
1252	Amide III Unordered
830, 850	Tyrosine
1340, 1360	Tryptophan
976	Phenylalanine
	CSU
1660	Amide I α-Helix
-	Amide I β-sheets
1673	Amide I Unordered
1276	Amide III α-Helix
1235	Amide III β-sheets
1253	Amide III Unordered
830, 850	Tyrosine
1340, 1360	Tryptophan
976	Phenylalanine
	RSU
1643	Amide I α-Helix
1662	Amide I β-sheets
1680	Amide I Unordered
1297	Amide III α-Helix
1230	Amide III β-sheets
1247	Amide III Unordered
830, 850	Tyrosine
-	Tryptophan
976	Phenylalanine

A disadvantage to this method occurs when trace amounts of fluorescent molecules are found in a sample, particularly proteins and peptides that contains natural fluorophores. This would make it is difficult to record an adequate Raman spectrum. In addition, the occurrence of thermal degradation, ('cooking' of the sample) may occur when using high laser intensities. Due to these challenges, Raman spectroscopy can be difficult to carryout.

In the present study, we report for the first time the preliminary results obtained from Raman spectroscopic studies of the structure of *E. coli* ATCase and its individual subunits. These results will be compared with earlier reported FTIR spectroscopic investigations of RSU.

4.2 Materials and Methods

4.2.1 Preparation of Enzymes

ATCase was purified as previously described in (Turnbull et al. 1992). Its subunits, CSU and RSU were isolated by the addition of mercurial agents. The enzyme purity was confirmed by non-denaturing polyacylamide gel electrophoresis (Native-PAGE). The protein concentrations were determined using BioRad Protein Assay as well as absorbance readings at 280 nm using coefficients of 0.59, 0.70, and 0.3 cm^2/ mg for the holoenzyme, CSU and RSU, respectively (Gerhart and Holoubek 1967).

For the co-addition experiments of the CSU and RSU Raman spectra, molecular weights for individual catalytic and regulatory chains of 33, 000 Da and 18, 600 Da, respectively, were used to calculate the monomer concentrations. To obtain equal molar ratios of the two different subunit components, 500 µl of CSU (6.6 µM monomer) and 150 µl (20.0 µM monomer) were used to compare with the holoenzyme. The isolated ATCase holoenzyme was prepared by taking 590 µl from a 3.2 µM monomer solution to give a final concentration of ~ 0.6 mg/ml. Protein samples were desalted and/or buffer exchanged with ddH_2O using commercially available pre-packed Sephadex gel filtration (NAP^{TM}) columns as described in the manufacturer's instructions. After this procedure, the samples were freeze-dried overnight using a Labconco Freeze dry system Lyph-Lock 4.5.

4.2.2 FT-Raman Spectral Analysis

The Raman scattering of samples placed in 1-mm glass capillaries were measured at ambient temperature on a Nexus 670 FT Raman spectrophotometer at a laser power of 0.93 W. The data was collected by the co-addition of 1024 scans from 100 to 3700 cm^{-1} at a resolution of 8 cm^{-1} and 100 aperture. The recorded spectra were analyzed using Omnic 6 software (Nicolet Inc., Madison, WI). The intensity was normalized on the phenylalanine peak at 976 cm^{-1}. The band assignments of the spectra (Table 4.2) were made on the basis of the literature from Table 4.1.

4.3 Results and Discussion

The positions of the main peaks found in the protein spectra are shown in Figure 4.1. The amide I region (Figure 4.2) between 1700-1600 cm^{-1} are examined and the band assignment for each of the secondary structures are shown in Table 4.3.

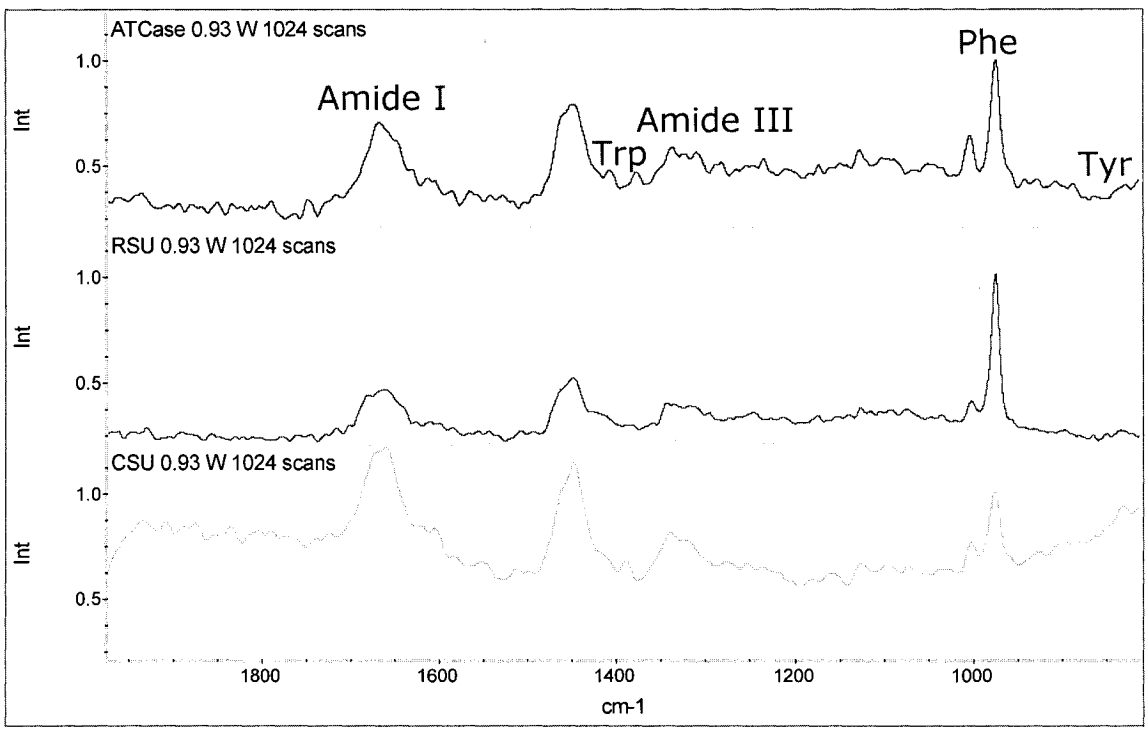

Figure 4.1: Raman spectra of the holoenzyme ATCase, RSU and CSU.

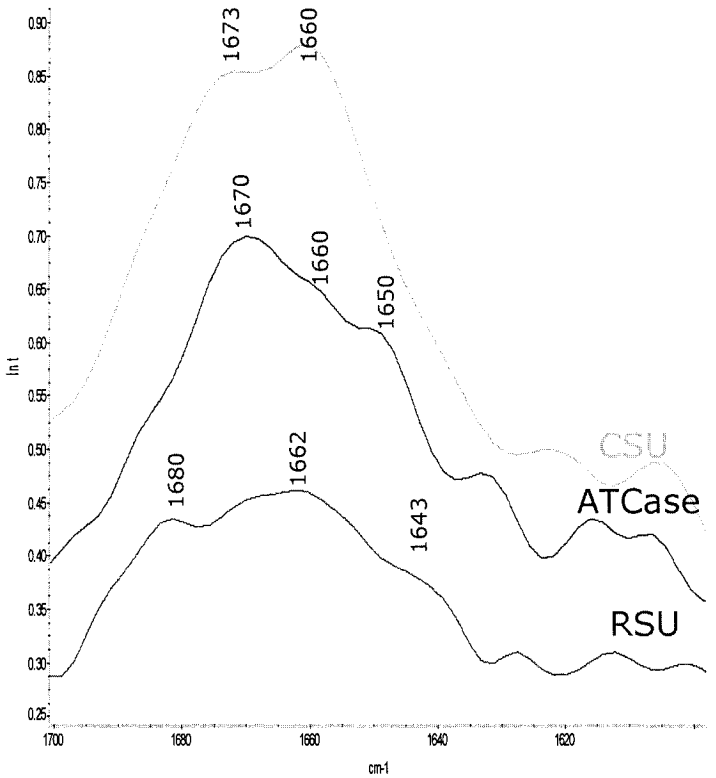

Figure 4.2: Overlaid Raman spectra of the amide I band of ATCase and its isolated subunits, CSU and RSU.

Table 4.3: Characteristic Raman bands in the Amide I region

Wavenumber (cm^{-1})	Assignment
	ATCase
1650	α-helix
1670	β-sheets
1660 (faint shoulder)	Unordered
	CSU
1660	α-helix
-	β-sheets
1673	Unordered
	RSU
1643	α-helix
1662	β-sheets
1680	Unordered

4.3.1 Amide I Band of RSU

Figure 4.3 shows the comparison of the amide I region of RSU using Raman and IR spectroscopy. The main secondary structures of the RSU are β-sheets and are assigned on the basis of the bands 1662 cm^{-1} (Raman) and 1627 cm^{-1} (IR). The β-sheets are easily identified in both techniques because of its symmetrical structure. The second most intense band is assigned to the α-helix structure at 1643 cm^{-1} for Raman and 1650 cm^{-1} in IR spectrum. The α-helices in the Raman spectra tend to be in the range of 1643-1660 cm^{-1}, this occurs because it is close to the H_2O band around 1660 cm^{-1}. The random coil bands are at 1680 cm^{-1} in the Raman spectrum and can be seen at 1665 cm^{-1} in the IR spectrum.

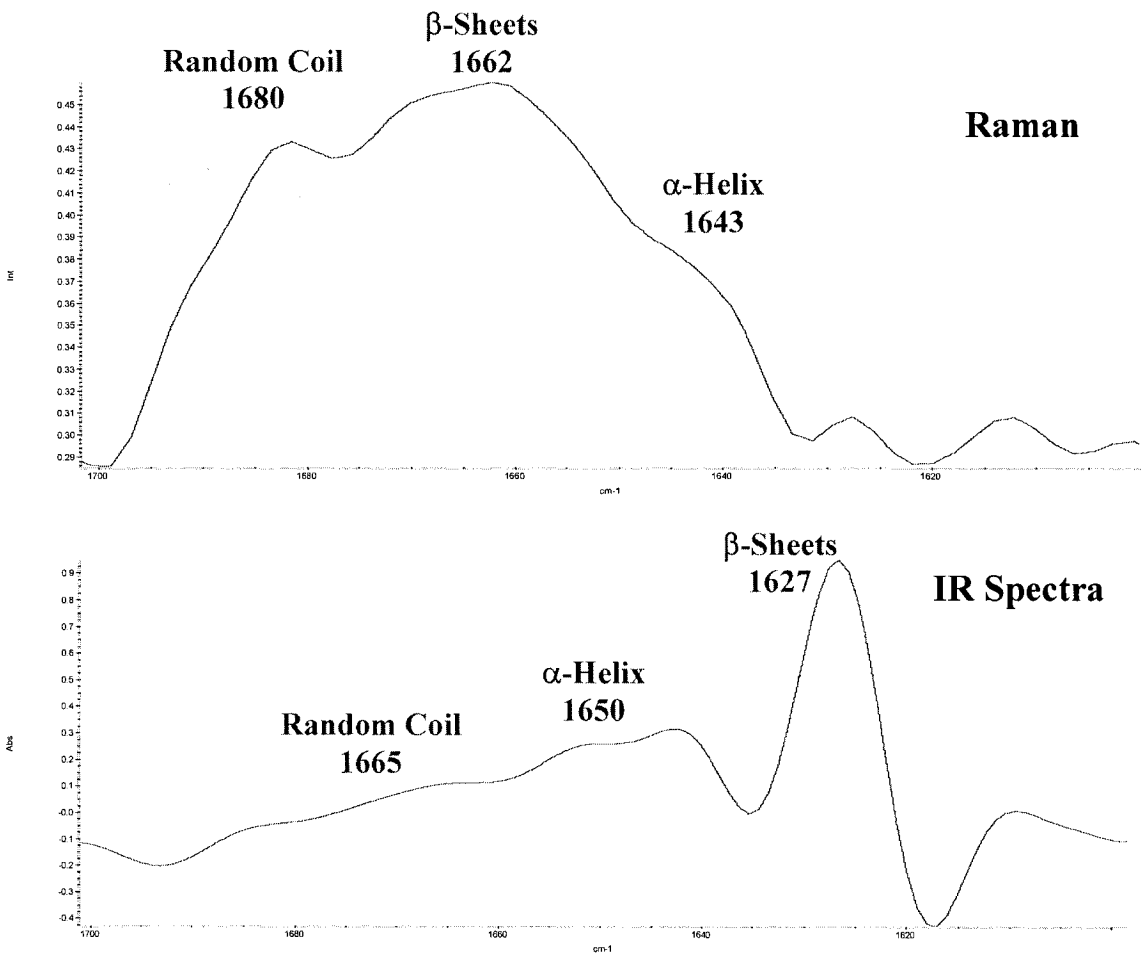

Figure 4.3: The comparison of the amide I region of RSU between the two spectroscopic techniques: Raman and IR spectroscopy.

4.3.2 Amide I band of ATCase

Figure 4.4 below shows the results of the co-addition of the CSU and RSU Raman spectra in the amide I region (top) compared to the spectrum of the isolated ATCase holoenzyme (bottom). The differences between the two sets of spectra suggest that structural changes arise from the interaction of the different subunits in the holoenzyme. The co-added spectrum shows an increase in intensity for the random coil structures, and a decrease in intensity of β-sheet and α-helix structures relative to the holoenzyme. Moreover, the holoenzyme displays a higher intensity for the β-sheet and α-helix bands, and a lower intensity for random structure compared to the co-added spectra of the individual subunits. It appears that the interaction stabilizes the secondary structure in the protein. The changes in intensity can not be quantified precisely because the S/N ratio of these spectra are low and the CSU spectra showed high levels of background fluorescence.

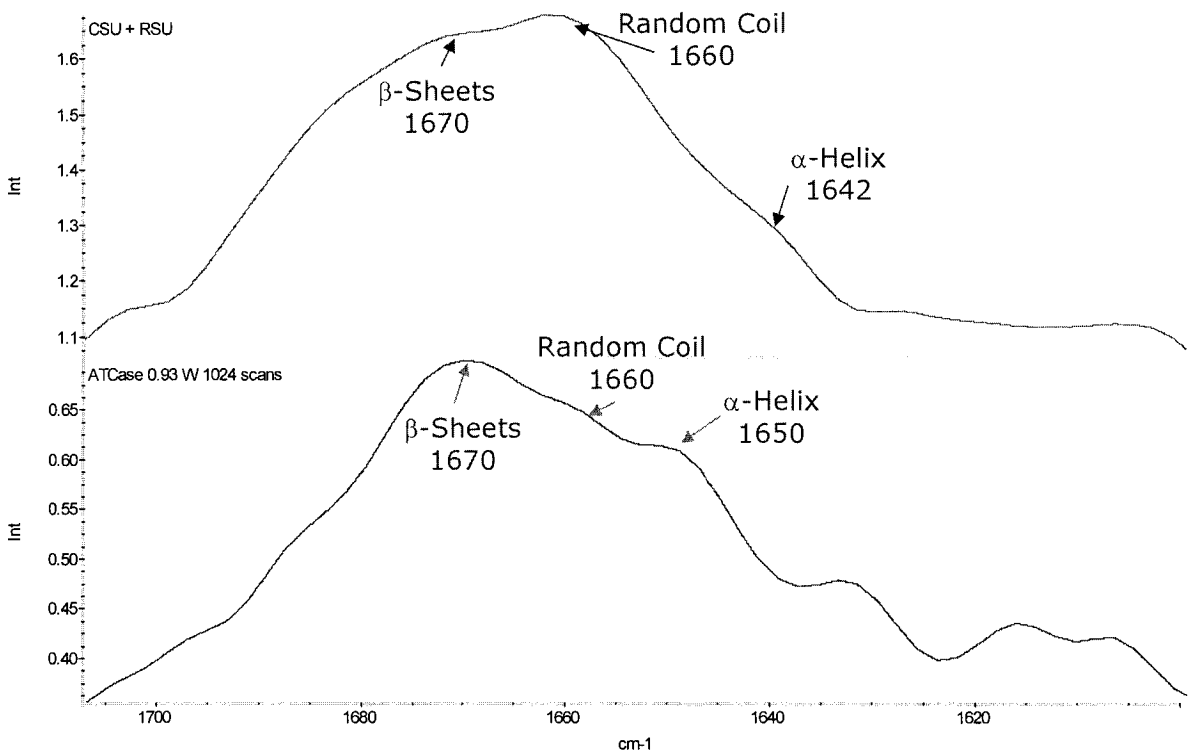

Figure 4.4: Amide I band of ATCase compared with the addition spectra of CSU and RSU.

Table 4.4 lists the proposed band assignments of ATCase, RSU and CSU for the amide III bands. It is interesting to note that the β-sheet structures for CSU has a band in the amide III region, which is very weak in the amide I region (data not shown).

Table 4.5 lists the band assignments for the aromatic amino acids for each protein. The ratios of intensities I_{1360}/I_{1340} for tryptophane and I_{850}/I_{830} for tyrosine indicate that these residues are in a hydrophilic region of the protein. These residues can be identified in the x-ray structure and are shown in Figure 4.5. It is of interest to note that the holoenzyme possesses a higher ratio (I_{1360}/I_{1340}) for tryptophan compared to CSU alone (RSU does not contain tryptophan residues). This indicates that the interaction between RSU with CSU shield some of the tryptophan residues, i.e. changes to a hydrophobic environment. In comparison, the I_{850}/I_{830} of tyrosine is slightly decreased in ATCase indicating that the interaction between RSU with CSU changes the buried tyrosine residues to becomes more hydrophilic and solvent exposed

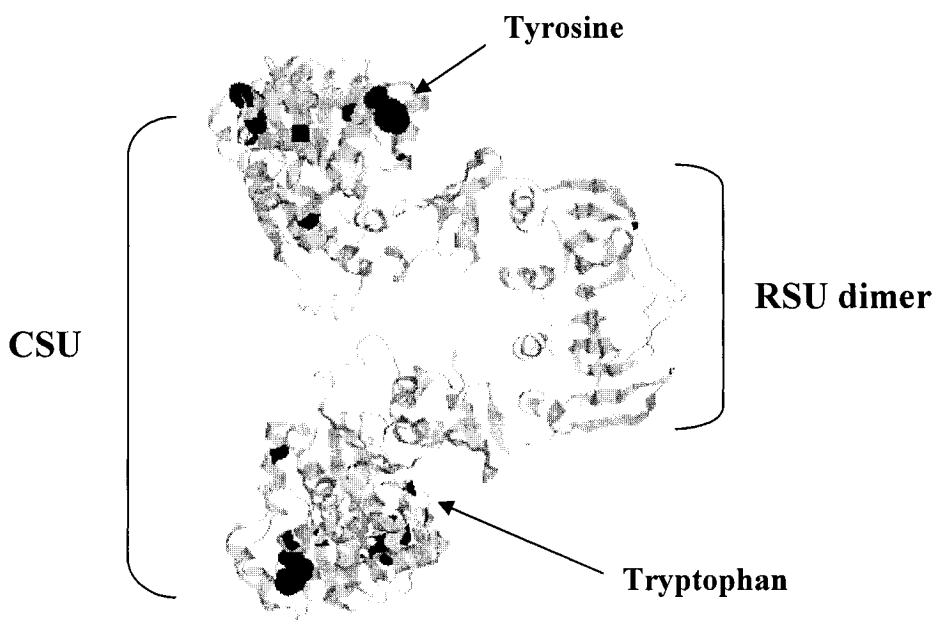

Figure 4.5: Crystal structure of two RSU-CSU pairs, highlighting the tyrosines (displayed as a spacefill) and tryptophans (displayed on the protein backbone) (Williams et al. 1998).

Table 4.4: Characteristic Raman bands in the Amide III region

Wavenumber (cm^{-1})	Assignment
	ATCase
1284	α-helix
1235 (sharp)	β-sheets
1252	Unordered
	CSU
1276	α-helix
1235	β-sheets
1253	Unordered
	RSU
1297	α-helix
1230	β-sheets
1247	Unordered

Table 4.5: Characteristic Raman bands of the aromatic amino acids

Wavenumber (cm^{-1})	Assignment
	ATCase
I_{850}/I_{830}= 0.839	Tyrosine
I_{1360}/I_{1340}= 1.17	Tryptophan
976	Phenylalanine
	CSU
I_{850}/I_{830}= 0.903	Tyrosine
I_{1360}/I_{1340}= 0.831	Tryptophan
976	Phenylalanine
	RSU
I_{850}/I_{830}= 0.921	Tyrosine
-	Tryptophan
976	Phenylalanine

4.4 Summary

Examination of the FT-Raman spectra of ATCase and its isolated subunits RSU and CSU components provided additional evidence in support of the FTIR spectroscopic studies. The RSU possessed predominantly β-sheets and CSU possessed predominantly α-helical structures. The crystal structure of CSU within the holoenzyme confirms that tyrosines and tryptophans are surface exposed (Williams et al. 1998); this was also confirmed by the intensity of the ratios obtained from the Raman spectra. Conformational changes are observed in both the RSU and CSU when they are combined to form ATCase. In particular, the change in the relative intensities of the I_{1360}/I_{1340} of tryptophan indicates that RSU binding to CSU results in shielding some of the tryptophan groups from solvent. Moreover, the interaction of RSU and CSU exposes the tyrosine residues to a more hydrophilic environment, as indicated by the relative intensities I_{850}/I_{830}.

CHAPTER 5

Strategies for the Production of Segmentally Labeled Isotopic Proteins: Regulatory Subunit as a Model System

5.1 Introduction

The purpose of this chapter is to demonstrate how to ligate two independently expressed domains of the regulatory subunit (RSU) of *E. coli* aspartate transcarbamylase (ATCase) using intein technology. The genes encoding the two domains of RSU (allosteric and Zn-binding domains) were subcloned into a pTWIN1 vector from the IMPACT^{TM}-TWIN system. This novel system allows each of the two RSU domains to be expressed as fusion proteins with an intein-chitin binding domain (IPL). Affinity purification with a chitin resin, is followed by a change in pH and/or an addition of a thiol reagent to cleave the two RSU domains from their respective intein tags allowing the reactive ends of the two domains to ligate together to form a peptide bond by intein-mediated protein ligation (IPL). The ultimate goal of this work is to establish a strategy for the selective labeling of either the nucleotide or Zn-binding domain of RSU by ^{13}C and ^{15}N isotopes to aid in the elucidation of the unfolding pathway individual domains by isotope-edited FTIR spectroscopy in conjugation with 2D IR correlation analysis.

5.1.1 Application of Intein Technology to Study the Production of Segmentally Labeled RSU

In the present study, the RSU will be obtained from a plasmid that carries the *pyr*B-*pyr*I operon encoding the catalytic and regulatory subunits of ATCase, respectively. The gene *pyr*I is the region that will be amplified and consists of 153 amino acid residues. Crystallographic data of the holoenzyme suggests that the allosteric domain encompasses residues 1-99 and the Zn-binding domain residues 100-153 (Markby et al. 1991). Although residues 99 and 100 present the boundaries between the two domains, we have interrupted the two domains at sites that have an optimal amino acid sequence for cleavage from the intein tag and for protein ligation (see Chapter 2, Table 2.2).

According to the IMPACT TWIN (New England Biolabs) instruction manual, to facilitate cleavage at the C-terminus of the intein tag, the N-terminus of the target protein

(Zn-binding domain) is recommended to have either Cys-Arg, Gly-Arg, or Ser-Arg. Furthermore, to facilitate cleavage at the N-terminus of the intein, the C-termini of the other target protein (allosteric domain) should have a Met residue. A site that is surface exposed is also selected (if possible), to facilitate the cleavage reaction. Several different sites were proposed in order to facilitate separate expressions of the Zn-binding and allosteric domains. One site is located between residues Lys94 and Ser95. This region in the sequence is relatively surface exposed and near the interface of the two domains (see Figure 5.1). The DNA encoding this region was amplified by PCR and subcloned into the intein expression vector (Figure 5.2). The primers for the clones also contained gene changes to incorporate the following mutations. Lys94 was changed to Met and the Ser95 was changed to Cys, in order to fulfill the requirements for a successful cleavage/ligation site. An alternate cut site was proposed and located between residues Val83 and Asn84. It has been shown that a Zn-binding domain (amino acids 84-153) can be expressed and purified as a stable protein (Markby et al. 1991). Furthermore, residues 83-84 are relatively surfaced exposed. Accordingly, Val83 must be changed to Met, and Asn84 changed to Cys (IMPACT^{TM}-TWIN Instruction Manual). In both strategies, Arg proceeded Cys at the N-terminus of the Zn-binding domain (ie. Arg85 and Arg97). Separating the domains at these positions should not disrupt any major secondary structural segments of the proteins.

Another cleavage site proposed for the independent expression of the Zn-binding domain was at 99-100, a surface exposed loop between the domains. However, this site wasn't chosen because residues 100-153 were reported to be unstable when expressed and purified (Markby et al. 1991).

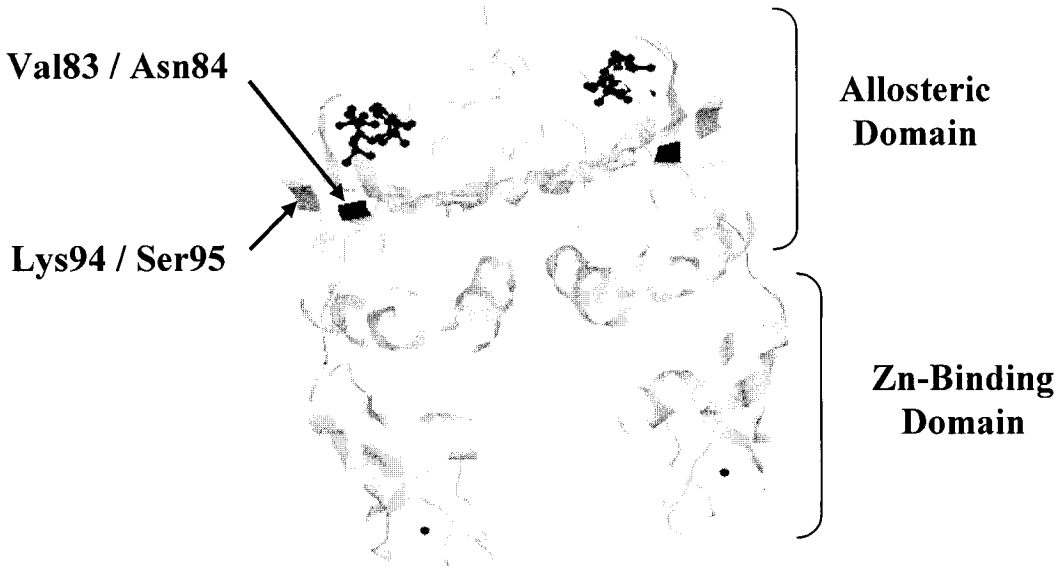

Figure 5.1: Crystal structure of the RSU dimer (Kosman et al. 1993). Two different sites were proposed in order to facilitate separate expressions of the Zn-binding and allosteric domains. These regions of the protein are relatively surface exposed and near the interface of the two domains. The sites are located between residues 94-95 and between residues 83-84.

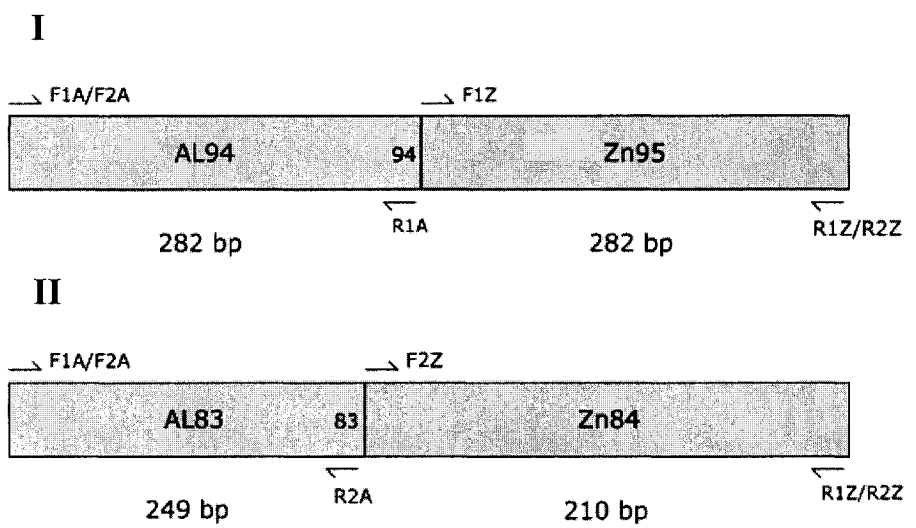

Figure 5.2: Two strategies for designing primers for the independent expression of the RSU domains. The DNA template pYY19RES from *E.coli* HS 1190 was used to amplify the two RSU domains by PCR.

5.2 Materials and Methods

5.2.1 Construction of Vectors Encoding Allosteric and Zn-Binding Domains

5.2.1.1 PCR Amplification of Allosteric and Zn-Binding Domains

Two plasmids, pTwAl94 and pTwAl83 were constructed for expression of the allosteric-intein fusion protein with allosteric fragments of different lengths. Al94 and Al83 in the plasmid names represent residues 1-94 and 1-83, respectively. Each gene was amplified separately using the plasmid pYY19RES as template DNA from HS1190 (a generous gift from H.K. Schachman). Figure 5.3 shows the cloning strategy for constructing the plasmids pTwAl94 and pTwAl83, as well as for pTwZn95 and pTwZn84. In order to insert the genes into the pTWIN1 vector, two restriction sites were introduced at both ends. *Nde*I was inserted at the 5'end and *Sap*I at the 3' end. All the primers were purchased from Biocorp, Montreal. The forward primer (F1A) for both Al94 and Al83 was 5' GGAAATACAT*ATG*ACACACG 3'. The reverse primer (R1A) for Al94 was 5' CGGCAGAGCTCTTCTGCA**CAT**ACCCACCACTTCATAG 3' and the other reverse primer (R2A) for Al83 was 5' CTTCATAGTTGGCTCTTCTGCA**CAT** CGTGGCTTGCGG 3'. Bases coding for restriction enzymes are underlined, and bases encoding the amino acid Met at position 94 and 83 are shown in bold. Also, this domain requires a start codon (shown in italic) since it will have an intein fused to its C-terminal end.

The Zn-binding domain (Zn95 and Zn84) was amplified using forward (F1Z, F2Z) and reverse (R1Z) primers. The primers introduced two restriction sites both at the 5'end and 3'end of the gene, *Sap*I and *Pst*I, respectively (underlined) and the residue Asn 84 and Ser94 of the Zn-binding domain was changed to Cys (bold). The forward primer (F1Z) for Zn95 was 5'CTATGAAGGCTCTTCTAA**CTG**CCGCCCAAGTCTG 3' and the other forward primer (F2Z) for Zn83 was 5' GCGCCGCGCTCTTCTAA**CTG** CCGTATCGACAAC 3' and the reverse primer (RZ) for both Zn95 and Zn84 was 5' CCAACTGCAG*TTA*ATTGGCCAGCACCAC 3' (BioCorp). The bases that were changed to incorporate restriction enzymes are shown in bold. The Zn-binding domain requires a stop codon (italic) since an intein is fused to its N-terminal.

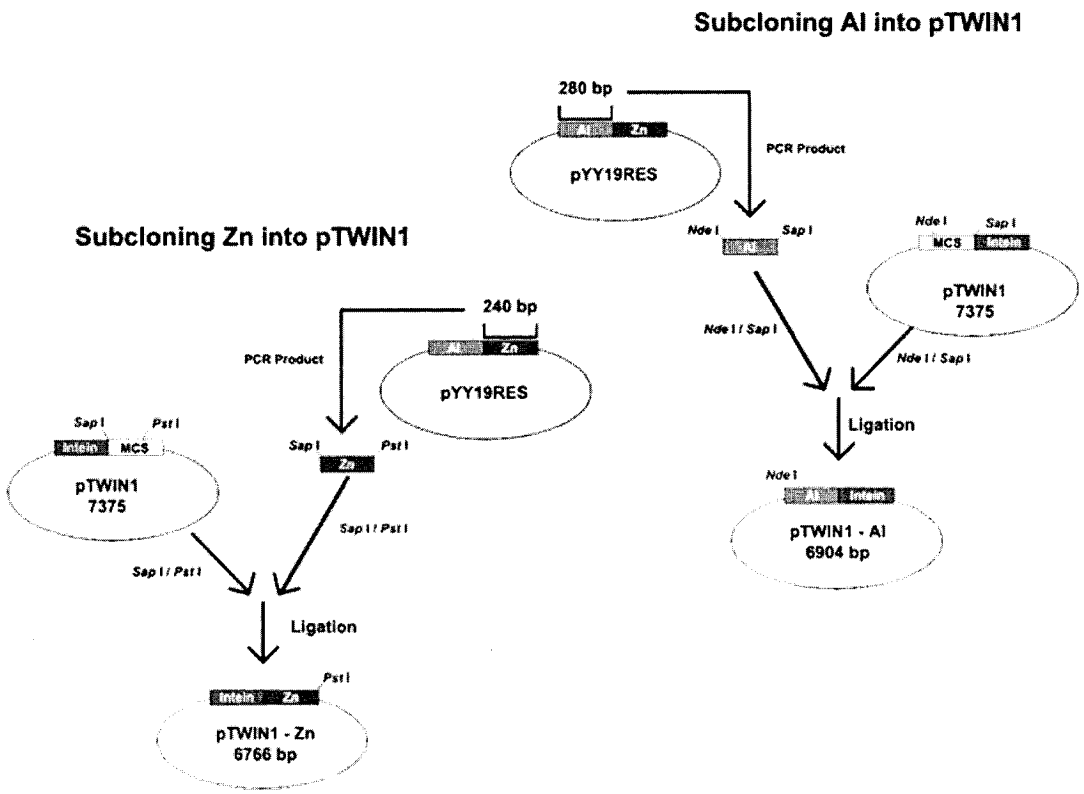

Figure 5.3: Schematic illustration of subcloning the PCR products (Al83 and Zn84) into intein expression vector pTWIN1.

The PCR reactions (of 100 µl reaction volume) were performed in triplicate and were pooled to have a total of 300 µl of solution. Each PCR reaction for Al94 and Al83 included: 76.5 µl ddH_2O, 1 µl pYY19RES (60 ng/µl), 1 µl F1A (20 µM), 1 µl of R1A or R2A (20 µM), 7 µl $MgCl_2$ (25 mM) (MBI, Fermentas), 10 µl of 10X PCR Buffer (MBI, Fermentas), 3 µl of deoxynucleoside triphosphates (dNTPs) (10 mM each) (MBI, Fermentas). The PCR reaction was held in a thermocycler, and programmed with a hot start at 94°C for 30 sec to add 0.5µl *Taq Polymerase* (5 U/µl) (MBI, Fermentas) to the solution. The program for amplification involved denaturation at 94°C for 1 min, annealing at 50°C for 1 min, and extension for 72 °C for 1 min. The PCR reaction repeated 25 times in total with the final extension at 72°C for 10 min to end the reaction. Amplification of Zn95 and Zn84 followed the same conditions with the exception of the primers (see above). The PCR products were purified using a PCR purification kit (Qiagen) according to the manufacturer's instructions and were verified by 1% agarose gel. Elution buffer was 50 µl of 10 mM Tris buffer, pH 8.0.

5.2.1.2 Restriction Enzyme Digestion and Purification of Double Digested PCR Fragments

Al94 and Al83 fragments (purified as described above) were digested with 2 restriction enzymes, *Nde*I and *Sap*I. The total reaction volume was 50 µl and included: 43 µl (~0.6 µg/µl) of Al94 or Al83 in 10 mM Tris-HCl, pH 8.0, 5 µl of 10X NEBuffer 4 (New England Biolabs), 1 µl *Nde*I (20,000 U/ml) (New England Biolabs), and 1 µl *Sap*I (2,000 U/ml) (New England Biolabs). The incubation took place in a 37°C water bath for 2 hr. The purified Zn95 and Zn84 PCR products were digested with two enzymes separately, first with *Sap*I, then with *Pst*I. The digestion with *Sap*I contained a total reaction volume of 50 µl and included: 43 µl (~0.6 µg/µl) of Zn95 or Zn84 in 10 mM Tris-HCl, pH 8.0, 5 µl of 10X NEBuffer 4 (New England Biolabs) and 1 µl of *Sap*I (2,000 U/ml) (New England Biolabs). The incubation also occurred in a 37°C water bath for 2 hr. Zn95 and Zn84 was digested with *Sap*I then purified by the Qiagen Kit and eluted with 50 µl of 10 mM Tris buffer, pH 8.0. The DNA was further digested with *Pst*I. The total volume of reaction was 50 µl and included: 43 µl of DNA (~0.6 µg/µl), 5 µl of 10X NEBuffer 3 (New England Biolabs, and 1 µl of *Pst*I (20,000 U/ml). The

mixture was placed at 37°C for 2 hr. These digested PCR products were gel purified as described below.

5.2.1.3 Restriction Enzyme Digestion and Purification of Double Digested pTWIN1

The vector pTWIN1 (200 ng/µl) must undergo two restriction enzyme digestions in order to allow insertion of Al94, Al83, Zn95 and Zn84 (prepared as described above). To accomplish this, the vector was first cleaved with the restriction enzyme *Sap*I, then with *Nde*I or *Pst*I. Briefly, the digestion was done with *Sap*I in duplicates, each with 20 µl aliquots and consisted of: 7 µl of ddH_2O, 10 µl pTWIN1 (200 ng/µl), 2 µl of 10X NEBuffer 4 (New England Biolabs), and 1 µl of *Sap*I (2,000 U/ml) (New England Biolabs). Incubation occurred in a 37°C water bath for 2 hr.

One 20 µl aliquot of pTWIN1 treated with *Sap*I was further digested with *Nde*I by adding 1 µl of *Nde*I (20,000 U/ml) (New England Biolabs) directly to the mixture for a total volume of 21 µl and incubating the solution for 1 hr in a 37°C water bath. The second 20 µl aliquot underwent digestion with *Pst*I. However, since *Pst*I is only 50% active in the buffer used for *Sap*I digestion, the DNA was precipitated by ethanol then resuspended in a buffer more compatible with this second digestion. Briefly, the pelleted DNA (pTWIN1 digested *Sap*I) was resuspended with 26 µl of ddH_2O then to it was added 3 µl of 10X NEBuffer 3 (New England Biolabs) and 1 µl of *Pst*I (20,000 U/ml) (New England Biolabs) to give a total reaction volume of 30 µl. The sample was incubated in a 37°C water bath for 2 hr.

PCR fragments and vector DNA were gel purified prior to further use. Briefly, Al94 and Al83 digested with *Nde*I and *Sap*I and Zn95 and Zn84 digested with *Sap*I and *Pst*I (50 µl each) were loaded onto a 1.0% agarose gel while their respective vectors, pTWIN1 digested with *Nde*I and *Sap*I (21 µl), and pTWIN1 digested with *Sap*I and *Pst*I (30 µl) were loaded on a 0.6% agarose gel. Electrophoretic separation was performed at 100 V for 1.5 hr. The DNA bands were visualized by using a UV transilluminator box at 312 nm and excised from the gel with a razor blade. The insert and its respective vector were purified together in the same eppendorf using the Qiagen Kit and the DNA mixture was eluted with 17 µl ddH_2O.

5.2.1.4 Ligation of the Digested PCR Fragments into pTWIN1

Four ligation reactions were prepared to construct pTwAl94, pTwAl83, pTwZn95 and pTwZn84. The constructs pTwAl94 and pTwAl83 should encode an intein fused to the C-terminus of the allosteric domain, and the constructs pTwZn95 and pTwZn84 should encode an intein fused to the N-terminus of the Zn-binding domain. Each ligation mixture included: 17 μl of the DNA mixture (~ 0.6 μg/μl) containing vector and PCR product (mentioned in the section above), 1 μl of T4 DNA Ligase (1 Weiss Unit/ μl, Promega), and 2 μl of 10X Ligase buffer (Promega) in a total reaction volume of 20 μl. The reaction occurred at 16°C overnight in a water bath.

5.2.1.5 Transformation

Recombinant plasmids pTwAl94, pTwAl83, pTwZn95 and pTwZn84, along with their respective controls were used to transform competent *E. coli* cells, DH5α. Under sterile conditions, 200 μl of DH5α were added to 10 μl of DNA and incubated on ice for 40 min. Following incubation, the solution underwent heat shock (45 sec at 42°C), and cooled on ice for 1 min. A volume of 800 μl of LB was added to the solution, and the cells were grown at 37°C, with 150 rpm of shaking for 1 hr. After incubation, 100 μl of solution were plated onto fresh LB plates that were supplemented with ampicillin (~100 μg/ml final concentration per plate). The plates were incubated at 37°C overnight.

5.2.1.6 Screening Transformants with Inserts

Single colonies were randomly selected from the LB plates containing the transformants. The plasmid DNA was purified using the alkaline lysis minipreparation.

5.2.1.7 Verification of Constructs pTwAl94, pTwAl83, pTwZn95 and pTwZn84

Screening for positive pTwAl94 and pTwAl83 transformants was performed by randomly choosing 24 colonies from the transformation plates and purifying the plasmids using the alkaline lysis minipreparation (Sambrook and Russell, 2001). The purified plasmid was eluted with 50 μl of TE buffer (10 mM Tris-HCl (pH 8.5), 1 mM EDTA) and stored at –20°C until further use. The purified plasmids underwent restriction enzyme analysis to verify that the inserts were present in these positive transformants.

Two following methods were used: (1) Plasmids were digested with *Bgl*II since this restriction site is found only in the insert Al94 and Al83. The reaction consisted of: 6.5 µl of ddH_2O, 2 µl (~0.6 µg/µl) of purified plasmid DNA, 1 µl of 10X REACT3 (GibcoBRL), and 0.5 µl *Bgl*II (10 U/µl) (GibcoBRL) for a total volume of 10 µl. The samples were incubated in a 37°C water bath for 1 hr. Resolving the linear DNA (containing vector plus insert) on a 0.7% agarose gel should yield a product of 6.8 kbp. (2) Plasmids were digested with *Nde*I and *Aat*II then the size of the vector and insert DNA were verified by 1% agarose gel electrophoresis using a 1 kbp ladder as a size marker. The digestion reaction included: 6 µl of ddH_2O, 20 µl (~0.6 µg/µl) of purified plasmid, 3 µl of 10X NEBuffer 4 (New England Biolabs), and 1 µl of *Aat*II (20,000 U/ml) (New England Biolabs) for a total reaction of 30 µl. Following the incubation in a 37°C water bath for 1 hr, 1 µl of *Nde*I (20,000 U/ml) (New England Biolabs) was added to the mixture and incubated under the same conditions.

Positive transformants pTwZn95 and pTwZn84 were identified by randomly choosing 12 colonies from the transformation plates and purifying the DNA by alkaline lysis method. Presence of the plasmids was verified by running them on a 0.6% agarose gel. From this analysis, six colonies (out of 12 samples) were strategically selected for further analysis. Their plasmids were isolated by the Wizard kit (Promega) due to protein contamination of the sample while using the alkaline lysis method, i.e. the DNA wasn't pure. The plasmids were eluted from the minicolumn with 50 µl of TE buffer and stored at –20°C until further use. A single digestion with the restriction enzyme *Eco*RV was performed since pTwZn84 has two *Eco*RV sites, one in the Zn84 insert and the other in the vector DNA. The digestion included: 14.5 µl of ddH_2O, 3 µl (~ 0.6 µg/µl)of purified plasmid, 2 µl of 10X Buffer B (Boehringer) and 0.5 µl *Eco*RV (10 U/µl) (Boehringer). The samples were incubated in a 37°C water bath for 1hr. The results of digestion were analyzed by subjecting the samples to 1.0% agarose gel electrophoresis using a 1 kb ladder as a marker. If the genes were successfully inserted into the vector then digestion of plasmid DNA with *Eco*RV should yield DNA fragments of sizes ~ 3.0 kb and ~ 4.0 kb.

Another clone was reconstructed to encode three stop codons at the C-terminal end of the Zn-binding domain gene, pTw-mZn84 where 'm' corresponds to modified Zn84. The procedures used to amplify and ligate the mZn84 gene into the pTWIN1 vector were the same for Zn84, with the exception of the reverse primer for PCR: 5' GCCAACTTTTAT**CTGCAG***TTATTATTA*ATTGGCCAGCACCAC 3' (Biocorp, Montreal). The bases that incorporated the restriction enzyme *Pst*I are shown in bold and the three stop codons are shown in italic. Verification of these clones was achieved by restriction analysis with *Bgl*II (10 U/μl) (GibcoBRL). DNA sequencing of the new plasmid pTw-mZn84 (modified with three stop codons) was performed to verify that the gene was subcloned correctly, and the DNA sequence was in-frame and 100% correct.

After confirmation, the successfully cloned constructs were transformed into *E.coli* strain ER2566 (New England Biolabs) using the same procedures as outlined previously. This strain is suitable for the expression of the intein-tagged fusion proteins (IMPACT^{TM}-TWIN Instruction Manual). In addition, each vector was sent for DNA sequencing (Bio S & T, Montreal) to confirm the correct ligation of the insert into the pTWIN1 plasmid.

5.2.2 Over-Expression of the Allosteric and Zn-Binding Domain-Intein Fusion

The constructs pTwAl94, pTwAl83, pTwZn95 and pTwZn84 in ER2566 were streaked out on LB plates supplemented with ampicillin (100 μg /ml final concentration) and grew overnight at 37°C. An overnight culture was prepared by inoculating a single colony into 10 ml of LB/amp (100 μg /ml final concentration) and grew at 37°C with 250 rpm shaking. A 500 ml LB/amp broth was inoculated with the freshly prepared overnight culture and grew at 37°C with 250 rpm shaking until the OD_{600} reached ~ 0.5. Protein expression was induced by the addition of isopropyl-B-D-thiogalactoside (IPTG) to a final concentration of 0.3 mM before transferring the culture into 15°C air shaker. The induction allowed to continue overnight (16 hr) with shaking at 250 rpm. The cells were then harvested by centrifuging the culture at 5000 x g for 15 minutes at 4°C. The supernatant was discarded and the cell pellets were stored at -20°C until further use.

5.2.3 Affinity Purification of Fusion Proteins, Induction of On-Column Cleavage, and Elution of the Allosteric Domain

All purification procedures were performed at 4°C. Purification of the allosteric domain (purified from a 500 ml culture) was performed using a column of 5 ml of chitin beads bed volume (NEB) in an Econo-Column (2.5 cm x 10 cm, Bio-Rad, Hercules, CA). The chitin column was equilibrated with 200 ml of Buffer B2 (20 mM Tris-HCl (pH 6.5), 500 mM NaCl, 1 mM EDTA). The cell pellet from a 500 ml culture was resuspended with 25 ml of cold cell lysis Buffer B2 supplemented with a protease cocktail containing 5 μg/ml each of leupeptin, pepstatin and antipain and 170 μg/ml PMSF as final concentrations. The cells were then lysed by using a French Press (2 passages) then ultracentrifuged at 45 000 x g for 45 min to obtain the clarified cell extract or supernatant. The remaining cell pellet was saved and resuspended with 25 ml of Buffer B2 for analysis.

The clarified cell extract was loaded onto the equilibrated chitin column at a flow rate of 0.5-1 ml/min. The chitin column was then washed with 100 ml of Buffer B2 at a rate of 2 ml/min. The column buffer was exchanged by washing the chitin resin with 20 ml of Buffer B4 (20 mM Tris-HCl, **pH 8.0,** 500 mM NaCl, **100 mM MESNA**, 1 mM EDTA) at a rate of 1 ml/min. This buffer is necessary for the generation of a thioester-tagged protein for intein-mediated protein ligation. After the wash, the column was stoppered and on-column cleavage reaction proceeded overnight (12-18 hr). The allosteric domain was then eluted by washing the column with 20 ml of Buffer B4 and fractions (1.5 ml in an eppendorf tube) were collected and stored at 4°C. Protein concentrations were estimated by using a BioRad assay (Bradford 1976).

Figure 5.4 shows the chemistry of the cleavage reaction. By incubating the chitin-bound fusion protein (~38 kDa) with thiol-compounds, causes the N-S acyl shift rearrangement at the Cys1 of the intein to form a linear thioester intermediate. Next, the nucleophillic attack by the sulfur containing side of a thiol reagent causes the excision of the allosteric domain protein (9 kDa) to yield a reactive C-terminal thioester. It is this reactive group that is necessary for ligating to the Zn-binding domain.

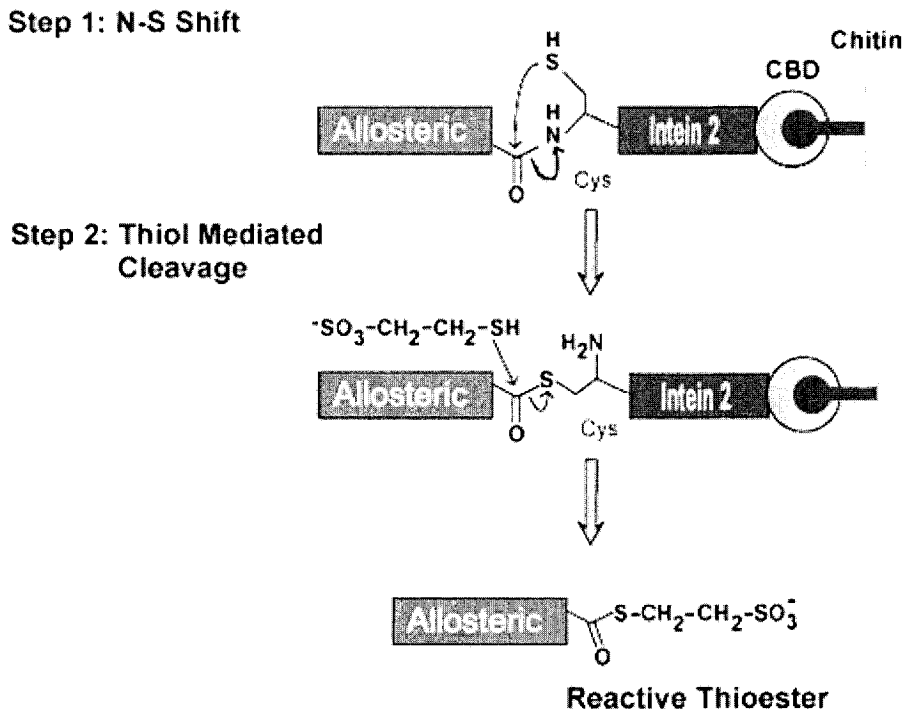

Figure 5.4: Chemistry of the cleavage reaction releasing the allosteric domain from the intein tag, resulting with a reactive thiosester at its C-terminus.

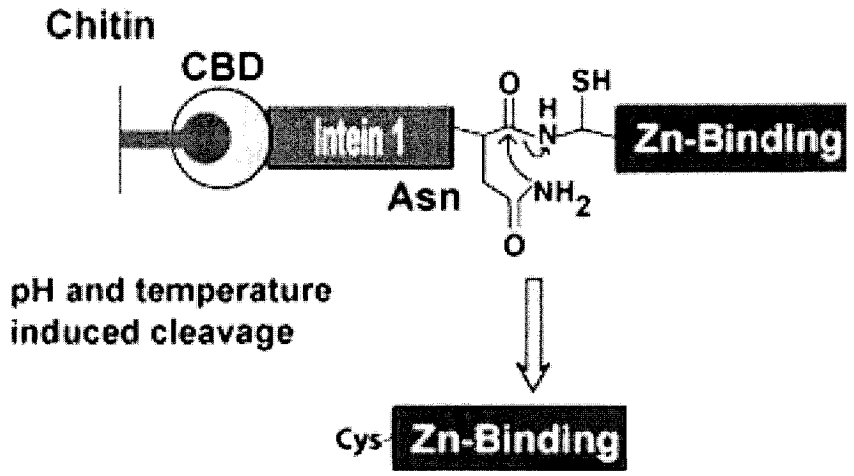

Figure 5.5: Chemistry of the cleavage reaction releasing the Zn-binding domain from the intein tag, resulting with a cysteine at its N-terminus.

5.2.4 Affinity Purification of Fusion Proteins, Induction of On-Column Cleavage, and Elution of the Zn-Binding domain

Procedures were performed as described for the allosteric domain (Section 5.2.3) except with the following modifications: Buffer B1 (20 mM Tris-HCl **pH 8.5**, 500 mM NaCl, 1 mM EDTA) was used for cell lysis as well as column equilibration and washing. Induction of on-column cleavage from the intein tag was initiated by exchanging the column buffer for Buffer B2 (20 mM Tris-HCl, **pH 6.5**, 500 mM NaCl, 1 mM EDTA). This buffer is necessary for the generation of an exposed N-terminal Cys for intein-mediated protein ligation. The on-column cleavage reaction proceeded overnight (12-18 hr) at **25°C**. The Zn-binding domain was then eluted with 20 ml of Buffer B2 (fraction size 1.5 ml) and stored at 4°C. Figure 5.5 (previous page) shows the chemistry behind the cleavage reaction. This one step reaction causes a specific rearrangement between the Asn at the C-terminal of the intein and the Cys at the N-terminus of Zn-binding domain, succinimide formation occurs causing the release the Zn-binding domain protein that houses an N-terminal Cys for IPL.

The protein concentration of each fraction was determined by Bio-Rad and analyzed by SDS-PAGE. In addition, protein was stripped from 200 µl aliquot of the chitin resin according to the IMPACT^{TM}-TWIN system Instruction Manual and analyzed by SDS-PAGE to verify the cleavage efficiency.

5.2.4.1 Verification of Zn-Binding Domain-Intein Fusion by Western Blot Analysis

The soluble protein was resolved by SDS-PAGE (15 % acrylamide) and the gel was placed on a piece of nitrocellulose membrane that was pre-soaked in semi-dry transfer buffer (39 mM glycine, 48 mM Tris, 0.037 % SDS, 20% v/v methanol, pH 9.2). The transfer of proteins from the gel onto the nitrocellulose membrane was achieved by layering them between 2 pieces of filter paper (2 mm thick) that was pre-soaked in the same buffer. A Semi-dry Western Blotting Transfer machine (BioRad) was used at 15 V for 15 min. The membrane was then washed with TBS (20 mM Tris-HCl pH 7.5, 0.5 M NaCl) for 15 min, then blocked with 5% skim milk at 4°C overnight and rinsed twice with 15 ml TTBS (20 mM Tris-HCl (pH 7.5), 0.5 M NaCl, 0.05% v/v Tween 20) for 15 min with gentle agitation.

The membrane was then incubated with 10 ml of 1:5000 diluted primary antibody (polyclonal anti-chitin binding domain, NEB) in TTBS at room temperature for 1 hr with gentle agitation. The membrane was then washed twice with TTBS for 15 min at room temperature, then incubated the membrane with 10 ml of 1:7500 diluted secondary antibody (anti-rabbit IgG (Fc)), alkaline phosphatase conjugate, Promega) in TTBS for 1hr at room temperature with gentle agitation. The membrane was then washed twice with TTBS for 15 min, and TBS for 15 min, then transferred to 10 ml of reaction buffer (100 mM Tris-HCl, pH 9.5; 100 mM NaCl, 5 mM $MgCl_2$, 0.66 % v/v NBT (nitro blue tetrazolium, 50 mg/ml, Promega), 0.33 % v/v BCIP (5-bromo-4-chloro-3-indolyl-phosphate, 50 mg/ml, Promega) and shaken with gentle agitation until bands appeared on the membrane. The reaction was stopped by discarding the transfer buffer and washing with ddH_2O. The membrane was then blotted dry and stored in the dark.

5.2.4.2 Verification of Zn-Binding Domain-Intein Fusion by MALDI-MS

The dried protein samples were dissolved in 10 µl of 5 % MeOH, 0.1 % TFA and de-salted with a $ZipTip_{C18}$ from Millipore. 1.5 µl of 60% ACN and 0.1% TFA were used to elute the peptides bound to the $ZipTip_{C18}$ column. To this 1.5 µl of sinapinic acid (saturated solution in 60 % dH_2O, 40 % ACN, 0.06 % TFA) matrix was added and 1 µl of the mixture was spotted on a stainless steel MALDI (matrix assisted laser desorption ionization) target plate. MALTI-ToF analysis was performed on a Micromass MALDI-LR mass spectrometer. A nitrogen laser source (337 nm) was pulsed at a rate of 5 Hz. A pulse voltage of 1737 V was used to accelerate the ions into the flight tube in linear mode. A microchannel plate detector was used to detect the ions. The instrument was calibrated with three external standards, cytochrome C (12360 Da), myoglobin (16951 Da) and trypsinogen (23980 Da). The instrument is capable of mass accuracy of 300 ppm as tested for trypsinogen and resolution of 1000 as tested for cytochrome C. Each spectrum is an accumulation of 25 shots. Data acquisition and analysis were performed with the MassLynx 4.0 package.

5.2.5 Protein-Protein Ligation Using IPL

Freshly isolated allosteric domain (thioester-tagged) (7.5 ml) and Zn-binding domain (containing N-terminal cysteine residue) (7.5 ml) were mixed together at 4°C. Starting concentrations for each domain were between 1-200 μM. The solution was concentrated using the Centriprep YM-3 (Millipore) apparatus to yield a final between 0.15-1.2 mM for each protein (Evans et al. 1999). The solution was supplemented with 0.1 mM Zn chloride and 1mM β-mercaptoethanol and incubated at 4°C overnight to facilitate the ligation reaction.

Cleavage from the intein tags produces reactive ends necessary for protein ligation. The allosteric domain possesses the C-terminal thioester, and the Zn-binding domain houses a reactive N-terminal Cys. Mixing the two domains together and concentrating the protein solutions (before or after mixing) should facilitate a chemo-selective reaction followed by an S-N acyl shift to form a peptide bond (Figure 5.6). As a result, the two domains should ligate together and create an intact RSU.

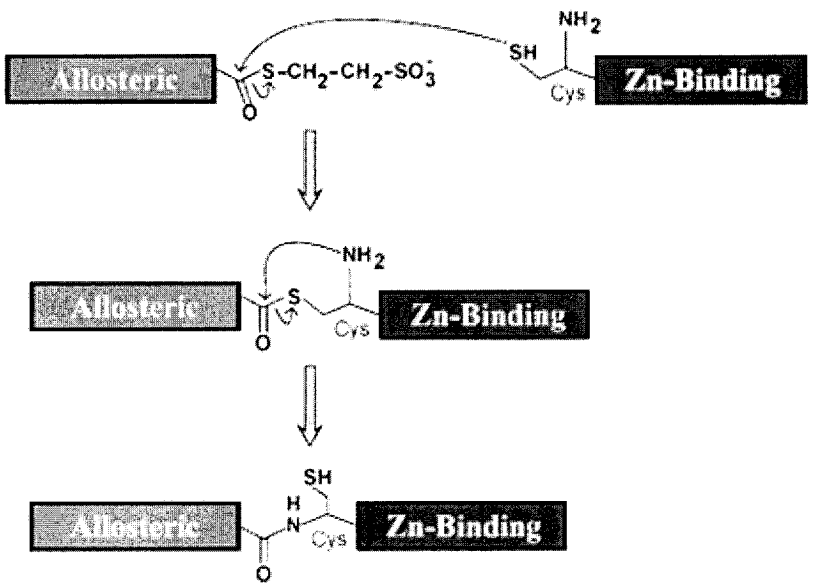

Figure 5.6: Chemistry of ligating the allosteric domain with the Zn-binding domain. Mixing and concentrating the two domains should facilitate a chemo-selective reaction, followed by an S-N acyl shift to form a peptide bond.

5.3 Results and Discussion

5.3.1 Construction of Vectors Encoding Allosteric and Zn-Binding Domains

PCR amplification of genes Al94 (Figure 5.7A) and Al83 (Figure 5.8) was conducted at annealing temperature of 50°C, whereas mZn95, mZn84, (Figure 5.7B) and Zn84 (Figure 5.8, lane 3) was conducted at 53 °C and 45 °C, respectively. The yields of the PCR products were adequate and they ran as expected based on predicted sizes of 281 bp and 241 bp for Al83 and Zn84, respectively (Figure 5.8, lanes 2 and 3). A faint band above the main dark band of mZn95 and mZn84 was observed (Figure 5.7B and Figure 5.8), suggesting that non-specific binding of primers to the template DNA had occurred. Increasing the temperature to 55°C did not eliminate the second weaker band in lane 3 (data not shown).

The concentration of $MgCl_2$ used in the PCR reaction greatly affected the yield of products since *Taq* polymerase is Mg^{2+}-dependent. After numerous trials, 7µl of 25 mM $MgCl_2$ (final concentration of 1.75 mM) was found to be the optimum concentration required for the reactions. *Taq* polymerase was chosen because of its relatively low cost and high efficiency in amplifying short fragments of DNA (Davis et al. 1994).

In order to ligate the genes encoding the allosteric or Zn-binding domain into the multiple cloning site of the vector pTWIN1, the PCR products and the vector first had to be digested with the appropriate restriction enzymes (Figure 5.3: Cloning Strategy). Al genes were then ligated into pTWIN1 to allow expression of the allosteric domain fused with an intein at its C-terminus, while Zn genes were inserted into pTWIN1 to yield the Zn-binding domain fused at its N-terminus to an intein. The amplification of the Al94 and Zn95 genes were successful and in adequate quantities, however, inserting the gene into the double digested vector resulted in low yield, i.e. the quantity of Zn95 after digesting with *Sap*I and *Pst*I was too low to observe on the 1% agarose gel. Due to time constraints, the ligation of Al94 and Zn95 into the pTWIN1 vector was not performed.

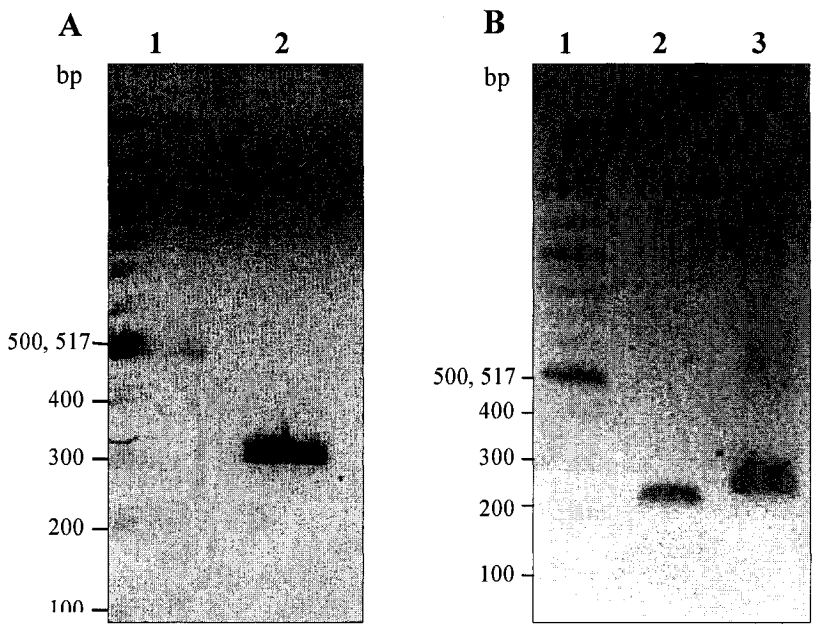

Figure 5.7: **A.** Verification of PCR product Al94 by a 1 % agarose gel. Lane 1: 100 bp DNA ladder (New England Biolabs); lane 2: PCR product Al94. **B.** Verification of PCR products by a 1% agarose gel electrophoresis. Lane 1: 100 bp DNA ladder (New England, Biolabs); lane 2: PCR product mZn95; lane 3: PCR product mZn84.

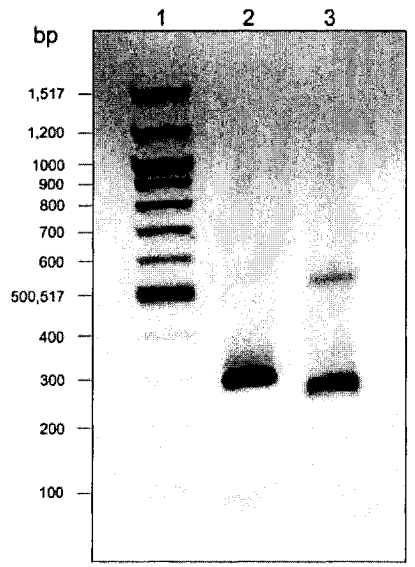

Figure 5.8: Verification of PCR products Al83 and Zn84 by a 1% agarose gel electrophoresis. Lane 1: 100 bp DNA ladder (New England Biolabs); lane 2: PCR product Al83; lane 3: PCR product Zn84.

After digestion of Al83 and Zn84 with their respective restriction enzymes, they were ligated separately into double digested pTWIN1 vector. Positive transformants of pTwAl83 were identified by restriction enzyme analysis of the plasmid DNA isolated from randomly picked colonies (see Materials and Methods). Since the insert Al83 was ligated into the *Nde*I and *Sap*I sites of the pTWIN1 vector's multiple cloning site, these enzymes would have been the most suitable for confirmation. However, the *Sap*I site was deleted after the ligation reaction and hence this enzyme cannot be used (IMPACT^{TM}-TWIN system Instruction Manual). DNA was analyzed by digestion with a single restriction enzyme *Bgl*II, and by double digestion with *Aat*II and *Nde*I as described in Materials and Methods. The results of the electrophoretic separation are shown in Figures 5.9 A and B, respectively. The enzyme *Bgl*II was used because the restriction site for *Bgl*II is found only in the insert Al83. As excepted, digestion with *Bgl*II yields a single 6.8 kb fragment

Positive transformants of pTwZn84 were also identified by restriction enzyme analysis of the plasmid DNA isolated from randomly picked colonies. Figure 5.10 confirms that the size of the purified uncut plasmid has the correct size of ~ 7.0 kb, which is close to its predicted size of 6.7 kb. Also, the sample digested with *Eco*RV (Figure 5.10, lane 3) resulted in two DNA fragments of ~3.0 and 4.0 kb, which are close to the expected fragment sizes of 2.9 kb and 3.8 kb.

In conclusion, both pTwAl83 and pTwZn84 constructs were verified to have the correct sizes of 6.8 kb and 6.7 kb, respectively. Commercial DNA sequencing was performed to confirm the nucleotide sequences of the inserts; they were indeed successfully ligated in-frame into the pTWIN1 plasmids.

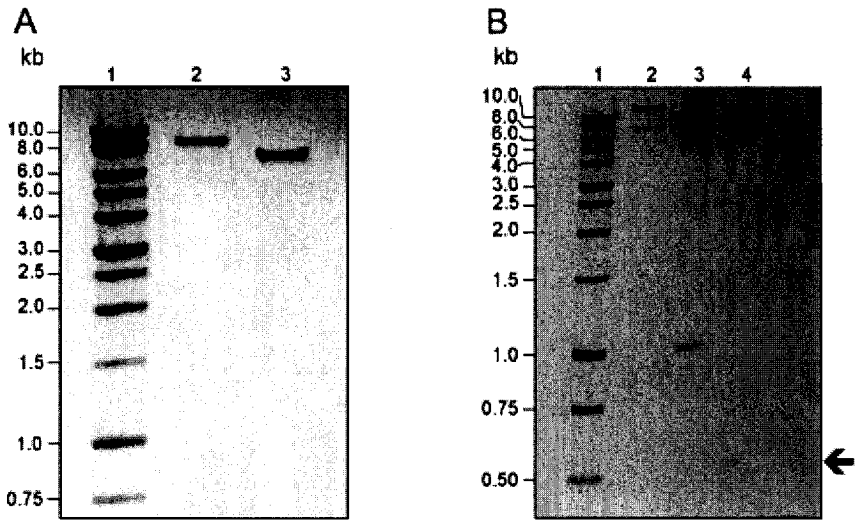

Figure 5.9: Confirmation of pTwAl83. **A.** Verification of pTwAl83 digested with *Bgl*II by a 0.7% agarose gel electrophoresis. Lane 1: 1kb DNA ladder (Promega); lane 2: purified undigested pTwAl83; lane 3: purified pTwAl83 digested with *Bgl*II. **B.** Verification of pTwAl83 digested with *Nde*I and *Aat*II by a 1% agarose gel electrophoresis. Lane 1: 1kb DNA ladder (Promega); lane 2: purified undigested pTWIN1; lane 3: purified pTWIN1 digested with *Nde*I and *Aat*II releasing an insert (arrow) ; lane 4: purified pTwAl83 double digested with *Nde*I and *Aat*II.

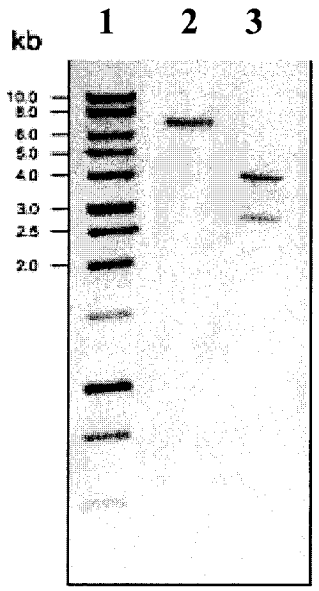

Figure 5.10: Confirmation of pTwZn84. Verification of pTwZn84 digested *Eco*RV by a 0.7% agarose gel electrophoresis. Lane 1: 1kb DNA ladder (Promega); lane 2: purified undigested pTwZn84; lane 3: purified pTwZn84 digested with *Eco*RV.

5.3.2 Optimization of Intein Fusion Protein Expression

Intein fusion protein has been used to purify target proteins from their recombinant precursors without the addition of exogeneous proteases (Chong et al. 1997; Chong et al. 1998; Evans et al. 1999). In our study, the allosteric domain was fused to the N-terminus or upstream of an intein while the Zn-binding domain was fused to the C-terminus (downstream) of a second intein. Figure 5.11 outlines the overall strategy of intein-mediated protein ligation (IPL) for the RSU. Two constructs were designed to purify the two domains of the regulatory subunit separately. The presence of the two fusion proteins are observed by analyzing the clarified cell extract (soluble protein) and the pellet (non-soluble protein) by SDS-PAGE (Figure 5.12 A and B). In this figure, the growth conditions of proteins from N- and C-terminal cleavage constructs were optimized for soluble protein overexpression using small test expression with 50 ml cultures. Protein expression was studied at varying cell growth temperatures and times by SDS-PAGE. Enrichment in soluble protein from both the N- and C- terminal cleavage constructs were observed by growing the cells at a lower temperature for a longer time (15^{o}C for 16 hr).

The expression of fusion proteins from a larger (500 ml) cell culture was also analyzed by SDS-PAGE (Figure 5.13). Regrettably, this gel shows that a significant amount of allosteric domain fusion protein, and was expressed as an insoluble fraction of the cell. For the Zn-binding domain fusion protein, two bands are visible; (shown in Figure 5.13, lane 6) one at ~38 kDa (the more highly expressed protein band) and one at 32 kDa (lighter band). Surprisingly, the weaker band (32 kDa protein) matched the predicted mass of the Zn fusion protein. The identity of the well expressed higher molecular weight protein was not obvious.

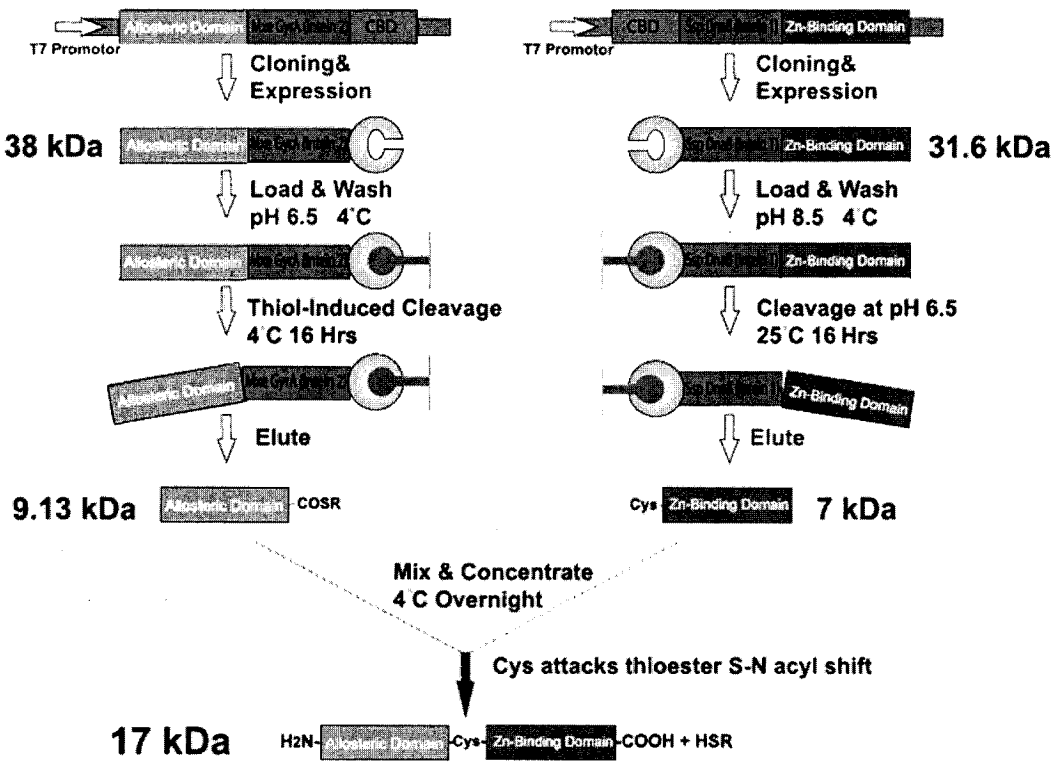

Figure 5.11: Overall strategy of intein-mediated protein ligation (IPL) of RSU. IPL reaction allows the ligation of the bacterially expressed Zn-binding domain with an N-terminal cysteine residue to the bacterially expressed allosteric domain with a C-terminal thioester to result in a peptide bond.

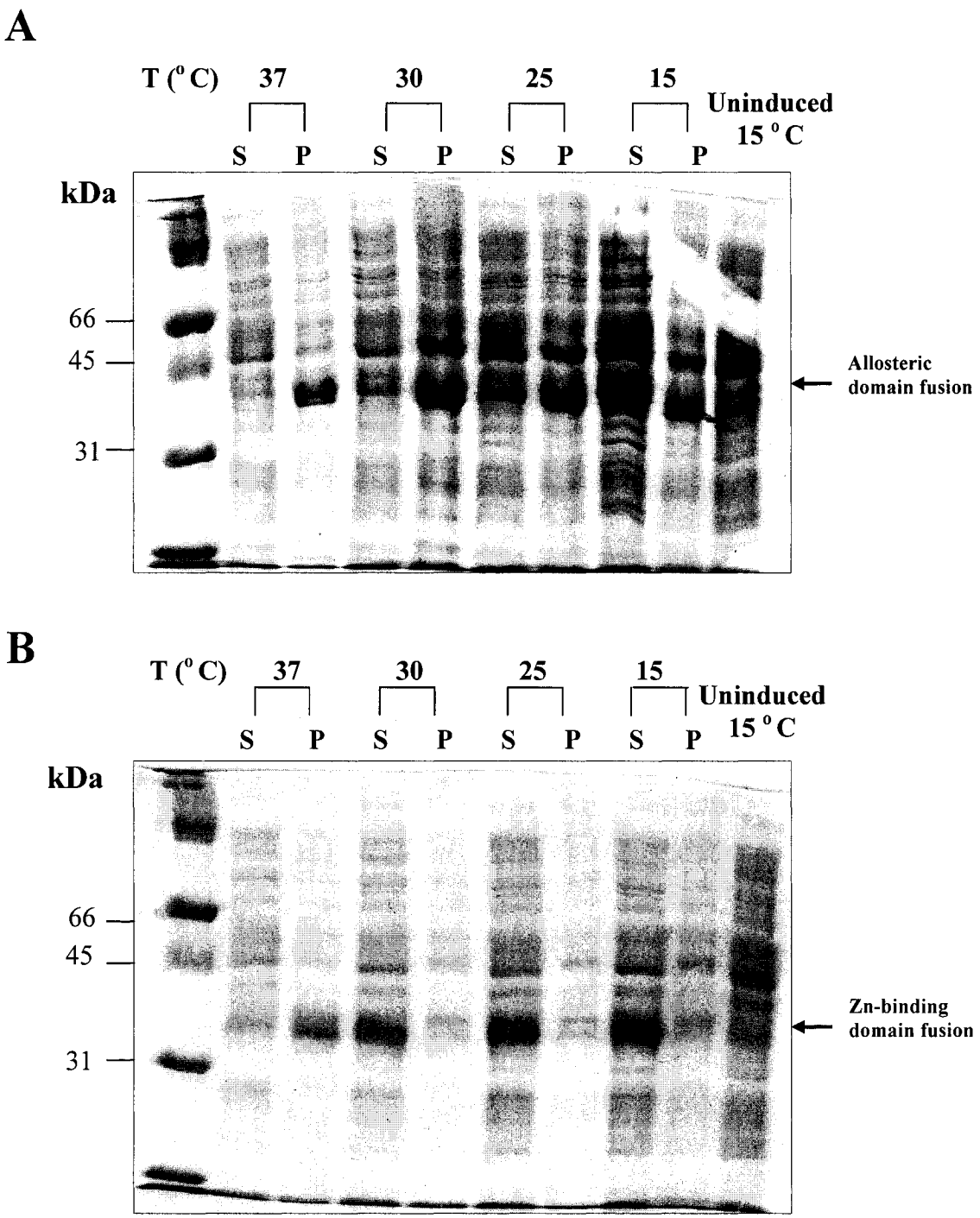

Figure 5.12: **A and B.** Growth conditions were optimized for soluble protein over-expression analyzed by SDS-PAGE (13% acylamide). Fusion protein was analyzed at varying temperatures and time; 37°C for 2 hr, 30°C for 3 hr, 25°C for 6 hr, and 15°C for 16 hr. Most soluble protein was observed by growing the cells at 15°C for 16 hr. This illustrates the increase of soluble protein band in the supernatant (S) and decrease in pellet (P) band with decreasing growth temperatures.

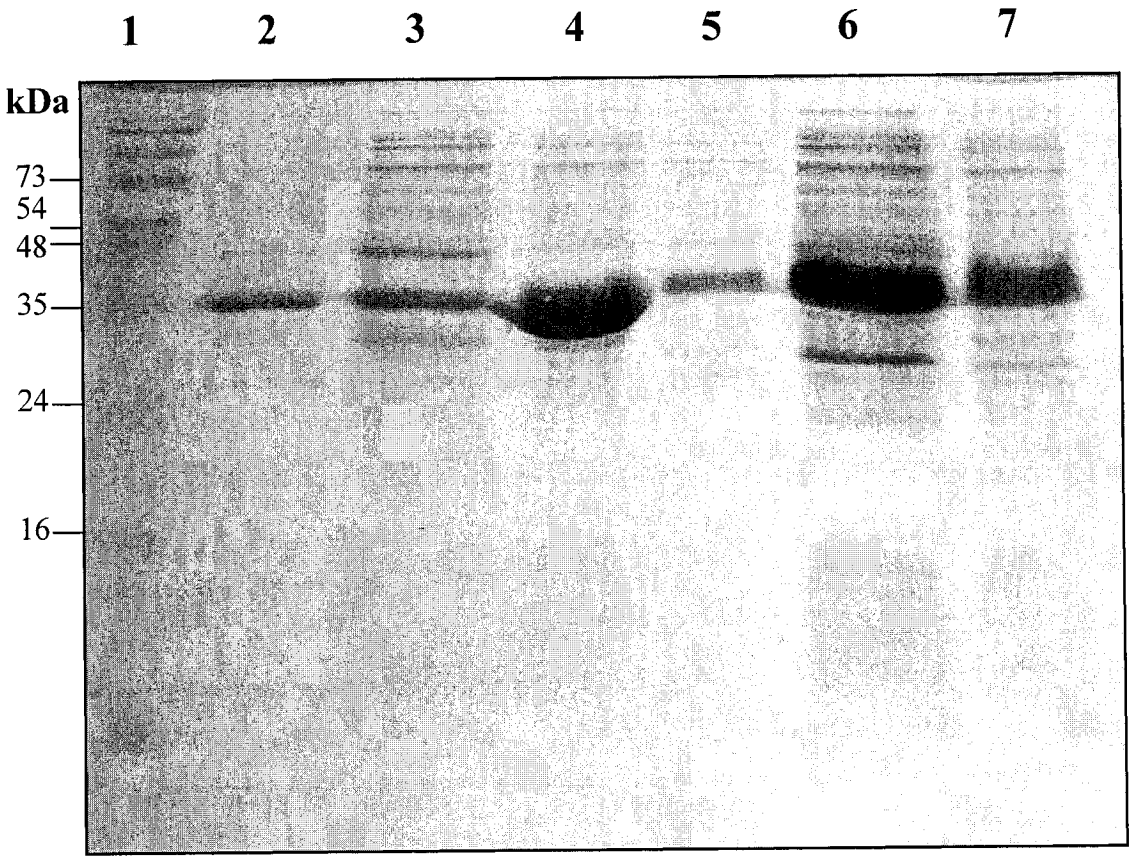

Figure 5.13: Over-expression of fusion proteins from a 500 ml cell culture analyzed by SDS-PAGE (13% acrylamide). Lanes 2-4 represents expression of allosteric fusion protein and Lanes 5-7 represents expression of Zn-binding domain fusion protein. Lane 1: molecular weight protein marker; lane 2: total cell extract following induction of protein expression diluted 1/20; lane 3: clarified cell extract (soluble protein); lane 4: pellet (non-soluble protein); lane 5: total cell extract following induction of protein expression diluted 1/20; lane 6: clarified cell extract (soluble protein); lane 7: pellet (non-soluble protein).

Several possibilities existed: (1) the well-expressed protein was our fusion protein of interest and was running anomalously on SDS-PAGE. The fainter band might represent the Zn-binding domain cleaved from the intein *in vivo*. (2) Both proteins were CBD fusion protein but the darker band on SDS-PAGE represented a protein larger than expected and expressed as a result of "reading through" the vector's termination codon and transcription termination loop. To address the second possibility, several Western Blot experiments were first performed with the polyclonal anti-CBD (provided with the IMPACT-TWIN kit) on the clarified cell extract of the Zn-binding-domain fusion (Figure 5.14 A and B). No antibodies were available to detect the presence of the RSU. The results from the Western Blot and SDS-PAGE analysis of the clarified cell lysate showed that the two proteins expressed (~32 kda and ~38 kda) and housed the CBD at their N-termini.

To determine if the expression of the higher molecular weight protein was due to a "read-through" problem, a modified clone (pTw-mZn84) was reconstructed to encode three successive stop codons at the 3' end of the Zn-binding domain gene. The results from the expression of the modified fusion protein are shown on a SDS-PAGE (Figure 5.15). The most prominent band has a molecular weight of ~38 kDa, similar to the protein transcribed without the two extra stop codons. As noted previously, a higher level of soluble fusion protein was obtained by growing the cells at 15°C for 16 hr.

MALDI-MS was then used to determine the mass of the two bands resolved by SDS-PAGE. Both the Zn-binding fusion protein (one stop codon) and the protein with three stop codons were analyzed. The results show that the heavier band had a mass of 33011.75 kDa and the lower band was at 26200.14 kDa (spectra not shown). The lower molecular weight species is most likely the degraded form caused by *in vivo* cleavage of the Zn-binding domain from the intein tag, since the Western Blot analysis confirmed that the protein houses a CBD at its N-terminus. Indeed, MS data confirmed that the Zn-binding fusion ran anomalously on a SDS-PAGE gel. Metal bound proteins have been noted to previously to migrate slower than expected by SDS-PAGE (personal communication with Dr. Armando Jardim, McGill University).

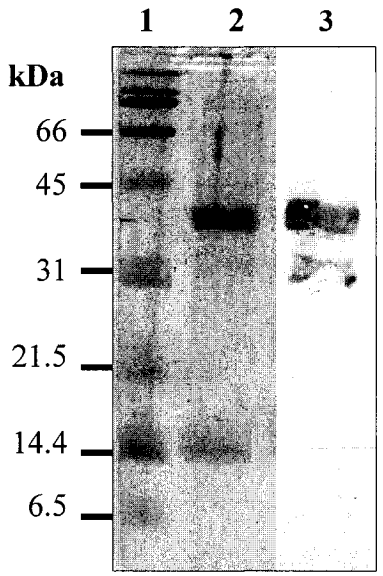

Figure 5.14: Coomassie stained gel (lanes 1 and 2) and western blot analysis (lane 3) of the supernatant containing the Zn-binding domain fusion protein (SDS-PAGE, 13% acrylamide). Lane 1: molecular weight protein marker; lane 2: clarified cell lysate; lane 3: western blot analysis of the clarified cell lysate using polyclonal anti-CBD provided by the IMPACT-TWIN kit.

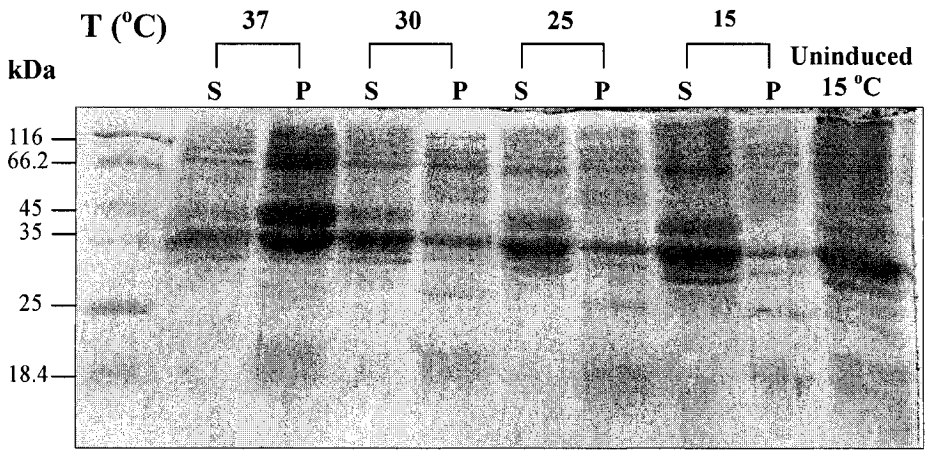

Figure 5.15: Growth conditions were optimized for soluble protein over-expression of the modified Zn-binding domain fusion protein (3 stop codons) analyzed by SDS-PAGE (13% acylamide). Fusion proteins were grown and analyzed at varying temperatures and time; 37°C for 2 hr, 30°C for 3 hr, 25°C for 6 hr, and 15°C for 16 hr. Most soluble protein was observed by growing the cells at 15°C for 16 hr.

An attempt to resolve this anomalous migration, a portion of the clarified cell extract was treated with 500 mM EDTA, but the fusion protein still ran at a molecular weight of ~ 38 kDa. The Western Blot analysis of both the N- and C- terminus constructs were also performed using a monoclonal anti-chitin binding domain (obtained by Tom Evans, New England Biolabs) as a probe of the clarified cell lysate (data not shown). The results confirmed that the allosteric domain fusion protein had a molecular weight of 38 kDa and the Zn-binding domain fusion protein was ~ 32 kDa.

The N-terminal cleavage construct (allosteric domain fused to the N-terminus of the intein tag) showed variability on its degree of expression. Test cultures of 50 ml, 500 ml, 1L and 2 L, differed greatly; the larger the culture, the greater the amount of insoluble protein expressed (SDS-PAGE data not shown). Previous labs have shown that there are higher levels of expression when the target protein is fused to the C-terminus not the N-terminus of the intein (Chong et al. 1998). This is due to the favorable amino acid sequence at the N-terminus of the intein-tag (supplied by the IMPACT kit). Hence, the lower expression level of the allosteric-domain fusion protein compared to the Zn-binding domain fusion protein agreed with the results found in literature. In addition, the protein expression may be related to the nature of the target protein (Evans et al. 1999).

5.3.3. Affinity Purification of Fusion Proteins, Induction of On-Column Cleavage, and Elution of the Allosteric Domain

Figure 5.16 shows the SDS-PAGE analysis of the expression and purification of the allosteric domain. After IPTG induction, the allosteric-intein fusion accumulated as a soluble product (observed in the clarified cell extract) (Figure 5.16, lane 2). After passing the supernatant over the chitin resin, most of the fusion precursor was bound, as indicated by the disappearance of the band in the last flow-through fraction (lane 3). The column was extensively washed to remove most nonspecifically bound proteins. (lanes 4 and 5). The column was then flushed with 100 mM MESNA and incubated overnight at **4 °C** to trigger the intein-mediated cleavage reaction. The allosteric domain (9 kDa) was expected to be released from the column bound intein-CBD protein. Unfortunately, negligible amounts of allosteric domain were obtained (lane 6). The SDS-PAGE analysis of the chitin resin after the cleavage reaction showed abundance of precursor in lane 7, in keeping with insufficient cleavage of the allosteric domain.

In order to increase the cleavage efficiency, the cleavage reaction was permitted to take place overnight at room temperature (25 °C) rather than 4 °C. In addition, Buffer B4 contained 50 mM NaCl rather than 500 mM NaCl for induction of on-column cleavage of the allosteric domain. The cleavage reaction was examined by taking a sample of the chitin resin after the induced cleavage reaction and analyzing the supernatant by SDS-PAGE. (Figure 5.17, lane 4). The sample was boiled before loading it onto the gel, and didn't contain any DTT in the sample buffer. Lane 4 shows that there are three prominent species; one at 38 kDa, one at 29 kDa and another at 9 kDa. These bands represent the uncleaved fusion protein, the intein-CBD tag and the allosteric domain, respectively. The allosteric domain was quite abundant, and is very promising. However, the eluate after overnight cleavage reaction did not contain protein of the expected molecular weight (9 kDa), rather only a band corresponding to the intein-CBD tag which presumably leached off the resin (29 kDa) (data not shown).

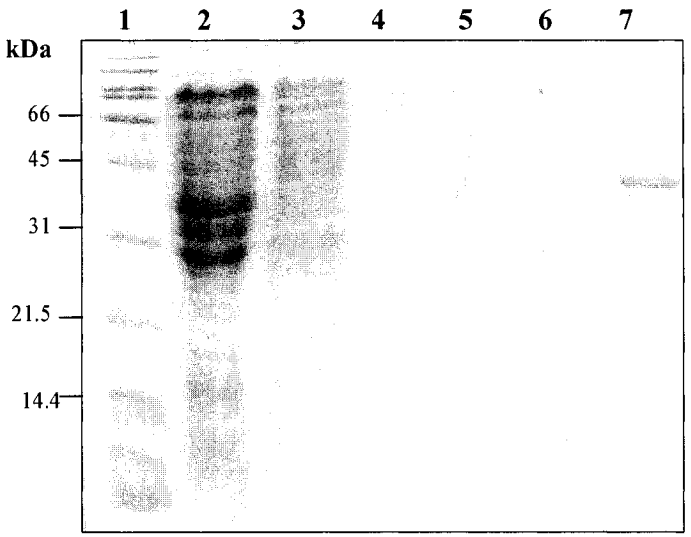

Figure 5.16: Purification of the allosteric domain from the intein tag analyzed by SDS-PAGE (13% acrylamide). Lane 1: Molecular weight protein marker; lane 2: supernatant loaded onto chitin column (4 °C); lane 3: flow through; lane 4 and 5: column wash (pH 8.5); lane 6: protein eluate after cleavage reaction, wash buffer + MESNA (pH 8.5), 4°C, 16 hr, (acetone precipitated protein); lane 7: analysis of resin after cleavage reaction.

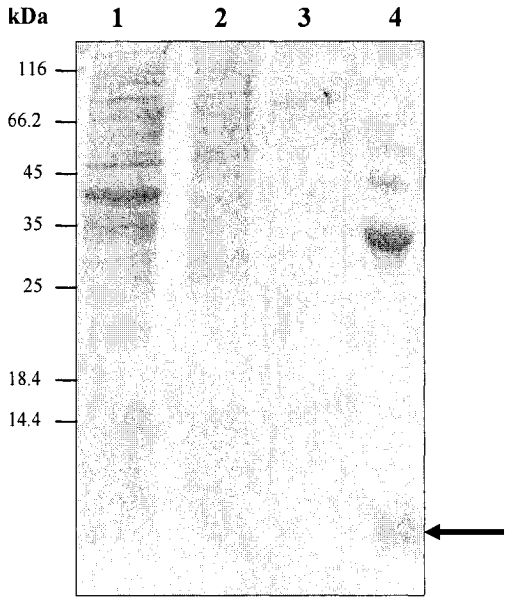

Figure 5.17: Cleavage efficiency analysis of the allosteric domain by SDS-PAGE (13% acylamide). Lane 1: supernatant loaded onto chitin column (4 °C); lane 2: last flow-through fraction; lane 3: column wash (pH 8.5); lane 4: analysis of resin after cleavage reaction (wash buffer + MESNA (pH 8.5), 25 °C, 16 hr). The arrow represents the allosteric domain (9 kDa).

These results could be explained if the allosteric domain is cleaved from the intein tag, but is trapped in the column, i.e. it is insoluble after cleavage. To test the cleavage efficiency, the protein loaded resin was washed with MESNA, and then the column was flushed with buffer lacking thiol-reducing reagents after. Lastly, both the eluate and the resin were analyzed by SDS-PAGE the following day at 25 °C. The gel indicated that the eluate contained the intein-CBD tag as well as the allosteric domain (data not shown). This result indicated that the cleavage reaction was partially successful. To test whether of not the cleaved allosteric domain precipitated on the column, the column could have been washed with 8 M urea: releases solubilized allosteric domain. This experiment still remains to be done.

5.3.4 Affinity Purification of Fusion Proteins, Induction of On-Column Cleavage, and Elution of the Zn-Binding domain

Similar to the methods outlined for the allosteric domain, the gene of the Zn-binding domain was cloned into the intein expression vector to produce a fusion protein that has the intein-CBD tag at the N-terminus. The supernatant was loaded onto the chitin resin at 4°C and pH 8.5; the fusion protein is expected to bind to the chitin beads. Extensive washing of the column should remove nonspecific bound protein.

The SDS-PAGE gel (Figure 5.18) illustrates the results that were obtained from the purification of the Zn-binding domain. A 500 ml culture was processed as described in Materials and Methods (5.2.4). Lane 2 represents the supernatant containing the soluble protein. The Zn-domain fusion protein is expressed as illustrated by the band at about 38 kDa. Analysis of the flow-through (lane 3) shows represents that most of the fusion protein bound to the column. The column was washed extensively with buffer. Lane 4 represents a fraction at the end of the wash procedure and shows that most contaminating proteins were eliminated. Lane 5 represents the Zn-binding domain eluted after the cleavage reaction. It is acetone precipitate protein, and therefore already concentrated in order to visualize it on a Coomassie stained gel. This domain was successfully cleaved from the intein-tag but some higher molecular weight species are present.

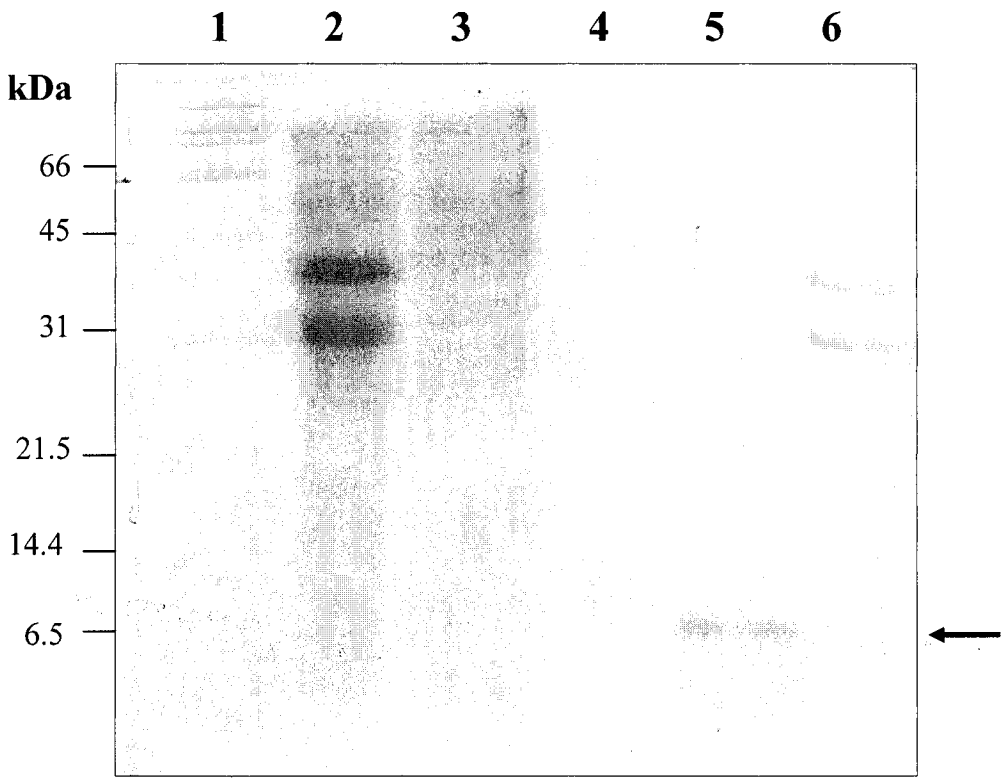

Figure 5.18: Purification of the Zn-binding domain from the intein tag analyzed by SDS-PAGE (13% acrylamide). Lane 1: molecular weight protein marker; lane 2: supernatant loaded onto chitin column (4 °C); lane 3: last flow-through fraction; lane 4: column was (pH 8.5), last fraction of the column wash; lane 5: protein eluate after cleavage reaction, wash (pH 6.5, 25 °C, 16 hr) acetone precipitated of the Zn-binding domain, indicated by the arrow; lane 6: analysis of resin after cleavage reaction.

Lane 6 (Figure 5.18) represents the analysis of an aliquot of chitin after the cleavage reaction. Two protein bands with apparent molecular weights of 38 kDa and 32 kDa, are the same bands that are also seen in the supernatant in lane 2. These bands represent the intact fusion protein and the protein with the Zn-binding domain cleaved away. Perhaps there is some *in vivo* cleavage that occurs within the cells. Nevertheless, our results indicate that we can successfully isolate the Zn-binding domain from the cleavage reaction.

5.3.5 Intein-Mediated Protein Ligation

The efficiency of the ligation has been shown to be increased by having a high concentration of the two target proteins (Evans et al. 1999). Efficiencies as high as 60-80% have been reported previously (Otomo et al. 1999). Intein-mediated ligation of the allosteric and Zn-binding domains followed the procedure outlined in section 5.2.5, and was adapted from a method originally outlined by Evans *et al* for the ligation of a C-terminal thioester on *E. coli* maltose-binding protein and an intein generated cysteine at the N-terminus of T4 DNA ligase (Evans et al. 1999).

SDS-PAGE analysis of the reaction is shown in Figure 5.19. Lanes 2 and 3 show the isolated allosteric and Zn-binding domain, respectively, which were acetone precipitated for visualizion. Unfortunately, the yields of the two isolated domains are low. The concentration of allosteric domain appears negligible since it is not visible on the Coomassie stained gel (lane 2). Alternatively, it may be that the allosteric domain stains very poorly by Coomassie Blue. In contrast, isolated Zn-binding domain is visible and displays the correct molecular weight of 7 kDa, predicted from the primary sequence of the protein. The higher molecular weight species at ~30 kDa, corresponds to the cleaved intein-CBD tag. Lane 4 shows the products of the IPL reaction, and is indicate of a successful ligation reaction. The band at 17 kDa corresponds to the predicted molecular weight of an intact RSU. However, there are other bands at about 66 kDa of unidentified higher molecular weight aggregates (see lanes 2, 3 and 4).

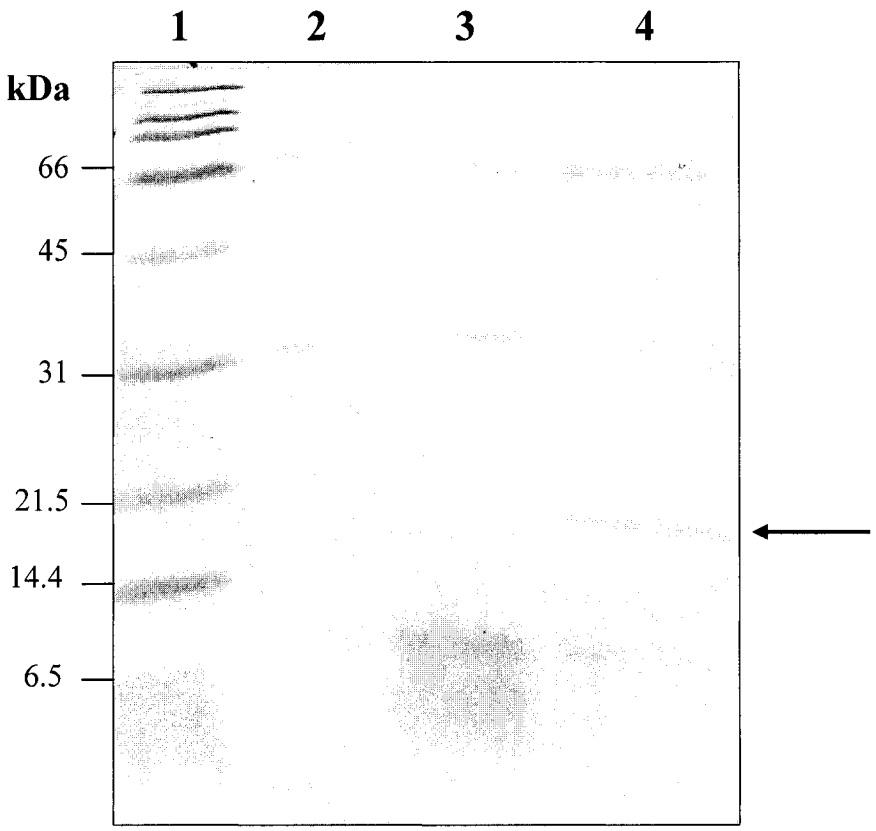

Figure 5.19: Intein-mediated protein ligation of the two domains of RSU. Lane 1: Molecular weight protein marker; lane 2: isolated allosteric domain (acetone precipitated. protein); lane 3: isolated Zn-binding domain (acetone precipitated protein); lane 4: protein products after IPL reaction. The arrow indicates the RSU dimer at 17 kDa.

In order to obtain a more purified sample, further chromatography steps must be performed, such as size exclusion-HPLC or running the sample through another chitin column to remove these aggregates. The yields of the desired proteins can be found in Table 5.1, it summarizes the overall yield of protein content after selected purification steps. A 500 ml bacterial culture yields less than 1 mg of intein-mediated ligated RSU (assuming that the RSU constitutes 10% or less of the protein resolved on the gel). The low yield (7%) of isolated allosteric domain (as visualized by SDS-PAGE in Figure 5.16, lane 6) is likely the limiting reagent in the ligation reaction. By increasing its cleavage efficiency from the intein-CBD tag and its solublility after cleavage, should result in increased amounts of ligated RSU. The Zn-binding domain was isolated with better yields (28%); however, more chromatography steps are required to obtain a pure domain (see Figure 5.19, lane 4).

Table 5.1: Purification Table of the Allosteric and Zn-binding Domains of RSU

Purification Step	**Allosteric Domain**		**Zn-binding Domain**	
	Total Protein (mg)	% Yield	Total Protein (mg)	% Yield
Clarified Cell Lysate (supernatant)	43.5 (≤ 10%) ~ 4.35	100	24.9 (≤ 10%) ~ 2.49	100
Cleavage Reaction	0.3	7	0.7	28
Protein ligation (RSU)	853 µg/ 500 ml			

Intein-mediated ligation has been successful in previous labs; they have isolated 3-6 mg/ L cell culture of ligated *Hpa*I (Evans et al. 1998). In their study, they showed that the efficiency of thiol-induced cleavage is dramatically altered by the target protein's C-terminal residue. For example, when they used an alanine adjacent to the first residue of *Mxe* GyrA intein, they obtained an intact RNase A with a yield of 0.3 mg/L cell culture. However, by replacing the alanine to a methionine for producing an intact *Hpa*I fragment, they increased their yield to 3-6 mg/ml. This data shows that it would be worthwhile to investigate other suitable C-terminal residue other than the methionine at the C-terminus of the allosteric domain. It is also important to consider the most

effective thiol inducing reagent for increasing the efficiency of the cleavage reaction. Another reagent that showed to increase the rate of 'intein-mediated cleavage reaction' was thiophenol when using a *Sce* VMA intein fusion protein (Perler and Adam 2000). However, they were only able to obtain a yield of 30% cleavage. Another lab used DTT as a thiol reagent for purifying Cre recombinase (Cantor and Chong 2001), but IPL reaction was not required after the purification. They have obtained a purified protein with a concentration of 4 mg /L of cell culture using the intein system. Muir and coworkers have demonstrated that it is feasible to ligate a phosphotyrosine peptide to the C-terminus of the protein tyrosine kinase C-terminal Src kinase using inteins (Muir et al. 1998). They obtained ~0.5 mg per 2.5 L of cell culture of ligated protein; their protocol differed from the traditional IPL because it involved ligating a synthetic peptide which contained a thioester instead of using DTT or MESNA to induce cleavage. To conclude, protein ligation using intein technology can be a promising technique to manipulate proteins.

5.4 Future Work

The constructs pTwAl83 and pTwZn84 were produced to further study the structure of the RSU and to test the feasibility of the IMPACT-TWIN^{TM} system to yield high levels of purified protein for IPL. However, the results from the IPL experiments have shown that ligation efficiency must be increased before isotopically labeling one domain. There are several ways to optimize ligation reaction:

First, the chosen cut sites should be in the surface exposed loop, whereas, the sites chosen were associated with β-strand regions of secondary structure not in a loop region. A method to do this is to add a linker in a loop area at the division of the domains. The choice where to split the protein in our case was based on the stability of the domains alone.

Second, the concentrated Zn-binding domain could be added to the chitin resin which contains the allosteric-fusion protein (after cleavage reaction) to facilitate the IPL reaction. It would be important to mix the beads so that the Zn-domain will ligate to the free allosteric domain. This modification might be very useful since it was found that the allosteric domain does cleave from the intein-CBD tag after the addition of MESNA, and

became insoluble after cleavage,; the addition of the Zn-binding domain may help make the allosteric domain soluble. Alternately, the addition of Triton X-100 or low concentrations of urea to the allosteric domain, or a change in the pH of the buffer below the pI of the protein may help its solubility. Moreover, the addition of a low concentration of urea in conjunction with MESNA may improve the thiol-reagent's accessibility to the cleavage site.

Third, the ligation reaction could be performed with misfolded protein purified from inclusion bodies via sucrose density gradient centrifugation, then denatured with chaotropic agents. This would increase the amount of protein reagents available for the ligation reaction. In addition, since soluble allosteric domain appears to be the limiting protein in the reaction, this domain could be isolated from a 2 L cell culture rather than 500 ml.

The ultimate goal is to obtain a cost effective segmentally labeled isotopic RSU where heavy isotopes are incorporated into one domain while the other is not labeled. This goal would be best met by growing the Zn-binding fusion protein with minimal media supplemented with ^{13}C and ^{15}N isotopes, since results from the present study suggests that the Zn-binding domain is well expressed in soluble form and the cleavage reaction yielding the Zn-binding domain is the most efficient.

5.5 Summary

Intein technology provides a novel means by which isotope editing can be performed to extract information on protein inter-domain and inter-subunit interactions by Fourier transform infrared (FTIR) spectroscopy. This project presented for the first time the feasibility of segmental labeling through intein-mediated protein ligation of RSU. In the first phase of this project, the regulatory subunit of ATCase, which houses a Zn-binding domain and a nucleotide binding domain, was reconstructed from its isolated domains using commercially available intein-base expression vectors. As steps towards obtaining an isotope labeled RSU, we have fused each domain to a separate intein. Following affinity purification, the intein tags were chemically cleaved and the reactive ends of the two RSU domains were ligated together to form a peptide. Although ligation was successful, improved yields are required for future FTIR spectroscopic studies.

CHAPTER 6
General Conclusion

The results obtained from the first part of this work demonstrate the advantages of employing isotope edited FTIR spectroscopy to elucidate the changes in the secondary structure of the RSU upon CTP binding. Uniform ^{13}C-labeling of RSU resulted in shifting the amide I absorption band by ~ 45 cm^{-1} away from a strong absorption of CTP (centered at 1656 cm^{-1}). This facilitated the interpretation of the changes in the amide I region in the RSU-CTP complex. VT-FTIR spectroscopy was employed to examine the thermal denaturation of the RSU and the RSU-CTP complex. Analysis of the results revealed that the binding of CTP to RSU increased the thermal stability of the regulatory subunit. The onset of aggregation of the RSU-CTP complex occurred at 53°C as opposed to 47°C for RSU alone. 2D correlation analysis of the dynamic spectra was generated from the VT-FTIR studies. 1D analysis in conjunction with 2D correlation showed that the α-helical structures were more thermally labile than the β-sheet structures of the protein. In addition, the α-helical content unfolded more rapidly and more extensively in the RSU-CTP complex. The sequence of unfolding for RSU commenced with the unfolding of the β-sheet structures, followed by the α-helices, and then the intramolecular β-sheets culminate in the irreversible formation of intermolecular β-sheet aggregates. The sequence of unfolding for the RSU in the RSU-CTP complex was found to be comparable, except that the unfolding commenced at a higher temperature.

FT-Raman spectra of ATCase and its isolated subunits CSU and RSU provided additional evidence in support of the FTIR spectroscopic studies. The RSU is predominantly composed of β-sheets while the CSU possesses predominantly α-helical structures. In addition, the intensity ratios of some of the Raman bands provided evidence that the tyrosines and tryptophans are surface exposed. This is in agreement with the crystal structure of CSU within the holoenzyme (Kosman, 1993 #39). Conformational changes are observed in both the RSU and CSU when they are combined to form ATCase, specifically, the changes in the relative intensities of tryptophans (I_{1360}/I_{1340}), indicating that RSU binding to CSU results in shielding some of the

tryptophan groups from the solvent. Moreover, the relative intensities of tyrosine (I_{850}/I_{830}) indicates that the interaction between RSU with CSU changes the buried tyrosine residues to becomes more solvent exposed

The feasibility of achieving an intein-mediated protein ligation of RSU was undertaken. In the first phase of this work, the regulatory subunit of ATCase, which houses a Zn-binding domain and a nucleotide binding domain, were reconstructed from its isolated domains using commercially available intein-base expression vectors. Each domain was fused to a separate intein. Following affinity purification, the intein tags were chemically cleaved and the reactive ends of the two RSU domains were ligated together to form a peptide. While ligation was successful, improved yields are necessary for future FTIR spectroscopic studies.

Future work should be aimed at the production of segmentally labeled RSU in order to study the unfolding pathways of each domain in RSU and RSU-CTP complex. This work can also be extended to the study of domain unfolding in RSU in the context of the holoenzyme.

REFERENCES

www.neb.com/neb/inteins.html.

Arnold, U., Hinderaker, M.P., and Raines, R.T. 2002. Semisynthesis of ribonuclease A using intein-mediated protein ligation. *Thescientificworldjournal* **2:** 1823-1827.

Ayers, B., Blaschke, U.K., Camarero, J.A., Cotton, G.J., Holford, M., and Muir, T.W. 1999. Introduction of unnatural amino acids into proteins using expressed protein ligation. *Biopolymers* **51:** 343-354.

Beernink, P.T., Endrizzi, J.A., Alber, T., and Schachman, H.K. 1999. Assessment of the allosteric mechanism of aspartate transcarbamoylase based on the crystalline structure of the unregulated catalytic subunit. *Proceedings of the National Academy of Sciences of the United States of America* **96:** 5388-5393.

Blaschke, U.K., Silberstein, J., and Muir, T.W. 2000. Protein engineering by expressed protein ligation. *Methods in Enzymology* **328:** 478-496.

Bradford, M.M. 1976. A rapid and sensitive method for the quantitation of microgram quantities of protein utilizing the principle of protein-dye binding. *Analytical Biochemistry* **72:** 248-254.

Braisted, A.C., Judice, J.K., and Wells, J.A. 1997. Synthesis of proteins by subtiligase. *Methods in Enzymology* **289:** 298-313.

Camarero, J.A., and Muir, T.W. 1997. Chemoselective backbone cyclization of unprotected peptides. *Chem. Commun.*: 1369-1370.

Cantor, E.J., and Chong, S. 2001. Intein-mediated rapid purification of Cre recombinase. *Protein Expression & Purification* **22:** 135-140.

Chong, S., Mersha, F.B., Comb, D.G., Scott, M.E., Landry, D., Vence, L.M., Perler, F.B., Benner, J., Kucera, R.B., Hirvonen, C.A., et al. 1997. Single-column purification of free recombinant proteins using a self-cleavable affinity tag derived from a protein splicing element. *Gene* **192:** 271-281.

Chong, S., Montello, G., Zhang, A., Cantor, E., Liao, W., Xu, M., and Benner, J. 1998. Utilizing the C-terminal cleavage activity of a protein splicing element to purify recombinant proteins in a single chromatographic step. *Nucl. Acids. Res.* **26:** 5109-5115.

Chong, S., Shao, Y., Paulus, H., Benner, J., Perler, F.B., and Xu, M.Q. 1996. Protein splicing involving the Saccharomyces cerevisiae VMA intein. The steps in the splicing pathway, side reactions leading to protein cleavage, and establishment of an in vitro splicing system. *Journal of Biological Chemistry* **271:** 22159-22168.

Clore, G.M., and Gronenborn, A.M. 1994. Multidimensional heteronuclear nuclear magnetic resonance of proteins. *Methods in Enzymology* **239:** 349-363.

Cotton, G.J., and Muir, T.W. 1999. Peptide ligation and its application to protein engineering. *Chemistry & Biology* **6:** R247-256.

Cotton, G.J., and Muir, T.W. 2000. Generation of a dual-labeled fluorescence biosensor for Crk-II phosphorylation using solid-phase expressed protein ligation. *Chemistry & Biology* **7:** 253-261.

Cowburn, D., and Muir, T.W. 2001. Segmental isotopic labeling using expressed protein ligation. *Methods in Enzymology* **339:** 41-54.

David, R., Richter, M.P., and Beck-Sickinger, A.G. 2004. Expressed protein ligation. Method and applications. *European Journal of Biochemistry* **271:** 663-677.

Davis, L., Kuehl, M., and Battey, J. 1994. *In vitro amplification of DNA using the polymerase chain reaction (PCR). Basic Methods in Molecular Biology,*, 2nd ed.

Dawson, P.E., Muir, T.W., Clark-Lewis, I., and Kent, S.B. 1994. Synthesis of proteins by native chemical ligation. *Science* **266:** 776-779.

Dutta, P.L., and Foye, W.O. 1990. Synthesis and biological activity of a series of aspartate transcarbamoylase inhibitors: N-substituted diethyl aspartates and N-substituted-3-oxo-1,4-piperazine-2-acetic acid esters. *J Pharm Sci.* **79:** 447-452.

Evans, T.C., Jr., Benner, J., and Xu, M.Q. 1998. Semisynthesis of cytotoxic proteins using a modified protein splicing element. *Protein Science* **7:** 2256-2264.

Evans, T.C., Jr., Benner, J., and Xu, M.Q. 1999a. The cyclization and polymerization of bacterially expressed proteins using modified self-splicing inteins. *Journal of Biological Chemistry* **274:** 18359-18363.

Evans, T.C., Jr., Benner, J., and Xu, M.Q. 1999b. The in vitro ligation of bacterially expressed proteins using an intein from Methanobacterium thermoautotrophicum. *Journal of Biological Chemistry* **274:** 3923-3926.

Evans, T.C., Jr., and Xu, M.Q. 1999. Intein-mediated protein ligation: harnessing nature's escape artists. *Biopolymers* **51:** 333-342.

Gardner, K.H., and Kay, L.E. 1998. The use of 2H, 13C, 15N multidimensional NMR to study the structure and dynamics of proteins. *Annu Rev Biophys Biomol Struct.* **27:** 357-406.

Gerhart, J.C., and Holoubek, H. 1967. The purification of aspartate transcarbamylase of Escherichia coli and separation of its protein subunits. *Journal of Biological Chemistry* **242:** 2886-2892.

Gimble, F.S., and Thorner, J. 1992. Homing of a DNA endonuclease gene by meiotic gene conversion in Saccharomyces cerevisiae. *Nature.* **357:** 301-306.

Goto, N.K., and Kay, L.E. 2000. New developments in isotope labeling strategies for protein solution NMR spectroscopy. *Current Opinion in Structural Biology* **10:** 585-592.

Gray, C.W., Chamberlin, M.J., and Gray, D.M. 1973. Interaction of Aspartate Transcarbamylase with Regulatory Nucleotides. *J. Biol. Chem.* **248:** 6071-6079.

Harris, P.I., Robillard, G.T., van Dijk, A.A., and Chapman, D. 1992. Potential 13C and 15N labeling for studying protein-protein interactions using Fourier transform infrared spectroscopy. *Biochemistry* **31:** 6279-6284.

Hervé, G. 1989. *Aspartate transcarbamoylase from Escherichia Coli. In: Allosteric Enzymes.* CRC Press, Boca Raton, Florida.

Hoang, T.T., Ma, Y., Stern, R.J., McNeil, M.R., and Schweizer, H.P. 1999. Construction and use of low-copy number T7 expression vectors for purification of problem proteins: purification of Mycobacterium tuberculosis RmlD and Pseudomonas aeruginosa LasI and RhlI proteins, and functional analysis of purified RhlI. *Gene* **237:** 361-371.

Hofmann, R.M., and Muir, T.W. 2002. Recent advances in the application of expressed protein ligation to protein engineering. *Current Opinion in Biotechnology* **13:** 297-303.

Hondal, R.J., Nilsson, B.L., and Raines, R.T. 2001. Selenocysteine in native chemical ligation and expressed protein ligation. *Journal of the American Chemical Society* **123:** 5140-5141.

Hong, S.-H., Toyama, M., Maret, W., and Murooka, Y. 2001. High Yield Expression and Single Step Purification of Human Thionein/Metallothionein. *Protein Expression and Purification* **21:** 243-250.

Honzatko, R.B., Crawford, J.L., Monaco, H.L., Ladner, J.E., Ewards, B.F., Evans, D.R., Warren, S.G., Wiley, D.C., Ladner, R.C., and Lipscomb, W.N. 1982. Crystal and molecular structures of native and CTP-liganded aspartate carbamoyltransferase from Escherichia coli. *Journal of Molecular Biology* **160:** 219-263.

Ismoyo, F., Wang, Y., and A.A., I. 2000. Examination of the effect on the secondary structure of avidin and avidin-binding complex by resolution-enhanced two-dimentional correlation spectroscopy. *Applied Spectroscopy* **54:** 939-947.

Iwai, H., and Pluckthun, A. 1999. Circular [beta]-lactamase: stability enhancement by cyclizing the backbone. *FEBS Letters* **459:** 166-172.

Jin, L., Stec, B., Lipscomb, W.N., and Kantrowitz, E.R. 1999. Insights into the mechanisms of catalysis and heterotropic regulation of Escherichia coli aspartate transcarbamoylase based upon a structure of the enzyme complexed with the bisubstrate analogue N-phosphonacetyl-L-aspartate at 2.1 A. *Proteins* **37:** 729-742.

Johnson, R.K., Swyryd, E.A., and Stark, G.R. 1978. Effects of N-(phosphonacetyl)-L-aspartate on murine tumors and normal tissues in vivo and in vitro and the relationship of sensitivity to rate of proliferation and level of aspartate transcarbamylase. *Cancer Research* **38:** 371-378.

Kainosho, M. 1997. NMR Suppl. *Nature Structural Biology* **4:** 858-861.

Kane, P.M., Yamashiro, C.T., Wolczyk, D.F., Neff, N., Goebl, M., and Stevens, T.H. 1990. Protein splicing converts the yeast TFP1 gene product to the 69-kD subunit of the vacuolar H(+)-adenosine triphosphatase. *Science* **250:** 651-657.

Kantrowitz, E.R., and Lipscomb, W.N. 1990. Escherichia coli aspartate transcarbamoylase: the molecular basis for a concerted allosteric transition. *Trends in Biochemical Sciences* **15:** 53-59.

Kigawa, T., Muto, Y., and Yokoyama, S. 1995. Cell-free synthesis and amino acid-selective stable isotope labeling of proteins for NMR analysis. *Journal of Biomolecular NMR* **6:** 129-134.

Klabunde, T., Sharma, S., Telenti, A., Jacobs, W.R., Jr., and Sacchettini, J.C. 1998. Crystal structure of GyrA intein from Mycobacterium xenopi reveals structural basis of protein splicing.[see comment]. *Nature Structural Biology* **5:** 31-36.

Kosman, R.P., Gouaux, J.E., and Lipscomb, W.N. 1993. Crystal structure of CTP-ligated T state aspartate transcarbamoylase at 2.5 A resolution: implications for ATCase mutants and the mechanism of negative cooperativity. *Proteins* **15:** 147-176.

Krause, K.L., Volz, K.W., and Lipscomb, W.N. 1985. Structure at 2.9-A resolution of aspartate carbamoyltransferase complexed with the bisubstrate analogue N-(phosphonacetyl)-L-aspartate. *Proceedings of the National Academy of Sciences of the United States of America* **82:** 1643-1647.

Krause, K.L., Volz, K.W., and Lipscomb, W.N. 1987. 2.5 A structure of aspartate carbamoyltransferase complexed with the bisubstrate analog N-(phosphonacetyl)-L-aspartate. *Journal of Molecular Biology* **193:** 527-553.

LiCata, V.J., and Allewell, N.M. 1997. Is substrate inhibition a consequence of allostery in aspartate transcarbamylase? *Biophys Chem.* **64:** 225-234.

Li-Chan, E.C.Y. 1996. The Application Of Raman Spectroscopy in Food Science. *Trends in Food Science & Technology.* **7:** 361.

Li-Chan, E.C.Y., Ismail, A., Sedman, J., and van de Voort, F. 2002. *Vibrational spectroscopy of food and food products. In "Handbook of Vibrational Spectroscopy".* Wiley & Sons Ltd, West Sussex, England., pp. 3629-3662.

Lipscomb, W.N. 1994. Aspartate transcarbamylase from Escherichia coli: activity and regulation. *Advances in Enzymology & Related Areas of Molecular Biology* **68:** 67-151.

Liu, L., Wales, M.E., and Wild, J.R. 2000. Allosteric Signal Transmission Involves Synergy between Discrete Structural Units of the Regulatory Subunit of Aspartate Transcarbamoylase. *Archives of Biochemistry and Biophysics* **373:** 352-360.

Lovrinovic, M., Seidel, R., Wacker, R., Schroeder, H., Seitz, O., Engelhard, M., Goody, R.S., and Niemeyer, C.M. 2003. Synthesis of protein-nucleic acid conjugates by expressed protein ligation. *Chemical Communications*: 822-823.

Markby, D., Zhou, B., and Schachman, H. 1991. A 70-Amino Acid Zinc-Binding Polypeptide from the Regulatory Chain of Aspartate Transcarbamoylase Forms a Stable Complex with the Catalytic Subunit Leading to Markedly Altered Enzyme Activity. *PNAS* **88:** 10568-10572.

Mathys, S., Evans, T.C., Chute, I.C., Wu, H., Chong, S., Benner, J., Liu, X.Q., and Xu, M.Q. 1999. Characterization of a self-splicing mini-intein and its conversion into autocatalytic N- and C-terminal cleavage elements: facile production of protein building blocks for protein ligation. *Gene* **231:** 1-13.

Mills, K.V., Lew, B.M., Jiang, S., and Paulus, H. 1998. Protein splicing in trans by purified N- and C-terminal fragments of the Mycobacterium tuberculosis RecA intein. *Proceedings of the National Academy of Sciences of the United States of America* **95:** 3543-3548.

Monod, J., Wyman, J., and Changeux, J.P. 1965. On the Nature of Allosteric Transition: A Plausible Model. *J Mol Biol.* **12:** 88-118.

Muchmore, D.C., McIntosh, L.P., Russell, C.B., Anderson, D.E., and Dahlquist, F.W. 1989. Expression and nitrogen-15 labeling of proteins for proton and nitrogen-15 nuclear magnetic resonance. *Methods in Enzymology* **177:** 44-73.

Muir, T.W. 2001. Development and Application of Expressed Protein Ligation. *SynLett* **6:** 733-740.

Muir, T.W. 2003. Semisynthesis of Proteins by Expressed Protein Ligation. *Annu. Rev. Biochem.* **[epub ahead of print].**

Muir, T.W., Sondhi, D., and Cole, P.A. 1998. Expressed protein ligation: a general method for protein engineering. *Proceedings of the National Academy of Sciences of the United States of America* **95:** 6705-6710.

Navre, M., and Schachman, H.K. 1983. Synthesis of aspartate transcarbamoylase in Escherichia coli: transcriptional regulation of the pyrB-pyrI operon. *Proceedings*

of the National Academy of Sciences of the United States of America **80:** 1207-1211.

Noren, C.J., Wang, J., and Perler, F.B. 2000. Dissecting the Chemistry of Protein Splicing and its Applications. *Angewandte Chemie Int. Ed.* **39:** 450-466.

Nyanguile, O., Dancik, C., Blakemore, J., Mulgrew, K., Kaleko, M., and Stevenson, S.C. 2003. Synthesis of adenoviral targeting molecules by intein-mediated protein ligation. *Gene Therapy* **10:** 1362-1369.

Otomo, T., Ito, N., Kyogoku, Y., and Yamazaki, T. 1999a. NMR observation of selected segments in a larger protein: central-segment isotope labeling through intein-mediated ligation. *Biochemistry* **38:** 16040-16044.

Otomo, T., Teruya, K., Uegaki, K., Yamazaki, T., and Kyogoku, Y. 1999b. Improved segmental isotope labeling of proteins and application to a larger protein. *Journal of Biomolecular NMR* **14:** 105-114.

Pauza, C.D., Karels, M.J., Navre, M., and Schachman, H.K. 1982. Genes encoding Escherichia coli aspartate transcarbamoylase: the pyrB-pyrI operon. *Proc Natl Acad Sci U S A.* **79:** 4020-4024.

Perler, F.B. 1998. Protein splicing of inteins and hedgehog autoproteolysis: structure, function, and evolution. *Cell* **92:** 1-4.

Perler, F.B. 2000. InBase, the Intein Database. *Nucleic Acids Research* **28:** 344-345.

Perler, F.B., and Adam, E. 2000. Protein splicing and its applications. *Current Opinion in Biotechnology* **11:** 377-383.

Perler, F.B., Xu, M.Q., and Paulus, H. 1997. Protein splicing and autoproteolysis mechanisms. *Current Opinion in Chemical Biology* **1:** 292-299.

Rastogi, V.K., Swanson, R., Hartberg, Y.M., Wales, M.E., and Wild, J.R. 1998. Role of Allosteric:Zinc Interdomain Region of the Regulatory Subunit in the Allosteric Regulation of Aspartate Transcarbamoylase fromEscherichia coli. *Archives of Biochemistry and Biophysics* **354:** 215-224.

Redfield, A.G., McIntosh, L.P., and Dahlquist, F.W. 1989. Use of 13C and 15N isotope labels for proton nuclear magnetic resonance and nuclear Overhauser effect. Structural and dynamic studies of larger proteins and nucleic acids. *Archivos de Biologia y Medicina Experimentales* **22:** 129-137.

Rowland, R.L., Perry, W.L., Foreman, E.L., and Friedman, H.L. 1950. Mercurial diuretics. I. Addition of mercuric acetate to allyl ures. *Journal of American Chemistry Society* **72:** 3595-3298.

Roy, R.S., Allen, O., and Walsh, C.T. 1999. Expressed protein ligation to probe regiospecificity of heterocyclization in the peptide antibiotic microcin B17. *Chemistry & Biology* **6:** 789-799.

Sakash, J.B., Chan, R.S., Tsuruta, H., and Kantrowitz, E.R. 2000. Three of the six possible intersubunit stabilizing interactions involving Glu-239 are sufficient for restoration of the homotropic and heterotropic properties of Escherichia coli aspartate transcarbamoylase. *Journal of Biological Chemistry* **275:** 752-758.

Scheibner, K.A., Zhang, Z., and Cole, P.A. 2003. Merging fluorescence resonance energy transfer and expressed protein ligation to analyze protein-protein interactions. *Analytical Biochemistry* **317:** 226-232.

Scott, C.P., Abel-Santos, E., Wall, M., Wahnon, D.C., and Benkovic, S.J. 1999. Production of cyclic peptides and proteins in vivo. *PNAS* **96:** 13638-13643.

Severinov, K., and Muir, T.W. 1998. Expressed protein ligation, a novel method for studying protein-protein interactions in transcription. *Journal of Biological Chemistry* **273:** 16205-16209.

Shao, Y., and Kent, S.B. 1997. Protein splicing: occurrence, mechanisms and related phenomena. *Chemistry & Biology* **4:** 187-194.

Shingledecker, K., Jiang, S., and Paulus, H. 2000. Reactivity of the cysteine residues in the protein splicing active center of the Mycobacterium tuberculosis RecA intein. *Archives of Biochemistry & Biophysics* **375:** 138-144.

Southworth, M.W., Adam, E., Panne, D., Byer, R., Kautz, R., and Perler, F.B. 1998. Control of protein splicing by intein fragment reassembly. *EMBO Journal* **17:** 918-926.

Southworth, M.W., Amaya, K., Evans, T.C., Xu, M.Q., and Perler, F.B. 1999. Purification of proteins fused to either the amino or carboxy terminus of the Mycobacterium xenopi gyrase A intein. *Biotechniques* **27:** 110-114.

Stevens, R., and Lipscomb, W. 1992. A Molecular Mechanism for Pyrimidine and Purine Nucleotide Control of Aspartate Transcarbamoylase. *PNAS* **89:** 5281-5285.

Stevens, R.C., Chook, Y.M., Cho, C.Y., Lipscomb, W.N., and Kantrowitz, E.R. 1991. Escherichia coli aspartate carbamoyltransferase: the probing of crystal structure analysis via site-specific mutagenesis. *Protein Engineering* **4:** 391-408.

Stevens, R.C., Gouaux, J.E., and Lipscomb, W.N. 1990. Structural consequences of effector binding to the T state of aspartate carbamoyltransferase: crystal structures of the unligated and ATP- and CTP-complexed enzymes at 2.6-A resolution.[erratum appears in Biochemistry 1990 Dec 18;29(50):11146]. *Biochemistry* **29:** 7691-7701.

Stevens, R.C., and Lipscomb, W.N. 1990. Allosteric control of quaternary states in E. coli aspartate transcarbamylase. *Biochemical & Biophysical Research Communications* **171:** 1312-1318.

Stieglitz, K., Stec, B., Baker, D.P., and Kantrowitz, E.R. 2004. Monitoring the Transition from the T to the R State in E.Coli Aspartate Transcarbamoylase by X-Ray Crystallography: Crystal Structures of the E50A Mutant Enzyme in Four Distinct Allosteric States. *J.Mol.Biol.* **341:** 853.

Sun, L., Ghosh, I., and Xu, M.Q. 2003. Generation of an affinity column for antibody purification by intein-mediated protein ligation. *Journal of Immunological Methods* **282:** 45-52.

Sydor, J.R., Mariano, M., Sideris, S., and Nock, S. 2002. Establishment of intein-mediated protein ligation under denaturing conditions: C-terminal labeling of a single-chain antibody for biochip screening. *Bioconjugate Chemistry* **13:** 707-712.

Takeda, S., Tsukiji, S., and Nagamune, T. 2004. Site-specific conjugation of oligonucleotides to the C-terminus of recombinant protein by expressed protein ligation. *Bioorganic & Medicinal Chemistry Letters* **14:** 2407-2410.

Tam, J.P., Lu, Y.A., Liu, C.F., and Shao, J. 1995. Peptide synthesis using unprotected peptides through orthogonal coupling methods. *Proceedings of the National Academy of Sciences of the United States of America* **92:** 12485-12489.

Tanner, J.J., Smith, P.E., and Krause, K.L. 1993. Molecular dynamics simulations and rigid body (TLS) analysis of aspartate carbamoyltransferase: Evidence for an uncoupled R state. *Protein Sci* **2:** 927-935.

Telenti, A., Southworth, M., Alcaide, F., Daugelat, S., Jacobs, W.R., Jr., and Perler, F.B. 1997. The Mycobacterium xenopi GyrA protein splicing element: characterization of a minimal intein. *Journal of Bacteriology* **179:** 6378-6382.

Turnbull, J.L., Waldrop, G.L., and Schachman, H.K. 1992. Ionization of amino acid residues involved in the catalytic mechanism of aspartate transcarbamoylase. *Biochemistry* **31:** 6562-6569.

van Vliet, F., Xi, X., Staercke, C., de Wannemaeker, B., Jacobs, A., Cherfils, J., Ladjimi, M., Herve, G., and Cunin, R. 1991. Heterotropic Interactions in Aspartate Transcarbamoylase: Turning Allosteric ATP Activation into Inhibition as a Consequence of a Single Tyrosine to Phenylalanine Mutation. *PNAS* **88:** 9180-9183.

Wallace, C. 1995a. Peptide ligation and semisynthesis. *Curr Opin Biotechnol.* **6:** 403-410.

Wallace, C.J. 1995b. Peptide ligation and semisynthesis. *Curr Opin Biotechnol.* **6:** 403-410.

Wang, Y., Murayama, K., Myojo, Y., Tsenkova, R., Hayashi, N., and Ozaki, Y. 1998. Two-dimensional Fourier-transform near infrared spectroscopy study of heat denaturation of ovalbumin in aqueous solutions. *Journal of Physical Chemistry* **102:** 6655-6662.

Watanabe, T., Ito, Y., Yamada, T., Hashimoto, M., Sekine, S., and Tanaka, H. 1994. The roles of the C-terminal domain and type III domains of chitinase A1 from Bacillus circulans WL-12 in chitin degradation. *Journal of Bacteriology* **176:** 4465-4472.

Wider, G., and Wuthrich, K. 1999. NMR spectroscopy of large molecules and multimolecular assemblies in solution. *Current Opinion in Structural Biology* **9:** 594-601.

Williams, M.K., Stec, B., and Kantrowitz, E.R. 1998. A single mutation in the regulatory chain of Escherichia coli aspartate transcarbamoylase results in an extreme T-state structure. *Journal of Molecular Biology* **281:** 121-134.

Wood, D.W., Derbyshire, V., Wu, W., Chartrain, M., Belfort, M., and Belfort, G. 2000. Optimized single-step affinity purification with a self-cleaving intein applied to human acidic fibroblast growth factor. *Biotechnology Progress* **16:** 1055-1063.

Wood, D.W., Wu, W., Belfort, G., Derbyshire, V., and Belfort, M. 1999. A genetic system yields self-cleaving inteins for bioseparations.[see comment]. *Nature Biotechnology* **17:** 889-892.

Wood, R.J., Tchack, L., Angelo, G., Pratt, R.E., and Sonna, L.A. 2004. DNA microarray analysis of vitamin D-induced gene expression in a human colon carcinoma cell line. *Physiological Genomics* **17:** 122-129.

Xi, X.G., De Staercke, C., Van Vliet, F., Triniolles, F., Jacobs, A., Stas, P.P., Ladjimi, M.M., Simon, V., Cunin, R., and Herve, G. 1994. The Activation of Escherichia coli Aspartate Transcarbamylase by ATP : Specific Involvement of Helix H2' at the Hydrophobic Interface Between the Two Domains of the Regulatory Chains. *Journal of Molecular Biology* **242:** 139-149.

Xi, X.G., van Vliet, F., Ladjimi, M.M., de Wannemaeker, B., de Staercke, C., Glansdorff, N., Pierard, A., Cunin, R., and Herve, G. 1991. Heterotropic interactions in Escherichia coli aspartate transcarbamylase. Subunit interfaces involved in CTP inhibition and ATP activation. *J Mol Biol.* **220:** 789-799.

Xu, R., Ayers, B., Cowburn, D., and Muir, T.W. 1999. Chemical ligation of folded recombinant proteins: segmental isotopic labeling of domains for NMR studies. *Proceedings of the National Academy of Sciences of the United States of America* **96:** 388-393.

Yamazaki, T., Otomo, T., Oda, N., Kyogoku, Y., Uegaki, K., Ito, N., Ishino, Y., and Nakamura, H. 1998. Segmental isotope labeling for protein NMR using peptide splicing. *J. Am. Chem. Soc.* **120:** 5591-5592.

Yang, Y.R., Kirschner, M.W., and Schachman, H.K. 1978. Aspartate transcarbamoylase (Escherichia coli): preparation of subunits. *Methods in Enzymology* **51:** 35-41.

Zuberek, J., Wyslouch-Cieszynska, A., Niedzwiecka, A., Dadlez, M., Stepinski, J., Augustyniak, W., Gingras, A.C., Zhang, Z., Burley, S.K., Sonenberg, N., et al. 2003. Phosphorylation of eIF4E attenuates its interaction with mRNA 5' cap analogs by electrostatic repulsion: intein-mediated protein ligation strategy to obtain phosphorylated protein. *Rna* **9:** 52-61.